Functional characterization of PLDγ1 in *Arabidopsis thaliana* innate immunity

Dissertation

der Mathematisch-Naturwissenschaftlichen Fakultät
der Eberhard Karls Universität Tübingen
zur Erlangung des Grades eines
Doktors der Naturwissenschaften
(Dr. rer. nat.)

vorgelegt von
M.Sc. Maria Alejandra Schlöffel
aus Ciudad Bolivar, Kolumbien

Tübingen
2019

Gedruckt mit Genehmigung der Mathematisch-Naturwissenschaftlichen Fakultät der Eberhard Karls Universität Tübingen.

Tag der mündlichen Qualifikation:	19.12.2019
Dekan:	Prof. Dr. Wolfgang Rosenstiel
1. Berichterstatter:	PD Dr. Andrea Gust
2. Berichterstatter:	Prof. Dr. Thorsten Nürnberger

CONTENT

LIST OF ABBREVIATIONS VII

LIST OF FIGURES IX

LIST OF TABLES X

1 INTRODUCTION 1

1.1 Plant Innate Immunity 1

1.1.1 General aspects 1

1.1.2 PRR mediated plant immunity 3

1.1.2.1 Flagellin sensing through LRR-RLKs – recognition and regulation 4

1.1.2.2 Chitin and Peptidoglycan recognition through LysM-receptor kinases 5

1.2 Phospholipases 6

1.2.1 General overview 6

1.2.2 PLDs and the role of PA in plant immunity 8

1.2.2.1 PLDα1 is involved in G-protein-mediated defence responses and beneficial interactions 8

1.2.2.2 PLDβ works as negative regulator in plant immunity on different signalling levels 9

1.2.2.3 PLDδ is an important player in fungal resistance and PLDζ is a negative regulator in MTI 9

1.2.2.4 PLDγ subfamily is mostly unknown to be involved in plant innate immunity .. 10

1.3 Aims of this study 11

2 MATERIAL AND METHODS 12

2.1 Material 12

2.1.1 General consumables 12

2.2 Media and Antibiotics 12

2.2.1 Vectors 13

2.2.2 Primers 14
2.2.3 Antibodies 15

2.3 Plants, Bacteria and Fungi – cultivation and transformation 16
2.3.1 Plant lines and cultivation 16
2.3.2 Stable transformation of *Arabidopsis thaliana* 17
2.3.3 Transient transformation of *Nicotiana benthamiana* 17
2.3.4 Bacteria strains and cultivation 18
2.3.5 Transformation of chemical competent bacteria 18
2.3.6 Transformation of electro-competent *Agrobacterium tumefaciens* 18
2.3.7 Preparation of electro competent *Agrobacterium tumefaciens* cells 19
2.3.8 Fungal strains 19

2.4 Molecular biology methods 19
2.4.1 Plasmid DNA extraction 19
2.4.2 Genomic DNA extraction from plants 19
2.4.3 Fungal DNA extraction 20
2.4.4 RNA extraction 20
2.4.5 DNase treatment 21
2.4.6 Reverse transcription 21
2.4.7 Polymerase Chain Reaction - Standard protocols and thermal profiles 21
2.4.8 Quantitative Real Time PCR 24
2.4.9 Separation and isolation of DNA via agarose gel electrophoresis 24
2.4.10 DNA quantification and analysis 25
2.4.11 Cloning 25
2.4.12 TALEN 25

2.5 Biochemical methods 26
2.5.1 Protein extraction in plants 26
2.5.1.1 Protein extraction for Co-immunoprecipitation 26
2.5.1.2 Protein extraction for MS analysis 26
2.5.2 Quantification of protein concentration 26
2.5.3 SDS-PAGE 27
2.5.4 Western blot analysis 27
2.5.5 Protein-Protein interaction assays 28
2.5.5.1 Co – Immunoprecipitation 28

2.5.6 Phosphosite analysis via mass spectrometry 28
2.5.7 Phospholipid labelling and extraction 29
2.5.8 Thin layer chromatography 30
2.5.9 Detection of salicylic acid and jasmonic acid 30

2.6 Bioassays 30
2.6.1 *Pst* infection 30
2.6.2 *Botrytis cinerea* infection 31
2.6.3 *Alternaria brassicicola* infection 31
2.6.4 Detection of reactive oxygen species 31
2.6.5 MAP-kinase activation assay 32

3 RESULTS 33

3.1 Phosphoproteomic analysis to find new signalling targets of CERK1 33

3.2 The role of PLDγ1 in plant innate immunity 40
3.2.1 PLDγ is a putative interactor of CERK1 40
3.2.2 Characterization of *PLDγ* T-DNA insertion lines 42
3.2.3 Bacterial and fungal infection in *Arabidopsis* is negatively regulated by PLDγ1 but not by PLDγ2 and PLDγ3 44
3.2.4 MAMP induced ROS-production is negatively regulated by PLDγ1 48
3.2.5 Generation of complementation lines *pldγ1-1 PLDγ1* 50
3.2.6 Resistance of *pldγ1* to *Pseudomonas* infection can be reversed in complementation lines 52
3.2.7 Identification of additional T-DNA insertions in *pldγ1-1* (Salk_066687) 56
3.2.8 Generation of a second, independent *pldγ1* mutant via TALEN 56

3.3 Finding the reason for the pldγ1-1 phenotype in different downstream pathways 59
3.3.1 PA levels are not affected in the *pldγ1-1* mutant 59
3.3.2 JA levels are elevated 60

3.4 PLDγ1 can be found in complex with BIR2 and BIR3 62
3.4.1 Transiently expressed PLDγ1 binds to BIR2 and BIR3 in *N. benthamiana* 62
3.4.2 Alternative methods to test interaction of PLDγ1 with BIR2 need to be optimized . 65

4 DISCUSSION 66

4.1 General aspects 66

4.2 PLDγ1 is part of the immune pathway in *Arabidopsis* as negative regulator ..67

4.3 Additional T-DNA Insertions in *pldγ1-1* and missing independent mutant line complicate the situation 70

4.4 The role of phosphatidic acid in PLDγ1 dependent stress signalling 71

4.5 Defence pathways must be tight regulated – PLDγ1 interplay with BIR2 and BIR3 73

4.6 Outlook 76

5 SUMMARY 77

6 ZUSAMMENFASSUNG 78

7 REFERENCES 79

8 APPENDIX 90

LIST OF ABBREVIATIONS

(v/v) *Volume per volume*
(w/v) *Weight per volume*
°C *Grad Celsius*
AtCP *Arabidopsis thaliana capping protein*
BAK1 *BRASSINOSTEROID INSENSITIVE 1- ASSOCIATED KINASE 1*
Bgh *Blumeria graminis f. sp. hordei*
BIK1 *BOTRYTIS-INDUCED KINASE1*
BIR1 *BAK1-INTERACTING RECEPTOR-LIKE KINASE 1*
BIR2 *BAK1-INTERACTING RECEPTOR-LIKE KINASE 2*
BIR3 *BAK1-INTERACTING RECEPTOR-LIKE KINASE 3*
BRI1 *BRASSINOSTEROID INSENSITIVE 1*
BSA *Bovine serum albumin*
Ca2+ *Calcium*
CERK1 *CHITIN ELICITOR RECEPTOR KINASE 1*
cm *Centimetre*
DAMPs *damage-associated molecular patterns*
ddH_2O *double distilled water*
DEPC *Diethyl pyrocarbonate*
DNA *Deoxyribonucleic acid*
dNTPs *Deoxyribonucleotide triphosphate*
DTT *Dithiothreitol*
EDTA *Ethylenediaminetetraacetic acid*
ET *ethylene*
ETI *Effector Triggered Immunity*
flg22 *22 amino acid long peptide of flagellin*
FLS2 *FLAGELLIN SENSITIVE 2*
fw F*orward*
g *Gram*
GFP *green fluorescent protein*
GlcNAc *N-acetylglucosamine*
h *Hour*
HAMP *herbivore-associated molecular pattern*
JA jasmonic acid
kb *Kilobase*
L *Litre*
LB *Lysogeny broth*
LiCl *Lithium chloride*
LIK1 *RLK1-INTERACTING KINASE 1*
LRR *Leucine-rich repeat*
LYK *LysM-Receptor Kinases*
LYK5 *LYSIN MOTIF RECEPTOR KINASE 5*
LysM *lysin motifs*
mA *Milliampere*
MAMP *microbe-associated molecular pattern*
MAPK *Mitogen Activated Protein Kinases*
MAPKKK.....*MAP kinase kinase kinase*
$MgCl^2$ *Magnesium chloride*
$MgSo^4$ *Magnesium Sulfate*
min M*inute*
MPK3 *MAP KINASE 3*
MPK4 *MAP KINASE 4*
MPK6 *MAP KINASE 6*
ms *Millisecond*
MS *Murashige and Skoog*
MTI *MAMP-triggered immunity*
MurNAc .....*N-acetylmuramic acid*
NaCl *Sodium chloride*
NAMP *nematode-associated molecular pattern*
ng *nanogram*
OD *Optical density*
*Os*CERK1 *Oryza sativa CHITIN ELICITOR RECEPTOR KINASE1*
OXI1 *OXIDATIVE SIGNAL-INDUCIBLE 1*
PA *phosphatidic acid*
ParAMP *parasite-associated molecular patterns*
PBL27 *AVRPPHB SUSCEPTIBLE1 (PBS1)-like 27*
PCR *Polymerase chain reaction*
PDB *Potato dextrose broth*

PDK1 *3'-PHOSPHOINOSITIDE-DEPENDENT PROTEIN KINASE 1*
PGN *peptidoglycan*
pH *Power of hydrogen*
PLA1 *Phospholipase A1*
PLA2 *Phospholipase A2*
PLB *Phospholipase B*
PLC *Phospholipase C*
PLD *Phospholipase D*
PP2A *protein phosphatase type 2A*
PRR *pattern recognition receptors*
Pst *Pseudomonas syringae pv. tomato DC3000*
qRT-PCR..... *Quantitative real time PCR*
RbohD RESPIRATORY BURST OXIDASE HOMOLOGUE D
RbohF *RESPIRATORY BURST OXIDASE HOMOLOG F*
rev *Reverse*
RLCK *receptor like cytoplasmic kinases*
RLK receptor like kinases
RLP *receptor like proteins*
RNA *Ribonucleic acid*
ROS *Reactive oxygen species*
RT *room temperature*
s *Second*
SA *salicylic acid*
SAR *systemic acquired resistance*
SDS *Sodium dodecyl sulfate*
SDS-PAGESodium dodecyl sulfate polyacrylamide gel electrophoresis
SOBIR1*SUPRESSOR OF BIR1*
SOC *Super Optimal Broth with catabolite repression*
TLC *Thin-layer chromatography*
U *Unified atomic mass*
V *Volt*

LIST OF FIGURES

Figure 1-1: Cellular responses in PRR-mediated immunity (adapted from Yu et al. (2017)) 2
Figure 1-2: Reaction scheme for the hydrolysis and transphosphatidylation of phosphatidylcholine by Phospholipase D (Nakazawa et al., 2011) 7
Figure 1-3: Overview of PLD and their biochemical properties (Hong et al., 2016) 8
Figure 3-1: Cell culture-based sample collection for quantitative phosphoproteomic analysis 34
Figure 3-2: GO terms of biological processes for the identified phospho-peptides. 35
Figure 3-3: T-DNA insertion lines of PLDγ family members 42
Figure 3-4: Transcript analysis of PLDγ1, PLDγ2 and PLDγ3 in corresponding T-DNA insertion lines by qRT-PCR 43
Figure 3-5: Mutants of pldγ1-1 were more resistant to Pseudomonas syringae pv. tomato DC3000 infection than pldγ2-1 and pldγ3-1 or wild-type plants. 44
Figure 3-6: Mutants of pldγ1-1 were more resistant to Botrytis cinerea infection compared to wild-type plants 45
Figure 3-7: pldγ1-1 mutants displayed smaller lesions upon infection with Botrytis cinerea 46
Figure 3-8: Infection with Alternaria brassicicola induced more severe infection symptoms on pldγ1-1 than to pldγ2-1 and pldγ3-1 mutant plants 47
Figure 3-9: The oxidative burst was enhanced in pldγ1-1 but not in pldγ2-1 and pldγ3-1 mutants compared to wild-type plants. 49
Figure 3-10: MAP kinases are not differently activated in pldγ1-1 and pldγ1-1 PLDγ1 complementation lines 50
Figure 3-11: Generation of pldγ1-1 PLDγ1 complementation lines 52
Figure 3-12: Complementation of pldγ1-1 with 35S::PLDγ1-GFP led to wild-type infection levels 53
Figure 3-13: Independent complementation of pldγ1-1 with 35S::PLDγ1-GFP showed partial phenotype reversion I Pst infection assays 54
Figure 3-14: Complementation of pldγ1-1 mutant could only reverse elevated ROS levels partially 55
Figure 3-15: Schematic display of working steps using TALENs to generate new mutants 58
Figure 3-16: Phosphatidic acid levels were not changed significantly in pldγ1 mutant lines compared to wild-type plants 60
Figure 3-17: SA-levels are not affected in pldγ1-1 mutants but JA levels are elevated 61
Figure 3-18: PLDγ1 does not interact with FLS2 or BAK1 62
Figure 3-19: PLDγ1 can be found in complex with BIR2 and BIR3 64

LIST OF TABLES

Table 2-1: Cultivation media 12
Table 2-2: Antibiotics 13
Table 2-3: Vectors 13
Table 2-4: Antibodies 15
Table 2-5: Arabidopsis thaliana lines used in this work 16
Table 2-6: Bacterial strains used in this study 18
Table 2-7: Fungal strains used in this study 19
Table 2-8: Taq Polymerase reaction mix 22
Table 2-9: Taq Polymerase thermal profile 22
Table 2-10: Pfu High-Fidelity DNA Polymerase reaction mix 22
Table 2-11: Pfu High-Fidelity DNA Polymerase thermal profile 23
Table 2-12: Q5® High-Fidelity DNA Polymerase reaction mix 23
Table 2-13: Q5® High-Fidelity DNA Polymerase thermal profile 23
Table 2-14: Standard reaction mix for qRT-PCR 24
Table 2-15: Thermal profile for qRT-PCR with melting curve 24
Table 2-16: Standard reaction mixture for 1 SDS-PAGE gel preparation 27
Table 3-1: GO terms of biological processes (GOBP) selection of enriched proteins of regulated phospho-peptides with a p-value < 0.05 36
Table 3-2: Proteins with regulated phospho-peptides in the GOBP category of innate immunity 39
Table 3-3: Putative interactors of CERK1 based on MIND-database analysis (data set from 04.03.2013) 41
Table 3-4: Summary of all ROS-burst experiments performed in pldγ mutants 49
Table 3-5: Overview of complementation lines 51

1 INTRODUCTION

1.1 PLANT INNATE IMMUNITY

1.1.1 General aspects

All forms of life must deal with different stresses. Besides abiotic factors such as climate, nutrition and environment, facing other organisms can be challenging too. Contrary to most other organisms, plants are sessile and have to cope with any stress at a fixed place. Thus, it is even more important for plants to acquire an efficient immune system. For this, plants evolved different defence strategies. The first layer consists of mechanical and chemical barriers. The cuticle, mainly a layer of wax, and the cell wall composed of cellulose and lignin prevent pathogens from entering the cells in a physical way (Malinovsky et al., 2014, Miedes et al., 2014). Moreover, compounds like secondary metabolites present in the plant apoplast often have antimicrobial or antifungal functions and also inhibit infection (Osbourn, 1996). The second layer of immunity compromises the recognition of potential pathogens and a rapid reaction on different cellular levels to fight them (Figure 1-1). These include extracellular alkalization and membrane depolarization, calcium (Ca^{2+})-influxes into the cell, production of reactive oxygen species in the apoplast, activation of mitogen activated protein kinases (MAPK) which leads to phytohormone production, cytoskeleton remodelling, callose deposition at the cell wall, stomata closure and eventually transcriptional adaptation and metabolic changes (Boller and Felix, 2009, Böhm et al., 2014, Yu et al., 2017, Saijo et al., 2018). In order to initiate these defence reactions, the plant needs to sense potential pathogens. Therefore, the plant evolved pattern recognition receptors (PRR) which can recognize specific patterns from molecules deriving from different organisms (Boller and Felix, 2009, Couto and Zipfel, 2016). These molecules can be summarized in a term of danger signals (Gust et al., 2017, Boller and Felix, 2009) which could be categorized into exogenous danger signals originating from microbes (MAMPs: microbe-associated molecular patterns) (Boller and Felix, 2009), herbivores (HAMPs: herbivore-associated molecular patterns) (Mithöfer and Boland, 2008), nematodes (NAMPs: nematode-associated molecular patterns) (Manosalva et al., 2015) or parasitic plants (ParAMPs: parasite-associated molecular patterns) (Kaiser et al., 2015, Hegenauer et al., 2016) and

endogenous danger signals deriving from the plant itself also known as damage-associated molecular patterns (DAMPs) (Rubartelli and Lotze, 2007). Generally, this layer is known as non-host resistance or MTI (MAMP-triggered immunity).

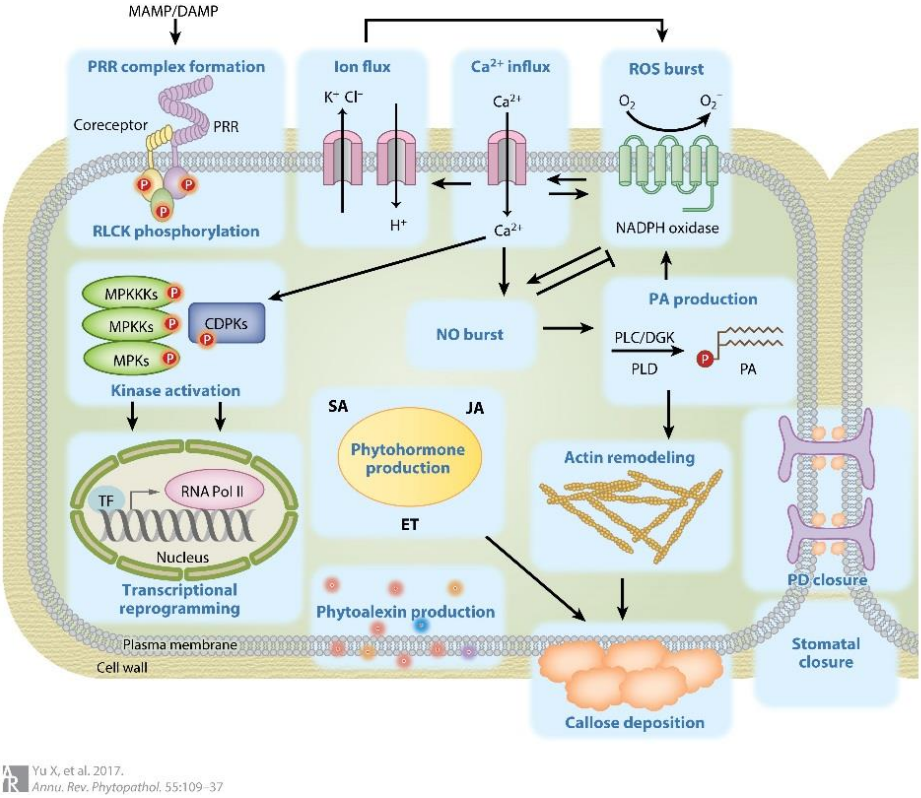

Figure 1-1: Cellular responses in PRR-mediated immunity (adapted from Yu et al. (2017))

Plant cell pattern recognition receptors (PRRs) recognize danger signals leading to a series of cellular and physiological responses. PRR complex formation with co-receptors is accompanied by rapid transphosphorylation in the complex and phosphorylation of receptor-like cytoplasmic kinases (RLCKs). Upon this mitogen-activated protein kinase (MAPK) cascades and calcium-dependent protein kinases (CDPKs) will be activated, which regulate gene transcriptional changes and other cellular responses. Danger signal- triggered immunity include responses such as calcium influx, ion efflux, actin filament remodelling, plasmodesmata (PD) and stomatal closure, callose deposition, and production of reactive oxygen species (ROS), nitride oxide (NO), phosphatidic acid (PA), phytoalexins, and phytohormones. Collectively, these responses contribute to plant resistance against a variety of pathogens. Abbreviations: DGK, diacylglycerol kinase; ET, ethylene; JA, jasmonic acid; PLC, phospholipase C; PLD, phospholipase D; SA, salicylic acid; TF, transcription factor.

According to the model of Jones and Dangl (2006) plants and pathogens fight an evolutionary battle over time. After plants gained non-host resistance, pathogens adapt to the defence mechanisms of the plant and can overcome these barriers by inactivating specifically PRR-mediated immune responses described earlier. For this, pathogens translocate specific virulence factors, called effectors, into the host which are then recognized by plant specific receptors and cause similar responses as in MTI (Boller and Felix, 2009, Spoel and Dong, 2012). This response is also described as Effector Triggered

Immunity (ETI) assuming that effectors and danger signals like MAMPs differ in structural appearance and their recognition mechanisms. However, sometimes this differentiation is difficult and the boundaries between MTI and ETI blur (Thomma et al., 2011). Consequently, effectors are also classified to the category of exogenous danger signals (Gust et al., 2017). Nevertheless, ETI is often associated to a stronger immune response than MTI and eventually leads to a specific pathogen induced resistance in the whole plant while MTI is regarded as an unspecific, broad spectrum disease resistance mechanism (Zhang et al., 2018b). ETI is often accompanied by the hypersensitive response, a reaction which results in cell death and necrosis at the infection site to avoid further spreading of the pathogen (Boller and Felix, 2009). High levels of SA (salicylic acid) are produced and induce systemic effects which are then considered as systemic acquired resistance (SAR) (Zhang et al., 2018b, Fu and Dong, 2013). SAR includes changes in transcription programming and induces SA dependent defence genes. A mobile signal, not SA itself, but methyl salicylic acid, or glycerol-3-phosphate for example are transferred to non-infected areas and induce SA accumulation there (Fu and Dong, 2013). SAR protects the plant from further infection by keeping the plant alert. The molecular mechanisms of SAR and the specific regulation of different hormones like SA, JA (jasmonic acid) and ET (ethylene) are reviewed in detail in several recent articles (Shine et al., 2019, Zhang et al., 2018b, Adam et al., 2018) and will not be described here further.

1.1.2 PRR mediated plant immunity

As described previously the detection of danger signal is crucial for establishing resistance against pathogens. Most of the danger signal receptors are located at the plasma membrane and belong to the classes of receptor like kinases (RLK) and receptor like proteins (RLP) (Saijo et al., 2018, Boutrot and Zipfel, 2017, Böhm et al., 2014). The extracellular domain of the receptors can be structured differently. They can contain Leucine-Rich-Repeat (LRR) motifs recognizing mainly proteinaceous components (Boutrot and Zipfel, 2017), while other motifs like for instance lysin motifs (LysM) recognize N-acetylglucosamine-containing carbohydrate ligands as chitin or peptidoglycan (PGN) (Schlöffel et al., 2019, Boutrot and Zipfel, 2017). In the next two chapters LRR-RLK and LysM-receptors are explained in more detail.

1.1.2.1 Flagellin sensing through LRR-RLKs – recognition and regulation

FLAGELLIN SENSITIVE 2 (FLS2) might be one of the best investigated receptors within PRR-mediated immunity in plants. This LRR-RLK found by Gómez-Gómez and Boller (2000) contains 24 LRRs in its ectodomain, a single transmembrane domain and an intracellular kinase domain. FLS2 can bind the 22 amino acid long epitope flg22 from the bacterial flagellum protein flagellin. Upon elicitor binding, BRASSINOSTEROID INSENSITIVE 1 (BRI1)-ASSOCIATED KINASE 1 (BAK1) (Chinchilla et al., 2009), another LRR-RLK, is recruited to build heterodimers with FLS2 (Chinchilla et al., 2007, Heese et al., 2007) which initiates downstream signalling. Transphosphorylation events between the two kinases lead to rapid activation and phosphorylation of RECEPTOR LIKE CYTOPLASMIC KINASES (RLCKs), like BOTRYTIS-INDUCED KINASE1 (BIK1). Then, BIK1 transphosphorylates FLS2 and BAK1 which results in dissociation of BIK1 from these two kinases (Lu et al., 2010) and mediation of downstream signalling, like activation of NADPH OXIDASE RESPIRATORY BURST OXIDASE HOMOLOG D (RBOHD) (Kadota et al., 2014) and MAP – kinase signalling cascades (Lin et al., 2014). RBOHD is mainly responsible for the ROS burst (Kadota et al., 2014) whereas MAP-kinase signalling leads to the activation of phytohormones, transcription factors and induction of defence related genes (Thulasi Devendrakumar et al., 2018b). After BIK1 dissociated and activated downstream signalling, endocytosis of FLS2 and subsequent degradation by several U-Box E3 ligases is conducted (Lu et al., 2011). Ligand induced PRRs such as FLS2 are in a steady turn-over process and recent findings show that FLS2 is localized in nanoclusters with BIK1 and the RLCK BRASSINOSTEROID SIGNALING KINASE 1 (BSK1) at the plasma membrane acting as preformed signalling platforms to ensure quick availability of all reaction components (Bücherl et al., 2017). Since the activation of FLS2 is crucial for establishing a successful defence but thereby affects other regulations in the plant, for example growth (Wan et al., 2018, Wang, 2012), it is necessary to regulate this system very tightly. Thus, in an unelicited status BAK1 and FLS2 are prevented from binding to each other by the LRR-pseudo kinase BAK1-INTERACTING RECEPTOR-LIKE KINASE 2 (BIR2) (Halter et al., 2014) and its closest homolog BIR3 (Imkampe et al., 2017) which bind to BAK1 in an unstimulated situation. BIR3 can also bind the receptor FLS2 itself and prevents BAK1 interaction. In response to flg22 stimulus, both pseudo kinases dissociate from BAK1 and FLS2 and the FLS2-BAK1-complex can be formed. BIR1

(BAK1-INTERACTING RECEPTOR-LIKE KINASE 1) is also involved in plant immunity especially as a negative regulator in cell death responses. In the absence of BIR1, BAK1 binds to SUPRESSOR OF BIR1 (SOBIR1) (Liu et al., 2016) which might indicate that BIR1 sequesters BAK1 and prevents BAK1 - SOBIR1 interaction (Ma et al., 2017). SOBIR1 is important for downstream signalling of receptor like proteins (RLP) lacking a functional kinase (Gust and Felix, 2014, Liebrand et al., 2014).

1.1.2.2 Chitin and Peptidoglycan recognition through LysM-receptor kinases

Other well characterized receptor proteins are the LysM-Receptor Kinases (LYK), of which there are five in *Arabidopsis.* They consist of two to three extracellular lysin motifs, a transmembrane domain and an intracellular kinase domain (Schlöffel et al., 2019, Bücherl et al., 2017, Gust et al., 2012). Among them the CHITIN ELICITOR RECEPTOR KINASE 1 (CERK1) and LYSIN MOTIF RECEPTOR KINASE 5 (LYK5) are involved in chitin perception. First it was assumed that CERK1 is the chitin receptor in *Arabidopsis*. CERK1 builds homodimers bridged by chitin octamers which leads to transphosphorylation of the kinase domains (Liu et al., 2012b). However, recent findings show that the pseudo-kinase LYK5 has a much higher affinity to bind chitin octamers and it was anticipated that LYK5 is the major chitin receptor (Cao et al., 2014). Nonetheless, *lyk5* mutants were only partially compromised in chitin induced innate immunity but did not show a complete loss. Only double mutants of *LYK5* and its close homolog *LYK4* were unable to trigger chitin induced immune response (Cao et al., 2014) , indicating that also LYK4 has a major impact in the recognition of chitin molecules . Although CERK1 has not such a high affinity to bind chitin, mutation in CERK1 leads to a full loss of chitin-triggered immunity (Petutschnig et al., 2010, Wan et al., 2008, Miya et al., 2007). This supports the assumption that CERK1 works as an essential adaptor protein in chitin induced immunity most likely due to its functional kinase domain. Chitin signalling was first studied in rice (*Oryza sativa*) with a similar signal cascade as in *Arabidopsis*. The functional homolog of LYK5 in rice is the LysM-RLP CHITIN ELICITOR-BINDING PROTEIN (CEBiP) which is the major chitin receptor in this plant (Kaku et al., 2006). While binding chitin oligomers, two CEBiP-molecules form a homodimer with the chitin fragment in between (Hayafune et al., 2014). Subsequently, *Oryza sativa* CHITIN ELICITOR RECEPTOR KINASE1 (*Os*CERK1) is recruited to the complex and mediates downstream signalling (Shimizu et al., 2010). The downstream signalling cascade is not fully understood yet,

but it is known that RLCKs are phosphorylated by CERK1 (Liang and Zhou, 2018). In *Arabidopsis,* these are for instance BIK1 (Zhang et al., 2010) and PBL27 (AVRPPHB SUSCEPTIBLE1 (PBS1)-LIKE 27) (Shinya et al., 2014) which was recently shown to work as the MAPKKK (MAP kinase kinase kinase) in the MAP-kinase signalling cascade (Yamada et al., 2016). Also, the RLK1-INTERACTING KINASE 1 (LIK1) was found to be phosphorylated by CERK1 and to negatively regulate this pathway (Le et al., 2014). LysM-Proteins are not only involved in chitin recognition but also important for peptidoglycan sensing (Schlöffel et al., 2019, Saijo et al., 2018, Gust et al., 2012). Peptidoglycan is a glycan polymer of alternating β (1,4)-linked N-acetylglucosamine (GlcNAc) and N-acetylmuramic acid (MurNAc) residues cross-linked by short peptide bridges (Gust et al., 2012). It is an important compound of the bacterial cell wall and the *Arabidopsis* LYSOZYME-LIKE ACTIVITY 1 (LYS1) (Liu et al., 2014) is able to break down the complex PGN structure in parts which then can be detected by the LysM-RPs LYM1 (LYSM-CONTAINING RECEPTOR PROTEIN 1) and LYM3 (Willmann et al., 2011). LYM1 and LYM3 belong to the group of LysM-receptor proteins lacking an intracellular kinase domain but similar to CERK1 containing three LysM-motifs. Therefore, they cannot transmit the signal and depend on CERK1 which is not able to bind PGN but binds to the LYM-complex to transmit the signal which was shown for the rice homologs OsLYP4 (*Oryza sativa* LysM PROTEIN 4) and OsLYP6 (*Oryza sativa* LysM PROTEIN 6) (Ao et al., 2014, Liu et al., 2012a). Whether and how chitin and PGN perception differ in downstream signalling is currently not clear and requires further investigation.

1.2 PHOSPHOLIPASES

1.2.1 General overview

Cell membranes of almost all organisms are constituted of three major lipids: Phospholipids, glycolipids and cholesterol/phytosterols. Phospholipids are divided into glycerophospholipids and sphingolipids. Glycerophospholipids are the most common structure in biological membranes and consists of two fatty acids bound to a glycerol backbone to which a phosphorylated alcohol is attached. Common alcohol residues are serine, ethanolamine, choline, glycerol, and the inositol. (Berg et al., 2018). Rearrangement of cell membranes is an essential process for living organisms. In this process phospholipases, beside lots of other proteins, are involved. Phospholipases

hydrolyse the bonds in phospholipids. According to their side of action they can be categorized into 4 major classes. Phospholipases A1 and 2 (PLA1 and PLA2)cleave one of the fatty acid chains bound to the glycerol molecule. Phospholipase B (PLB) can hydrolyse the bonds of both acyl groups and is also known as lysophospholipase. The glycerophosphate bond is hydrolysed by Phospholipase C (PLC), whereas Phospholipase D (PLD) removes the head group of the phospholipid (Aloulou et al., 2012). In plants only PLA1, PLA2, PLC and PLD are present (Wang et al., 2012). Within each group there are different subgroups which have different substrate specificities, cofactor requirements or reaction conditions (Qin and Wang, 2002). This study will mainly focus on PLDs, which hydrolyse the phosphodiesther bond on the headgroup side of the phospholipid. This reaction leads to the generation of phosphatidic acid (PA) and a soluble headgroup. Moreover, PLDs are able to catalyse the transphosphatidylation reaction in which a PLD transfers the phosphatidyl group to a primary alcohol, such as ethanol or methanol (Yang et al., 1967). In Figure 1-2 an example of PLD action on phosphatidylcholine is shown.

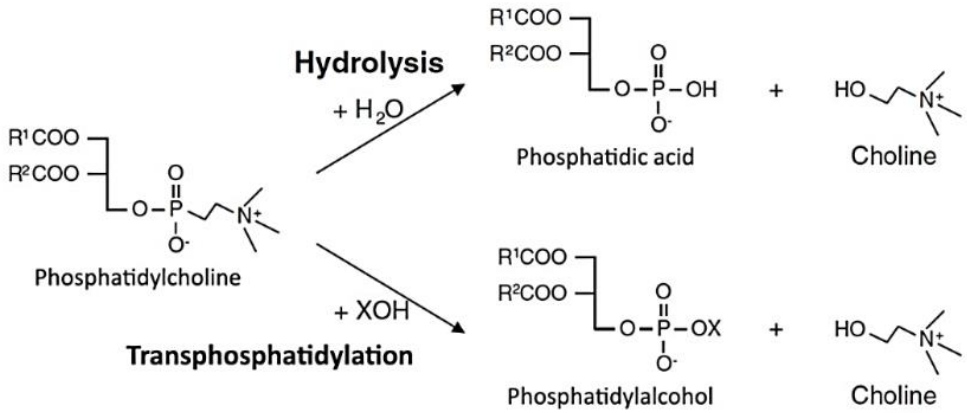

Figure 1-2: Reaction scheme for the hydrolysis and transphosphatidylation of phosphatidylcholine by Phospholipase D (Nakazawa et al., 2011)

Phospholipase D hydrolyses phosphatidylcholine in an aqueous solution into phosphatidic acid and choline. In the presence of primary alcohols, the phosphatidyl group is transferred onto the alcohol and generates a phosphatidylalcohol plus choline.

Arabidopsis thaliana has 12 PLDs grouped in several subfamilies as shown in Figure 1-3. PLDs are involved in lots of processes in the plant. For instance, PLDα was shown to mediate osmotic equilibrium in the plant by responding to drought (Sang et al., 2001), salt stress (Hong et al., 2008) and cold stress (Li et al., 2008). PLDδ was shown to be involved in freezing tolerance (Li et al., 2004) as well as in drought regulation (Katagiri

et al., 2001) but also has an impact in cytoskeleton organization (Gardiner et al., 2001). Nitrate and phosphorous household are regulated by PLDε and PLDζ, respectively (Cruz-Ramirez et al., 2006, Hong et al., 2009, Li et al., 2006). PLDζ was also found in vesicular trafficking and auxin response (Li and Xue, 2007). Beside all those important functions, except for PLDε and PLDζ, all other families of PLDs were somehow associated with plant immunity, as described in section 1.2.2 in more detail.

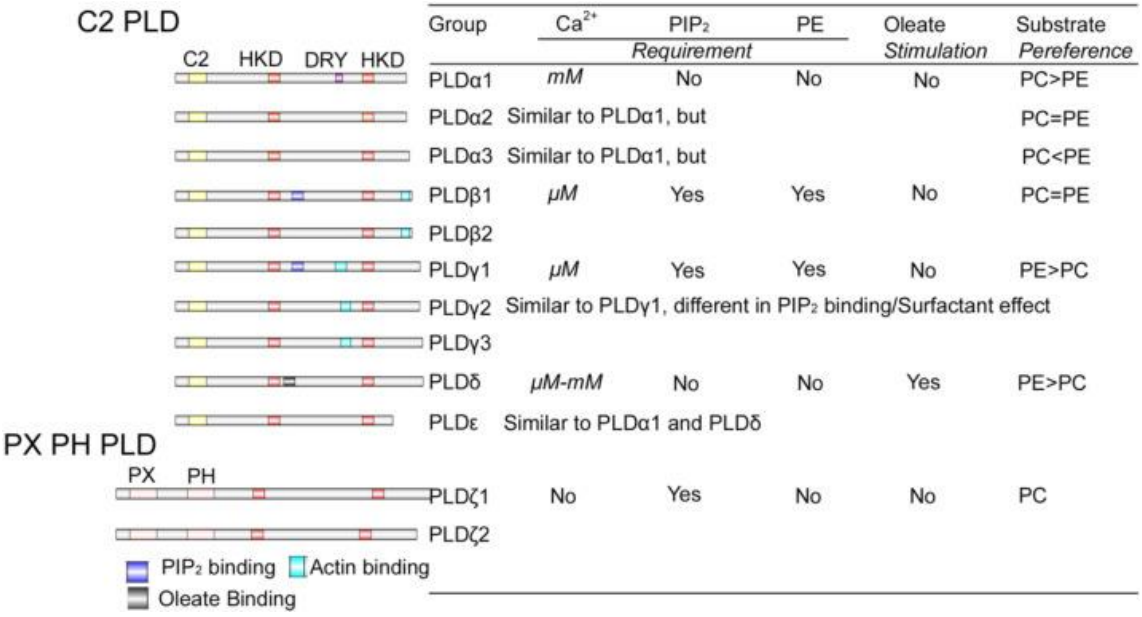

Group	Ca^{2+}	PIP_2	PE	Oleate	Substrate
	Requirement			*Stimulation*	*Pereference*
PLDα1	*mM*	No	No	No	PC>PE
PLDα2	Similar to PLDα1, but				PC=PE
PLDα3	Similar to PLDα1, but				PC<PE
PLDβ1	*μM*	Yes	Yes	No	PC=PE
PLDβ2					
PLDγ1	*μM*	Yes	Yes	No	PE>PC
PLDγ2	Similar to PLDγ1, different in PIP_2 binding/Surfactant effect				
PLDγ3					
PLDδ	*μM-mM*	No	No	Yes	PE>PC
PLDε	Similar to PLDα1 and PLDδ				
PLDζ1	No	Yes	No	No	PC
PLDζ2					

Figure 1-3: Overview of PLD and their biochemical properties (Hong et al., 2016)
Arabidopsis PLD domain structures and distinguishable biochemical properties. PC, phosphatidylcholine; PE, phosphatidylethanolamine; and PIP2, phosphatidylinositol 4,5-bisphosphate.

1.2.2 PLDs and the role of PA in plant immunity

Beside the fields described before, PLDs play an important role in plant immunity and disease resistance. In the past several years, PLDs were correlated and shown to be participating in various immunity signalling pathways (Zhao, 2015). Some of them are described in the next sections.

1.2.2.1 PLDα1 is involved in G-protein-mediated defence responses and beneficial interactions

PLDα1 was found to interfere with G-proteins at the plasma membrane. Upon infection, PLDα1 is translocated to the plasma membrane (Elmore et al., 2012) and binds to the Gα-protein (Zhao and Wang, 2013). As described in Zhong et al. (2018) G-proteins are important signalling components in LRR- RLP/RLK downstream signalling. The

interaction of PLDα1 with G-proteins could be another level of immune response regulation (Zhao, 2015). The exact mechanism and the impact of this interaction remains elusive. Moreover, PLDα1 was also found in the regulation of the growth promoting *Piriformospora indica* pathway. PA generated by PLDα1 activates the OXIDATIVE SIGNAL-INDUCIBLE 1 (OXI1) pathway which was shown to be essential for *Piriformospora indica* growth promotion (Camehl et al., 2011).

1.2.2.2 PLDβ works as negative regulator in plant immunity on different signalling levels

PLDβ is known to be a negative regulator in plant immunity in various plant species. Elevated defence responses upon elicitation in tomato cell suspension culture (Bargmann et al., 2006) or permanently activated immune responses in rice (Yamaguchi et al., 2009) were the result of lacking functional PLDβ. Similar results were obtained in *Arabidopsis PLDβ* deficient plants which were more resistant to *Pseudomonas syringae* pv. *tomato* DC3000 (*Pst)* infection, accumulated more ROS and showed elevated SA dependent gene expression whereas JA responses were down-regulated (Zhao et al., 2013a).

PLDβ was also shown to be an actin binding protein (Kusner et al., 2003). But more importantly, PLDβ-produced PA binds to the actin binding protein *Arabidopsis thaliana* CAPPING PROTEIN (AtCP) and induces acting polymerization (Huang et al., 2006). Cytoskeleton remodelling is a crucial response upon danger signal sensing (Li et al., 2012). Without infection AtCP binds to actin and prevents actin remodelling and filament growth (Li et al., 2012). Upon infection PLDβ produces PA which then binds to AtCP and induces the release of the protein from the actin molecules. Therefore, the cytoskeleton can be rearranged to support fast defence responses

1.2.2.3 PLDδ is an important player in fungal resistance and PLDζ is a negative regulator in MTI

In 2013, Pinosa et al. (2013) showed that PLDδ is directly involved in defence reactions against the fungal pathogen *Blumeria graminis* f. sp. *hordei* (*Bgh*). Mutation in *PLDδ* led to a higher penetration rate of *Bgh* in corresponding mutant plants. Recent findings indicate that not only PLDδ but also PLDα1 are important key players in fungal

resistance. They have opposite effects in establishing fungal resistance and work together in a SA/JA- independent pathway (Zhang et al., 2018a).

PLDζ was firstly found in correlation with vesicle trafficking and cytoskeleton formation (Zhao, 2015). Later studies showed then that PLDζ-produced PA binds to PP2A (PROTEIN PHOSPHATASE TYPE 2A) and BZR1 (BRASSINAZOLE RESISTANT1), which are parts of the brassinosteroid pathways, and works there as a negative regulator preventing activation of downstream gene expression triggered by RLK-mediated signalling (Gao et al., 2013, Wu et al., 2014).

1.2.2.4 PLDγ subfamily is mostly unknown to be involved in plant innate immunity

While for the other isoforms various information are available, for the subfamily of PLDγ very little is known. One study is showing that PLDγ1 is involved in establishing aluminium tolerance (Zhao et al., 2011). Further PLDγ1 was shown to be induced transcriptionally by pathogen infection (de Torres Zabela et al., 2002) and is then recruited to the plasma membrane (Elmore et al., 2012). Apart from this, very little information about PLDγ1 is available. In a study by Pinosa et al. (2013) PLDγ-deficient plants together with mutants for all other PLD isoforms were tested in infection assays using the fungus *Bgh,* but *pldγ* mutants never showed a phenotype that was different from the wild type response. Nevertheless, the family of PLDγs is interesting: PLDγ isoforms share up to 95 % sequence similarities (Qin and Wang, 2002) presumably a gene duplication (Qin et al., 2006). Although the three isoforms are very similar in sequence, the activity requirements in *in vitro* assays differ indicating that PLDγ isoforms are differently regulated and activated (Qin et al., 2006). However, these results might just give a putative explanation for the function of the different isoforms since the biological function of them remains unclear until now. Therefore, this study addresses the question of the function of PLDγ proteins, especially PLDγ1, in plant innate immunity.

1.3 AIMS OF THIS STUDY

Downstream signalling of PRR mediated plant immunity through RLKs like FLS2 or CERK1 is still not understood completely. Thus, using phosphoproteomic- and database analyses new candidates were searched and the three proteins of PLD gamma were focused for further investigation. As mentioned before PLDγ -proteins were found to be involved somehow in plant innate immunity. However, the exact role and impact of PLDγ1 in immune signalling was not known or described before. Therefore, the main aim of this work was to study the function of the proteins PLDγ1, PLDγ2 and PLDγ3 within plant innate immunity using a reverse genetic approach. Gen-deficient plant lines of PLDγ1, PLDγ2 and PLDγ3 but also new generated complementation lines with overexpressing PLDγ1 in the background of *pldγ1-1* mutants were tested in pathogen infection assays and early immune responses. Also, the effect of missing PLDγ1 and its biochemical product PA was studied. Eventually, transient expressed PLDγ1 was tested in interaction assays with known proteins involved in plant innate immunity to elucidate the function of PLDγ1.

2 MATERIAL AND METHODS

2.1 MATERIAL

2.1.1 General consumables

Chemicals were purchased from following companies: Sigma-Aldrich (Taufkirchen), Carl Roth (Karlsruhe), Merck (Darmstadt), Qiagen (Hilden), Invitrogen (Karlsruhe), Formedium (Hunstanton, UK), Duchefa (Haarlem, Netherlands), Molecular Probes (Leiden, Netherlands), Fluka (Buchs, Switzerland) and BD (Sparks, USA). Restriction enzymes, ligases and DNA modification enzymes were used from Thermo Scientific (Waltham) and New England Biolabs (Beverly, USA). Oligonucleotides were ordered from Eurofins MWG Operon (Ebersberg). Kits were purchased from SLG (Gauting).

2.2 MEDIA AND ANTIBIOTICS

All media used in this work are listed in Table 2-1. Solid media were prepared by adding agar-agar for bacterial cultivation media, select agar for plant media. All media were autoclaved (121 °C, 20 min) before use. For resistance-based selection of microbes, antibiotics (Table 2-2) were added at the indicated concentrations after autoclaving.

Table 2-1: Cultivation media

Medium	Ingredients for 1 L
LB	10 g bacto- tryptone, 5 g yeast extract, 5 g NaCl, pH 7.0
½ MS	2.2 g MS (Duchefa), pH 5.7 (KOH)
King's B	20 g glycerol, 40 g proteose pepton No. 3, addition of sterile 0,1 % (v/v) $MgSO_4$ and KH_2PO_4 after autoclaving
PDB	24g PDB (Formedium), pH 5.8 (NaOH)
SOC	20 g tryptone, 5 g yeast extract, 0.5 g NaCl, 0,19 g KCl and 3.6 g D-Glucose after autoclaving

Table 2-2: Antibiotics

Antibiotic	Final concentration	Solvent
Carbenicillin	50 µg/mL	water
Gentamycin	25 µg/mL	water
Hygromycin	50 µg/mL	water
Kanamycin	50 µg/mL	water
Rifampicin	50 µg/mL	DMSO
Spectinomycin	100 µg/mL	water

2.2.1 Vectors

In Table 2-3 the vectors used in this work are listed.

Table 2-3: Vectors

Vectors	Characteristics	reference
pCR8/GW/TOPO	Ori Puc, rrnB, T2, rrnB, T1, attP1, attP2, ccdB, Sm/Spr	Thermo Scientific
pGBKT7/GW	2a ori f1ori pUC ori attR1 and attR2 ccdB Cmr pADH1 TT7 & ADH1 GAL4 BD c-Myc Kanr TRP1	RfB/Invitrogen; Postel et al. (2010)
pGADT7/GW	2a ori pUC ori attR1 and attR2 ccdB Cmr pADH1 tADH1 GAL4 AD HA LEU2 Ampr	RfB/Invitrogen; Postel et al. (2010)
pB7YWG2/GW	35S promoter, YFP-fusion at the C-terminus	VIB, Ghent
pGWB14	p35S, t35S, attR1, attR2, ccdB, Kanr, Hygr, 3x-HA	Nakagawa et al. (2007)
pGWB17	p35S, t35S, attR1, attR2, ccdB, Kanr, Hygr, 4x-Myc	Nakagawa et al. (2007)
pGWB5	p35S, t35S, attR1, attR2, ccdB, Kanr, Hygr, GFP (green fluorescent protein)	Nakagawa et al. (2007)

2.2.2 Primers

Name	sequence 5`→ 3`	Characteristics
AtRuBisco-QF	GCAAGTGTTGGGTTCAAAGCTGGTG	qRT-PCR Arabidopsis RuBisco forward
AtRuBisco-QR	CCAGGTTGAGGAGTTACTCGGAATGCTG	qRT-PCR Arabidopsis RuBisco reverse
Basta_F	ATGAGCCCAGAACGACGCC	Selecetion marker BASTA forward
Basta_R	ATCTCGGTGACGGGCAGGAC	Selecetion marker BASTA reverse
Bc-actin-qF	CCTCACGCCATTGCTCGTGT	qRT-PCR Botrytis cinerea Actin forward
Bc-actin-qR	TTTCACGCTCGGCAGTGGTGG	qRT-PCR Botrytis cinerea Actin reverse
BIR2_fw	ATGAAAGAGATCGGCTCAAAACC	BIR2 forward
BIR2-Stop_rv	CACTTTCTCGTTCTCTTGCGTG	BIR2 reverse without Stop codon
BIR3_fw	ATGAAGAAGATCTTCATCACACTC	BIR2 forward
BIR3-Stop_rv	AGCTTCTTGTTTGTTGAAGAC	BIR3 reverse without stop codon
ef1a-100-f	GAGGCAGACTGTTGCAGTCG	qRT-PCR EF1α forward
ef1a-100-r	CACTTCGCACCCTTCTTGA	qRT-PCR EF1α reverse
EF1a-as	TTGATCTGGTCAAGAGCCTCAAG	EF1α reverese
EF1a-s	TCACATCAACATTGTGGTCATTGG	EF1α forward
FRK1-100-f	AGCGGTCAGATTTCAACAGT	qRT-PCR FRK1 forward
FRK1-100-r	AAGACTATAAACATCACTCT	qRT-PCR FRK1 reverse
GABI-Kat LB	CCCATTTGGACGTGAATGTAGACAC	GABI LB primer
GT-AT1G77460-f	CGGTTAAGATAAAACTGTGAATAG	Genotyping promotor region AT1G77460 forward
GT-AT1G77460-r	CTTTGTTTGGGTCTCCATTTG	Genotyping promotor region AT1G77460 reverse
GT-AT2G31130-f	GATATCAAATCTTATATATTGATTTTGATTGG	Genotyping promotor region AT2G31130 forward
GT-AT2G31130-r	GAGAAATTTCACGACTCGG	Genotyping promotor region AT2G31130 reverse
GT-PLDg1-LP	GGTGGGTTGCTAGTTTTTCG	Genotyping Salk_066687C GABI-Kat 264A03
GT-PLDg1-RP	CATCATGTTGCTATTCTCTGCTG	Genotyping Salk_066687C GABI-Kat 264A03
GT-PLDg2-LP	TGGAACTGGATGCCACTATTC	Genotyping Salk_078226
GT-PLDg2-RP	GGTTCCAACCTCTCTGTTTCC	Genotyping Salk_078226
GT-PLDg3-LP	GGTTGTTTCAGTTGCATTTCA	Genotyping Salk_084335
GT-PLDg3-RP	GAACCCATTAAGGCAAAATCG	Genotyping Salk_084335
PLDg1-fw	ATGGCGTATCATCCGGCTTATAC	PLDγ1 forward
PLDg1-rv	TCATATGGTGAGGTTTTCTTGTAGTG	PLDγ1 reverse
PLDg1-wos-rv	TATGGTGAGGTTTTCTTGTAGTG	PLDγ1 reverse without stop codon
PLDg2-fw	ATGTCAATGGGAGGAGGGTCAAAC	PLDγ2 forward
PLDg2-rv	TCAGATGGTGAGGTTTTCTTGTAGAGTAAG	PLDγ2 reverse
PLDg2-wos-rv	GATGGTGAGGTTTTCTTGTAGAGTAAG	PLDγ2 reverse without stop codon
PLDg3-fw	ATGGCGTATCATCCAGTTTATAAC	PLDγ3 forward
PLDg3-rv	TCATATGGTGAGGTTTTCTTCTACTA	PLDγ3 reverse
PLDg3-wos-rv	TATGGTGAGGTTTTCTTCTACTA	PLDγ3 reverse without stop codon
qRT-PLDg1-fw1	ACTTTTTCTGTCTTGGAACCAGAG	qRT-PCR PLDγ1 forward
qRT-PLDg1-rv1	GCATTTGCATTTGCGTTTGGCTGA	qRT-PCR PLDγ1 reverse
qRT-PLDg2-fw1	TGCTCCCTTTGCGTCTAGGTTTCT	qRT-PCR PLDγ2 forward
qRT-PLDg2-rv1	TCTATTCCAGCAGCAACACCACGA	qRT-PCR PLDγ2 reverse
qRT-PLDg3-fw1	GGTTTCCATAACACCCTTGTTGGT	qRT-PCR PLDγ3 forward
qRT-PLDg3-rv1	TTCTCACCATCCACTTTATGATTCCT	qRT-PCR PLDγ3 reverse
SALK LBb1.3	ATTTTGCCGATTTCGGAAC	Salk LB primer

2.2.3 Antibodies

During this work the antibodies listed in Table 2-4 were used.

Table 2-4: Antibodies

Antibody	Produced in	Working solution	company
α-Myc	rabbit	1:5000	Sigma-Aldrich
α-HA	mouse	1:5000	Sigma-Aldrich
α-GFP	goat	1:10 000	Sicgen
α-rabbit lgG, horseradish peroxidase conjugated	goat	1:10 000	Sigma-Aldrich
α-mouse lgG, horseradish peroxidase conjugated	rabbit	1:10 000	Sigma-Aldrich
α-goat lgG, horseradish peroxidase conjugated	rabbit	1:10 000	Sigma-Aldrich

2.3 PLANTS, BACTERIA AND FUNGI – CULTIVATION AND TRANSFORMATION

2.3.1 Plant lines and cultivation

In Table 2-5 all the plant lines used in this work are specified.

Table 2-5: Arabidopsis thaliana lines used in this work

Name	Locus	Line	Properties
Col-0			
pldγ1-1	At4g11850	Salk_066687C	T-DNA insertion
pldγ1-2	At4g11850	GABI-Kat 264A03	T-DNA insertion
pldγ2-1	At4g11830	Salk_078226	T-DNA insertion
pldγ3-1	At4g11840	Salk_084335	T-DNA insertion
cerk1-2	At3g21630	GABI_096F09	T-DNA insertion
bir2-1	At3g28450	GK-793F12	T-DNA insertion
pldγ1-1-PLDγ1 1	pGWB5-PLDγ1 transformed in *pldγ1-1*At4g11850	12-4-3-2	stable transformation
pldγ1-1-PLDγ1 2	pGWB5-PLDγ1 transformed in *pldγ1-1*	12-8-2-2	stable transformation
pldγ1-1-PLDγ1 3	pGWB5-PLDγ1 transformed in *pldγ1-1*	12-8-4-4	stable transformation
pldγ1-1-PLDγ1 4	pGWB5-PLDγ1 transformed in *pldγ1-1*	12-9-1-3	stable transformation
pldγ1-1-bc	At4g11850	Salk_066687C/Col-0 T3	Crossing *pldγ1-1* with Col-0

All plants were grown on soil under short day conditions (8 h light, 150 µmol/cm^{2}s light, 40-60 % humidity, 22 °C) and used for the experiments at an age of 5-6 weeks. Plants used for infection assays with *Pseudomonas syringae*, *Botrytis cinerea*, and *Alternaria brassicicola* were grown under translucent cover. For seedling assays, *Arabidopsis* plants were surface sterilized with chlorine gas. Therefore, a small amount of seeds was incubated with a beaker containing 50 mL (v/v) of 12 % sodium-hypochlorite solution and 1.5 mL (v/v) 37 % HCl in a desiccator for 4-5 h. Before transferring the seeds onto ½ MS-agar-plates the samples were placed open under a sterile bench for 30 min to allow evaporation of remaining chlorine gas. Seedling were then grown under long-day conditions (16 h light) on ½ MS-agar for 7-10 days. *Nicotiana benthamiana* plants were

grown in the greenhouse (16 h light, 22 °C). *Arabidopsis* suspension cell cultures were grown in MS medium (4.41 g/L MS salt, 6 % sucrose, 50 mg/L MES, 2mg/L 2, 4-D) at 150 rpm and sub-cultured every week.

2.3.2 Stable transformation of Arabidopsis thaliana

Stable transformed *Arabidopsis* lines were generated by using the floral dip method described in Clough and Bent (1998). *Agrobacteria* cell culture grown for 2 days in 28 °C were harvested and suspended in 5 % (w/v) sucrose, 0.01 % (v/v) Silwet. *Arabidopsis* plants with numerous immature floral buds were dipped into the cell suspension for several min. After floral dipping the plants were kept in a high humidity surrounding for one night. Successful transformed seed were selected by using either 0.2 % BASTA or hygromycin. Hygromycin selection of transformed plants was performed as outlined in Harrison et al. (2006).

2.3.3 Transient transformation of Nicotiana benthamiana

Transient protein expression in *N. benthamiana* was mediated by *Agrobacterium tumefaciens*. The bacterial strains carrying the appropriate expression constructs were cultured as described in section 2.3.4. After harvesting the cells by centrifugation for 10 min at 3,500 rpm, the pellet was washed for two times with 10 mM $MgCl_2$. The density of the culture was adjusted to an OD_{600} of 1 with 10 mM $MgCl_2$ and 150 µM acetosyringone. The bacterial suspension was then incubated at room temperature (RT) for 2 hours. Afterwards, the bacteria were mixed 1:1 with a suspension of bacteria carrying an p19 expression construct (Voinnet et al., 2003) and adjusted to an OD_{600} of 0.2. The mixture was infiltrated into the leaves of 3-week-old *Nicotiana benthamiana* plants. Leaf tissue was analysed 2-3 days post infection for the presence of the protein and used in protein-protein interaction studies (2.5.5).

2.3.4 Bacteria strains and cultivation

Bacterial strains used in this work are shown in Table 2-6.

Table 2-6: Bacterial strains used in this study

Species	Strain	Genotype	Reference
Escherichia coli	DH5α	fhuA2 lacΔU169 phoA glnV44 ϕ80' lacZΔM15 gyrA96 recA1 relA1 endA1 thi-1 hsdR17	(Hanahan, 1983)
Escherichia coli	One Shot® TOP10	F^- *mcr*A Δ(*mrr-hsd*RMS-*mcr*BC) ϕ 80*lac*Z (M15 Δ (*lac*X74 *rec*A1 *ara*D139 Δ (*ara-leu*)7697 *gal*U *gal*K *rps*L (Str^R) *end*A1 *nup*G	
Escherichia coli	One Shot® ccdB Survival™ 2 T1R	F^- *mcr*A Δ(*mrr-hsd*RMS-*mcr*BC) ϕ 80*lac*Z Δ M15 Δ *lac*X74 *rec*A1 *ara* Δ 139 Δ *(ara-leu)*7697 *gal*U *gal*K *rps*L (Str^R) *end*A1 *nup*G *fhuA::IS2*	
Agrobacterium tumefaciens	GV3101::pmP90	T-DNA- vir+ rif^R, pMP90 gen^R	(Koncz and Schell, 1986)
Pseudomonas syringae pv. tomato	DC3000	rif^R	

2.3.5 Transformation of chemical competent bacteria

Chemical competent E. coli Dh5α was prepared according to Inoue et al. (1990). Top10 One Shot cells were obtained from Thermo Scientific. 50 µL of competent cells were incubated with plasmid DNA for 15 min on ice and heat shocked in 42 °C for 45 s. Afterwards 250 µL SOC-medium was added and to the cells and shaken at 37 °C for 1 h. transformed bacteria were selected on LB-Agar plates with the respective antibiotics.

2.3.6 Transformation of electro-competent Agrobacterium tumefaciens

For the transformation of electro-competent *Agrobacterium tumefaciens* (section 2.3.7), 40 µL of cells were thawed on ice, mixed with 100 ng of plasmid DNA and stored on ice in an electroporation cuvette (1 mm electrode distance) for 15 min. The cells were pulsed one time with 1500V for 5 ms using an Electroporator2510 (Eppendorf). Directly after electroporation 600 µL LB-medium was added to the cuvette. The cells were transferred to a fresh reaction tube and incubated for 4 h at 28 °C with 180 rpm shaking. The bacteria cells were plated on selective LB-agar-plates and incubated for 48 h at 28 °C until colonies were visible.

2.3.7 Preparation of electro competent Agrobacterium tumefaciens cells

To generate electro competent *Agrobacterium tumefaciens* cells 500 mL LB medium with the corresponding antibiotics was inoculated with 500 µL of a fresh grown 5 mL bacteria culture and grown until a density of OD_{600} 0.5. Subsequent the cells were spun down at 4 °C with 3,500 rpm for 15 min and washed with 200 mL ice cold ddH_2O for the first time. After another centrifugation of 15 min with 3,500 rpm at 4 °C the cells were washed in 100 mL of ice cold ddH_2O for the second time and centrifuged as mentioned before. The cells were suspended in 4 mL of ice-cold 10 % (v/v) glycerol and centrifuged again as described above. In the final step the cells are taken into a volume of 1-1.5 mL of ice-cold 10 % (v/v) glycerol and aliquots of 40 µL were frozen in liquid nitrogen and stored at -80 °C.

2.3.8 Fungal strains

In Table 2-7 the fungal strains are showed.

Table 2-7: Fungal strains used in this study

Species	Strain	Reference
Alternaria brassicicola	MUCL 20297	Thomma et al. (1999)
Botrytis cinerea	B05-10	

2.4 MOLECULAR BIOLOGY METHODS

2.4.1 Plasmid DNA extraction

Bacterial plasmid DNA was extracted from 3 mL inoculated bacteria cell culture, grown overnight, using the purification kit HiYield® Plasmid Mini Kit (SLG) as stated in the manufacturer's protocol.

2.4.2 Genomic DNA extraction from plants

DNA was extracted from fresh or frozen plant material according to Edwards et al. (1991). Plant material was grounded in 300 µL extraction buffer (200 mM Tris/HCl, pH 7.5, 250 mM NaCl, 25 mM EDTA pH 8.0, 0.5 % (w/v) SDS). Afterwards 300 µL isopropanol was added and incubated for 10 min on RT. Samples were centrifuged for 15 min with

14,000 rpm to precipitated DNA. DNA pellet was washed with 70 % ethanol for two times, air dried and dissolved in 100 µL nuclease free water.

2.4.3 Fungal DNA extraction

Fungal biomass quantification was performed by extracting DNA from infected leave material. Therefore, 3 infected leaves/plant (see section 2.6.2) were frozen in a screw vials containing ceramic beads mix (2 mm and 0.5 mm diameter) in liquid nitrogen. Tissue was homogenised using Precellys 24 tissue homogenizer (Bertin instruments, Montigny-le-Bretonneux – France) for 2x 30 s at RT. After homogenization 300 µL extraction buffer (2.5 mM LiCl, 50 mM Tris-HCl pH 8, 62.5 mM EDTA 4 % (v/v) Triton X – 100) was added. The probes were incubated for 10 min at RT and then 300 µL of phenol-chloroform-isoamylalcohol was added and shook vigorously for 20 sec and incubated 5-10 min at RT. After centrifugation with 14, 000 rpm for 5 min the upper phase, containing the DNA, was carefully transferred to a fresh reaction tube and incubated with 2x vol pure ethanol for 30 min at -20 °C. Precipitated DNA was centrifuged for 10 min at 4 °C and washed two times with 70 % (v/v) ethanol. The pellet was air-dried for 20 min and then dissolved in 100 µL nuclease free water.

2.4.4 RNA extraction

In order to extract RNA from plant material the method which was used is based on the protocol from Chomczynski and Sacchi (1987). The ready-to-use extraction buffer peqGOLD TriFast™ (peqlab, VWR) was used according to the manufacturer instruction. 100 mg fresh plant material was ground in liquid nitrogen and mixed with 1 mL extraction buffer. 200 µL chloroform was added and incubate for 10 min at RT. After centrifugation at RT with 14,000 rpm for 15 min the upper phase, containing the RNA, was carefully transferred to a fresh reaction tube and incubated with isopropanol overnight at -20 °C. Precipitated RNA was centrifuged for 10 min at 4 °C with 14,000 rpm and subsequently washed with 500 µL 75 % (v/v) ethanol in DEPC-treated water for two times. The pellet was air-dried for 20 min and then dissolved in 15 µL nuclease free water.

2.4.5 DNase treatment

To remove residual genomic DNA in RNA samples 1 U of DNase I, RNase-free (Thermo Scientific) was mixed with the included 10x reaction buffer with $MgCl_2$ and 0.25 µL RiboLock RNase Inhibitor (40 U/µL; Thermo Scientific). 0.5 - 1 µg of RNA were added in a final volume of 10 µL. The reaction was incubated at 37 °C for 30 min and the reaction was afterwards terminated by adding 1 µL of 50 mM EDTA and incubation for 10 min at 65 °C.

2.4.6 Reverse transcription

cDNA was prepared by using 1 µL of the recombinant M-MuLV RT "RevertAid reverse transcriptase" (200 U/µL; Thermo Scientific) for 0.5 - 1 µg of DNase treated RNA (2.4.5), together with 4 µL 10x reaction buffer, 2 µL 10µM Oligo-dT, 1 µL random hexamers and 2 µL 2.5 mM dNTPs. Additionally, 0.5 µL RiboLock RNase Inhibitor (40 U/µL; Thermo Scientific) was added and the reaction was filled up to a final volume of 20 µL with nuclease free water. The reaction was incubated for 90 min at 42 °C, followed by enzyme deactivation at 70 °C for 10 min.

2.4.7 Polymerase Chain Reaction - Standard protocols and thermal profiles

Standard PCR reactions were performed using a home-made *Taq* DNA polymerase. For cloning, recombinant *Pfu* High-Fidelity DNA Polymerase (Thermo Scientific) or Q5® High-Fidelity DNA Polymerase (New England Biolab) with proofreading function were used.
In the following tables the standard reaction mix and thermal profiles for home-made *Taq* Polymerase (Table 2-8; Table 2-9), *Pfu* High-Fidelity DNA Polymerase (Table 2-10; Table 2-11) and Q5® High-Fidelity DNA Polymerase (Table 2-12; Table 2-13) are shown, respectively.

Table 2-8: Taq Polymerase reaction mix

Component	Volume
Template DNA	0.1 – 20 ng
10x *Taq* reaction buffer	2 µL
2,5 mM dNTP - mix	2 µL
10 µM of fw-/rev-primer	1 µL
Taq DNA polymerase	0.5 µl (1 U)
ddH_2O	up to 20 µL

Table 2-9: Taq Polymerase thermal profile

Step	Temperature °C	Duration	N° of Cycles
Initial Denaturation	95	5 min	1
Denaturation	95	30 s	
Annealing	T_m – 3	30 s	30
Elongation	72	1 min /1 kb	
Final extension	72	10 min	1
Cooling	12	∞	

Table 2-10: Pfu High-Fidelity DNA Polymerase reaction mix

Component	Volume
Template DNA	1 – 50 ng
10x *Pfu*-buffer + $MgSO^4$	5 µL
2,5 mM dNTP - mix	5 µL
10 µM of fw-/rev-primer	2,5 µL
Pfu High-Fidelity DNA Polymerase	1 µL
ddH_2O	up to 50 µL

Table 2-11: Pfu High-Fidelity DNA Polymerase thermal profile

Step	Temperature °C	Duration	N° of Cycles
Initial Denaturation	98	5 min	1
Denaturation	98	30 s	
Annealing	T_m – 3	30 s	30
Elongation	72	1 min /0.5 kb	
Final extension	72	10 min	1
Cooling	12	∞	

Table 2-12: Q5® High-Fidelity DNA Polymerase reaction mix

Component	Volume
Template DNA	< 1 µg
5x Q5 reaction Buffer	10 µL
2,5 mM dNTP - mix	4 µL
10 µM of fw-/rev-primer	2,5 µL
Q5 High-Fidelity DNA Polymerase	0,5 µL
ddH_2O	up to 50 µL

Table 2-13: Q5® High-Fidelity DNA Polymerase thermal profile

Step	Temperature °C	Duration	N° of Cycles
Initial Denaturation	98	30 s	1
Denaturation	98	5 -10 s	
Annealing	NEB T_m *	20 s	30
Elongation	72	20-30 s /1kb	
Final extension	72	2 min	1
Cooling	12	∞	

*https://tmcalculator.neb.com/#!/ (16.07.2018)

2.4.8 Quantitative Real Time PCR

Biorad iCycler with iQ5 multicolour real-time PCR detection system was used to conduct quantitative real time PCR (qRT-PCR). The standard reaction mix and thermal profile for qRT-PCR shown in Table 2-14 and Table 2-15, respectively. Relative gene expression was calculated according to the $2^{-\Delta ct}$ method (Livak and Schmittgen, 2001) to the housekeeping gene *EF1α*.

Table 2-14: Standard reaction mix for qRT-PCR

Component	Volume
Template cDNA 1:3 diluted	1 µL
Maxima SYBR Green/Fluorescein qPCR Master Mix (2x)	10 µL
10 µM of fw-/rev-primer	0.5 µL
Nuclease free water	Up to 20 µL

Table 2-15: Thermal profile for qRT-PCR with melting curve

Step	Temperature °C	Duration	N° of Cycles	Realtime detection
Initial Denaturation	95	10 min	1	
Denaturation	95	15 s		
Annealing	$T_m - 3$	15 s	40	
Elongation	72	10 s /100 bp		📷
Melting Denaturation	95	1 min	1	
Melting cooling	T_a	2 min	1	
Melting	T_a - 95	10 s /step	0.5 steps	📷/step

2.4.9 Separation and isolation of DNA via agarose gel electrophoresis

To separate DNA fragments a 1 % agarose gel mixed with peqGreen (peqLab) in 1x TAE buffer (4 mM Tris/acetate, 1 mM EDTA pH 8.0) was used in an electrophoresis. Samples were mixed with 10 x loading dye (10x loading dye: 87 % (v/v) glycerine, 30 mM Tris-HCl, 3 mM EDTA pH 8.0, 0.4 % bromphenol blue (w/v)) and loaded next to 5-10 µL GeneRuler 1 kb DNA ladder (Thermo Scientific) which was used as standard. Electrophoresis was performed at an electric field strength of 5 V/cm. DNA fragments were visualized in a

UV-transilluminator (Infinity-3026 WL/26 Mx, Peqlab) with the software InfinityCapt 14.2 (Peqlab). DNA purification from agarose gels was performed with the "HiYield® PCR Clean-up/ Gel Extraction Kit" from SLG according to the manufacturer's recommended protocol.

2.4.10 DNA quantification and analysis

Nucleic acid concentrations were determined with a NanoDrop 2000 spectrophotometer (Thermo Scientific) at 220-340 nm and evaluated with the NanoDrop Software. Sequencing of plasmid DNA was performed by GATC (Konstanz) and prepared as stated in the company's Material and Methods instructions. Sequences were analysed using the CLC Main Workbench (Qiagen). DNA restriction enzymes were used according to the manufacturer's protocol (Thermo Scientific).

2.4.11 Cloning

The vectors used in this work where generated by using the GATEWAY® cloning system according to the manufacturer's instructions. To generate entry clones PCR fragments containing an A-overhang were taken in the he pCR8/GW/TOPO Cloning kit (Invitrogen). To achieve an A-overhang 20 µL purified PCR-Fragments were incubated with 2.4 µL of 10x *Taq* buffer (100 mM Tris-HCl, 500 mM KCl, and 15 mM $MgCl_2$, pH 8.3), 1 µL 10 mM dATP, 1 µL homemade *Taq*-Polymerase for 30 min at 72 °C. To transfer the fragment of interest into the final expression vector, LR reaction between the entry clone and a Gateway destination vector was conducted using the Gateway® LR Clonase® II Enzyme Mix (Invitrogen).

2.4.12 TALEN

In order to generate a directed mutation in wild-type Col-0 plants. TAL-effector nucleases were used. Constructs were generated by Dr. Robert Morbitzer from the department of general genetics in the ZMBP via the golden gate cloning system (Engler and Marillonnet, 2014) and transformed to Agrobacteria (see section 2.3.6). Col-0 plants were stable transformed according to section 2.3.2 and selected via BASTA.

2.5 BIOCHEMICAL METHODS

2.5.1 Protein extraction in plants

2.5.1.1 Protein extraction for Co-immunoprecipitation

For total protein extracts 200 mg frozen leaf material ground in liquid nitrogen was re-suspended in 1.6 mL solubilisation buffer (25 mM TRIS-HCl pH 8.0, 150 mM NaCl, 1 % (v/v) NP40, 0.5 % (w/v) DOC, 2 mM DTT and 1 tablet of "cOmplete ULTRA Tablets, Mini, EASYpack" (Roche) per 10 mL). The samples were solubilized for 1 h at 4 °C in an overhead rotation shaker (5 rpm). Centrifugation for 10 min at 4 °C and 20 000g separated the soluble proteins from the cell debris and the supernatant was transferred to a new reaction tube and centrifuged for another 10 min at 4 °C and 20 000g. The supernatant was then used for further analysis.

2.5.1.2 Protein extraction for MS analysis

For quantitative phosphoproteomic analysis cell suspension of *Arabidopsis thaliana* accession *Landsberg erecta* was used. 7 mL cells were transferred to a 6-well plate and induced with 1 µM chitin for 45 seconds and harvested immediately by vacuum filtration in two 3 mL steps to absorb the medium. The 1 mL of the treated cell suspension left was saved for MAPK activation (section 2.6.5) control. The cells were collected on a nylon membrane (10 µm, Merck Millipore) and frozen in liquid nitrogen subsequently.
For total protein cell extraction the cells were thawed on ice and suspended in 600 µL protein extraction buffer (6M Urea; 2M Thiourea, Tris-HCl, pH 8; 1 % N-octylglucoside, 1 tablet of “phosSTOP EASYpack” and 1 tablet of “cOmplete ULTRA Tablets, Mini, EASYpack” (Roche) per 10 mL). Samples were incubated in an overhead shaker for 10 min with 7 rpm at 4 °C and then centrifuged for 30 min at 4 °C and 20 000 g. The supernatants coming from the same sample were pooled in a fresh reaction tube and protein concentration was measured described in section 2.5.2.

2.5.2 Quantification of protein concentration

The protein concentration was determined after the Bradford method (Bradford, 1976) using Roti-Quant solution (Carl Roth). A standard curve was calculated with bovine serum albumin (BSA).

2.5.3 SDS-PAGE

For SDS polyacrylamide gel electrophoresis the method based on the protocol of Laemmli (1970) was used. The acrylamid-bisacrylamid mixture (37.5:1) was used from Carl Roth (Rotiphorese Gel 30). Separating gels of 8 % and 10 % with 4 % stacking gels were used in a Mini PROTEAN 3 system (Biorad). Standard reaction mixes for separation and stacking gels are listed in Table 2-16. The protein separation was conducted at a constant current of 25 mA per gel. As protein marker the pre stained PageRuler™ protein ladder mix (Thermo Scientific) was used.

Table 2-16: Standard reaction mixture for 1 SDS-PAGE gel preparation

Percent of Gel	8 %	10 %	4 %
H_2O	2.3 mL	1.9 mL	1.7 mL
Acrylamid-bisacrylamid mixture (37.5:1)	1.3 mL	1.7 mL	0.45 mL
Tris-HCl pH 8.8 1.5 M	1.3 mL	1.3 mL	-
Tris-HCl pH 6.8 1M	-	-	0.75 mL
SDS 10 % (w/v)	0.05 mL	0.05 mL	0.03 mL
Aps 10 % (w/v)	0.05 mL	0.05 mL	0.03 mL
TEMED	0.005 mL	0.005 mL	0.003 mL

2.5.4 Western blot analysis

To transfer the proteins from a Laemmli SDS PA gel onto an Amersham™ Protran™ 0.2 µm NC membrane (GE Healthcare) either the Mini PROTEAN 3 system from Biorad or PerfectBlue semi-dry-blotting gadget from PeqLab was used. The transfer was conducted with the transfer-buffer (25 mM TRIS, 192 mM Glycine, 1 % (w/v) SDS, 20 % (v/v) methanol) for 1 h at 100V for the wet-blotting-system and 1 h at 1 mA/cm^2 for the semi-dry-blotting system. After that, membranes were stained with Ponceau S-Red (0.1 % (w/v) Ponceau S Red in 5 % (v/v) acetic acid) to verify successful protein transfer and scanned for later documentation. To block unspecific binding sites the membranes were then incubated with TBS-T (10 mM TRIS pH 7.5, 150 mM NaCl, 0.1 % Tween-20) containing 5 % (w/v) BSA or 5 % (w/v) milk for 1 – 2 h at RT. After blocking, the membranes were washed 3 times with 15 mL TBS-T for 10 min at RT and then incubated with the adequate primary antibody in 10 mL TBS-T containing 5 % (w/v) BSA or 5 % (w/v) milk, depending on the manufacturer instructions overnight at 4 °C. On the next

day the membranes were washed again for 3 times with 15 mL TBS-T for 10 min at RT before the membranes were incubated with the respective secondary antibody for 1 h in 10 mL TBS-T containing 5 % (w/v) BSA at RT. In the final step the membrane was 3 times washed with 15 mL TBS-T for 10 min at RT. To visualize the protein on membrane a chemiluminescent substrate (ECL; GE Healthcare) was applied for 5 min before exposure using an Amersham Imager600 detection system from GE Healthcare.

2.5.5 Protein-Protein interaction assays

2.5.5.1 Co – Immunoprecipitation

To analyse protein – protein interaction *in vivo*, plants were transformed as stated in section 2.3.3 and protein extraction was performed as described in section 2.5.1. The solubilised proteins were incubated with the pre-washed and in solubilisation buffer equilibrated trap-beads (ChromoTek), respectively. After 1 h of incubation at 4 °C with 6 rpm in an overhead rotation shaker the GFP-trap beads were then two times carefully washed with solubilisation buffer and two times with washing buffer (25 mM TRIS-HCl pH 8.0, 150 mM NaCl, 2 mM DTT). The precipitated beads were suspended in SDS-PAGE loading dye and boiled at 95 °C for 10 min. The supernatant was then analysed via SDS-PAGE (2.5.3) and following western blot analysis (2.5.4).

2.5.6 Phosphosite analysis via mass spectrometry

For the quantitative phosphoproteomic analysis, the cell suspension culture was used, and samples were extracted as described in section 2.5.1.2.

The raw protein extracts were sent to the proteomics Core Facility of the University of Tubingen, Proteome Centre Tubingen, headed by Prof. Dr. Boris Maček and further proceeded by M. Sc. Maja Šemanjski according to Spat et al. (2015). Protein extracts were reduced with DTT, alkylated with iodoacetamide and in-solution digested with endoproteinase Lys-C (Waco) and trypsin (MS grade; Thermo Scientific). Peptides were differentially labelled using dimethyl-labelling approach (Boersema et al., 2009). For that, peptides were loaded onto a SepPak C18 column and labelled with CH_2O (Sigma-Aldrich) and $NaBH_3CN$ (Fluka) for “light”, $^{13}CD_2O$ (Sigma- Aldrich) and $NaBD_3CN$ (Sigma-Aldrich) for “heavy” labelling. Peptides were eluted from the column using 80 % acetonitrile and 6 % trifluoroacetic acid solution and mixed in equal amounts. The samples were then enriched for phosphopeptides by TiO_2 chromatography in 10

consecutive rounds, as described in Spat et al. (2015). After purification, peptides were separated by an EASY-nLC 1000 (Thermo Scientific) on an in-house packed 20 cm long analytical column with reverse-phase ReproSil-Pur C18-AQ 1.9 µm particles (Dr. Maisch). Peptides were measured on a Q Exactive HF mass spectrometer (Thermo Scientific) operated in the positive ion mode (Cvetesic et al., 2016). All raw MS spectra were processed with MaxQuant software suite (version 1.5.2.8) (Cox et al., 2009) and default settings. Identified peaks were searched against a reference *A. thaliana* proteome (taxonomy ID 3702) obtained from Uniprot (33351 entries, released in January 2016), with the database search criteria explained in Spat et al. (2015). During the first search, peptide mass tolerance was set to 20 ppm and in the main search to 4.5 ppm. Light- and heavy- dimethylation labelling on peptide N-termini and lysine residues was defined. Methionine oxidation, protein N-terminal acetylation and Ser-Thr-Tyr phosphorylation (STY) were defined as variable modifications, and carbamidomethylation of cysteines was set as a fixed modification. Peptide and modified peptides were filtered using a target-decoy approach with a false discovery rate (FDR) of 0.01. Perseus software (version 1.5.0.31) was used to analyse significance of regulated phosphorylation events. Only phosphorylation sites with PEP < 0.001 and Andromeda score > 50 were used for the analysis. Phosphorylation site ratios were log2 transformed and plotted against the respective log10 transformed phosphorylation site intensities. Significantly regulated phosphorylation events were determined by significance B test with a *p*-value of 0.05.
Gene-annotation and KEGG enrichment analysis was performed using The Database for Annotation, Visualization and Integrated Discovery (DAVID) tool (version 6.7) with default parameters and p-value of 0.01 (Huang et al., 2008). UniProt IDs were used as an input for the enrichment and all identified proteins (5655 proteins) were used as a background.

2.5.7 Phospholipid labelling and extraction

To analyse the impact of PLDγ1 on phospholipids the procedure described in Munnik and Zarza (2013) was followed. Therefore, 3- to 5-days-old seedlings were placed into 200µl labelling buffer (2.5 mM MES/KOH buffer (pH 5.7), 1 mM KCl) and labelled with 10 µCi of ^{32}P-inorganic phosphate and incubated overnight. The elicitors or the same amount of control solution were added and incubated as indicated. To stop the stimulus perchloric acid (5 % (w/v), final concentration) was added (Malinovsky et al., 2014) and

shaken vigorously for 10 min. Afterwards the total solvent was removed. For lipid extraction 400 µL extraction buffer ($CHCl_3$ /MeOH/HCl (50/100/1, (v/v/v)) was added and shaken again for 10 min. To separate phases 400 µL $CHCl_3$ and 200 µL 0.9 % (w/v) NaCl was added and vortexed for 10 s before centrifugation for 1 min at 10,000 g. The organic lower phase was transferred to a new tube containing 400 µL of fresh buffer ($CHCl_3$/MeOH/1M HCl (3/48/47, (v/v/v))). After mixing and another centrifugation step, the upper phase was removed, and 20 µL isopropanol was added. Samples were dried in a vacuum centrifuge at 50 °C and dissolved in 100 µL $CHCl_3$.

2.5.8 Thin layer chromatography

Phospholipids were separated as reported in Liscovitch (1989) and Munnik and Laxalt (2013) by thin-layer chromatography (TLC) using an ethyl acetate solvent system with the organic upper phase of ethyl acetate/iso-octane/HAc/H,O (13:2:3:10 [v/v]). Radiolabeled phospholipids were visualized and quantified using a phosphoImager (GE Healthcare) and the program QuantityOne (Biorad).

2.5.9 Detection of salicylic acid and jasmonic acid

For salicylic acid (SA) and jasmonic acid (JA) quantification in Col-0, *pldγ1-1*, *pldγ1-1 PLDγ1 1* and *pldγ1-1 PLDγ1 3* 200 mg fresh weight leaf material of 8-week-old *Arabidopsis* plants were collected. The amount of salicylic acid and jasmonic acid were measured by gas chromatography coupled to mass spectrometry (Shimadzu TQ8040) in the analytical laboratories of Dr. Mark Stahl (ZMBP, Tübingen) by Dr. Joachim Kilian.

2.6 BIOASSAYS

2.6.1 Pst infection

Pseudomonas syringae pv. tomato DC3000 (Pst DC3000) was grown overnight in King's B medium, centrifuged, washed and diluted in 10 mM $MgCl_2$ to a density of 10^4 cfu/mL. Bacteria were pressure-infiltrated into primed *Arabidopsis* leaves and the plants were kept under translucent cover and high humidity. Leaves where harvested at day 0 and 4, surface sterilized in 70 % ethanol and washed in dd$H_2$0 for 1 min each. Two leaf discs (5 mm or 4 mm diameter) per leave were stamped out, ground in 200 µL of a 10 mM $MgCl_2$ solution, diluted serially 1:10 and plated on LB plates containing rifampicin and cycloheximide. After 2 days of incubation at 28 °C, colony-forming units were counted.

2.6.2 Botrytis cinerea infection

Spores of *Botrytis cinerea* isolate B0-10 were diluted to a final concentration of $5x10^6$ spores/mL in PDB medium. 5 µL spore solution were dropped on 5-6-week old Arabidopsis leaves and were and kept under translucent cover and high humidity for 2 days. Lesion sizes were determined using the Photoshop CS5 Lasso tool. Selected pixels were counted and the lesion size in cm^2 was calculated using a 0.5 cm^2 standard. *Botrytis* growth was also quantified by measuring *Botrytis* DNA (2.4.3) in a real-time PCR reaction (2.4.8).

2.6.3 Alternaria brassicicola infection

Alternaria brassicicola MUCL 20297 cultivation and spore production was performed as described in Thomma et al. (1999). For infection experiments 6-week-old *A. thaliana* plants were used. A glycerol stock of *A. brassicicola* spores with of 2 * 10^7 spores/mL was diluted with sterile water to $1x10^6$ spores/mL and brought to RT. Two leaves per plant were inoculated with 2-4 5 µL droplets of the spore solution. Plants were randomly distributed in a tray and were kept under high humidity under short-day conditions. Monitoring of the infection symptoms was done after 7, 10 and 13 days according to the following scheme: 1: no symptoms, 2: light brown spots at infection site, 3: dark brown spots at infection site, 4: spreading necrosis, 5: leaf maceration, 6: sporulation. The disease index (DI) was calculated with the following formula: DI = Σ i * ni. ‘‘i’’ is the symptom category, and ‘‘ni’’ is the percentage of leaves in ‘‘i”.

2.6.4 Detection of reactive oxygen species

For measurement of reactive oxygen species (ROS) production, small leaf pieces (~ 0,4 cm x 0,2 cm) of 5-week-old Arabidopsis plants were cut and floated overnight in ddH_2O. The next day, two leaf pieces were placed in one well of a 96-well plate containing placed in a 96-well-plate (two pieces/well) containing 90 µl of the reaction mix (final concentration in 100 µL: 20 µM Luminol L-012, Wako Chemicals USA, 5 µg/mL horseradish peroxidase, Applichem, Germany). The background was measured before adding 10 µL of the respective elicitor and luminol-chemiluminescence was quantified using a 96-well Luminometer (Mithras LB 940, Berthold Technologies) and the software MicroWin.

2.6.5 MAP-kinase activation assay

In order to analyse activation of MAP-kinases 2-week-old *Arabidopsis* seedling grown on ½ MS plates (see section 2.3.1) were transferred in a 12-well plate with 1.5 mL liquid ½ MS medium. After equilibrating the seedlings overnight, they were treated with the respective elicitors. Seedlings were then frozen after 0 min as control and 15 min after elicitation in liquid nitrogen. The samples were homogenized in 40 µL extraction buffer (50 mM Tris-HCl pH 7.5, Complete Protease Inhibitor Cocktail without EDTA (Roche), PhosStop Phosphatase Inhibitor Cocktail (Roche)) and centrifuged with 14,000 rpm at 4 °C for 30 min. The protein extracts were transferred to a fresh reaction tube and the concentration was determined (2.5.2). The protein levels were adjusted to the lowest concentration of total protein and then applied to a 10 % SDS-PAGE (2.5.3). After western blotting (2.5.4) with the PerfectBlue semi-dry-blotting gadget (PeqLab Erlangen), activated MAP kinases 6, 3 and 4 were detected using the phospho p44/42 MAPK (Erk1/2) primary antibody (Cell Signaling Technology) according to the supplier protocol.

3 RESULTS

3.1 PHOSPHOPROTEOMIC ANALYSIS TO FIND NEW SIGNALLING TARGETS OF CERK1

As already explained in the introduction, CERK1 is an important protein in the recognition of carbohydrate MAMPs such as chitin and PGN. Therefore, it was one of our aims to find out more about the further signalling cascades of CERK1. To reveal novel downstream signalling components of CERK1, quantitative phosphoproteomic analysis was performed together with Maja Šemanjski from the Proteome Centre Tübingen. In the first experiments 6-week old *Arabidopsis* plants of wild-type Col-0 and *cerk1-2* were infiltrated with either water as control or 1 µM chitin and 100 µg/mL PGN for 5 min. Protein extracts were prepared as explained in section 2.5.1.2. After measuring protein concentrations samples were analysed in the proteome centre. The results of the first runs (not shown) revealed that several parameters needed to be optimized. Most of the found peptides were either from proteins involved in metabolic pathways or photosynthesis and gene regulation. We could not find peptides for proteins known to be involved in early immune responses such as MAP-kinases. Moreover, the total proteome changes between the plant lines were too big and could not be compared. Therefore, the experimental design was changed. To avoid proteome changes between different organisms a cell culture derived from *Arabidopsis* wild-type *Landsberg* was used. Since PGN seems not to be recognized in cell cultures (data not shown, personal communication Dr. Xiaokun Liu), this experiment was conducted only with chitin octamers (C8). After elicitation with 1 µM chitin, an early time point for harvesting was chosen to prevent getting too many 'late' signalling proteins. The aim was to harvest the cells before MAP-kinases were activated. Therefore, pre-tests were performed to see whether elicitation and harvesting techniques would be successful. Figure 3-1 shows that MAP-kinases were only activated after 5 min of elicitation. The samples harvested after one minute showed no MAP-kinase activation. Thus, one minute was used as a time point to collect the samples.

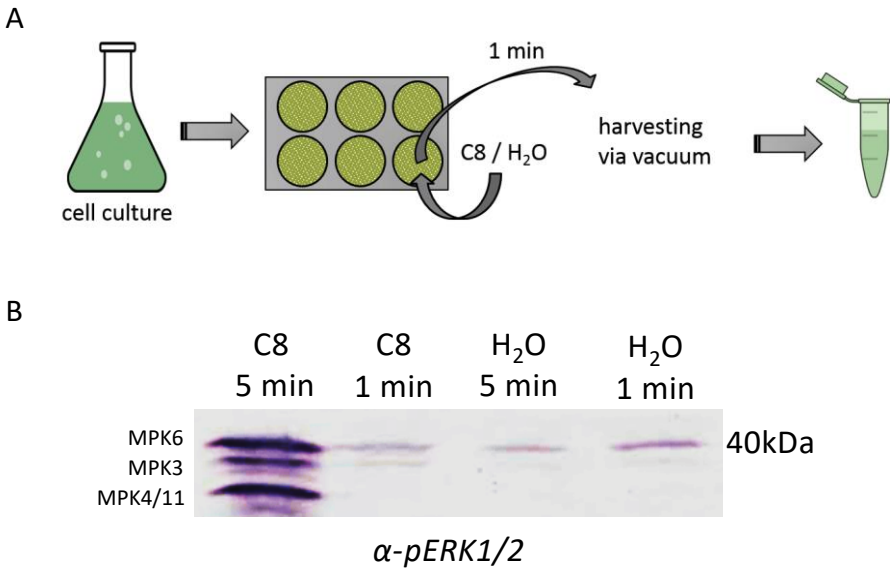

Figure 3-1: Cell culture-based sample collection for quantitative phosphoproteomic analysis

A Schematic display of improved sample collection for quantitative phosphoproteomic analysis. Cell cultures from *Arabidopsis thaliana* accession *Landsberg erecta* were transferred to a 6-well-plate and elicitated with 1 µM chitooctaose (C8) or water as control. Within 1 min of elicitation the samples were harvested on a nylon membrane by applying vacuum to remove the culture medium and then frozen in liquid nitrogen for protein extraction. **B** Appropriate time point for sample collection was achieved by testing MAP-kinase activation upon elicitation. This assay was performed with 1 mL cell culture which was elicited with 1 µM C8 or water for either 1- or 5-min. Activation of MAP-kinases was detected by the p44/p42 anti-phospho- antibody (α-pERK1/2).

Due to the homogenous cell culture and fast handling the overall proteome is expected not to show any drastic changes. Another advantage using cell cultures is to minimize the wounding response which might be induced by infiltration of leaves in earlier sample collections. In the phospho-proteome analysis performed with the cell culture extracts 5655 phospho-peptides were found. Indeed, overall proteome changes were not observed (data not shown). In the following process the identified peptides were further analysed as described in 2.5.6 and the candidates were categorized. For this, gene-annotation and KEGG (Kyoto Encyclopaedia of Genes and Genomes) enrichment analysis was performed using the 'Database for Annotation, Visualization and Integrated Discovery' (DAVID) tool (version 6.7). The results of the whole enrichment analysis for gene ontology (GO) terms of biological processes (GOBP) are displayed in Figure 3-2. To narrow down the candidate list, only proteins with matching phospho-peptides that had been significantly enriched with a p-value lower than 0.05, are shown in Table 3-1 in more detail.

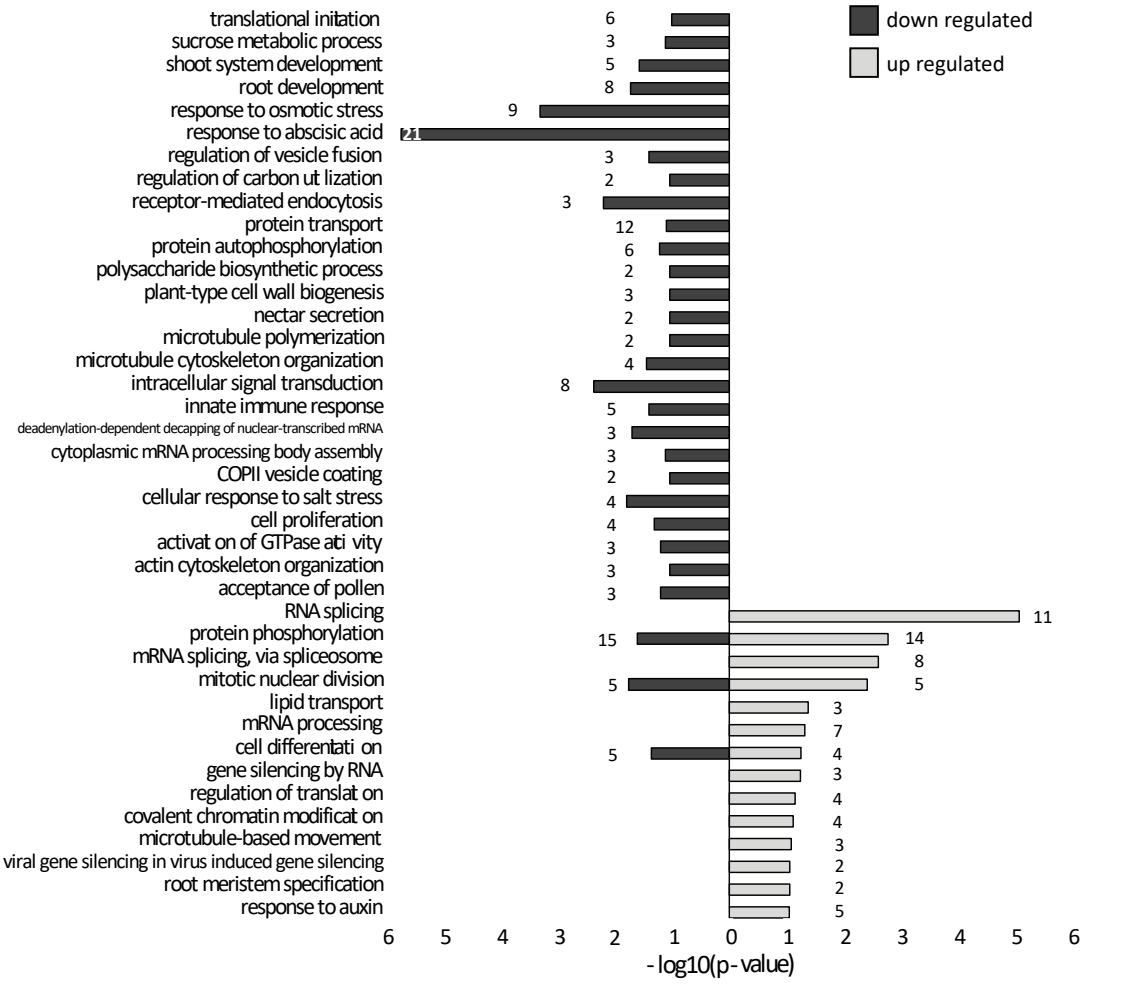

Figure 3-2: GO terms of biological processes for the identified phospho-peptides.

Annotation enrichment analysis of up- and down-regulated proteins with regulated phospho-peptides in C8 treated cell cultures using DAVID. The resultant *p*-values of each term were $-\log_{10}$ transformed. The number at the right or left side of each bar indicates the number of proteins that were significantly enriched in each GO term.

Table 3-1: GO terms of biological processes (GOBP) selection of enriched proteins of regulated phospho-peptides with a p-value < 0.05

	Up regulated			Down regulated		
	p-value < 0.05	Count / total hits	Genecode of Proteins	p-value < 0.05	Count / total hits	Genecode of Proteins
response to abscisic acid				1.79E-06	21/131	Q9LIL3, O80986, A8MR97, O80653, P54887, F4I7B6, Q9LES3, Q94K75, Q9SIB9, Q9FMM3, Q9XIE2, Q9ZUU4, Q9FXI5, Q9C778, Q9LQ55, Q9FIQ0, Q93VM8, F4J0N1, F4K9K4, Q39026, F4IGJ9
response to osmotic stress				4.80E-04	9/41	Q0WQF4, Q9S814, F4J0N1, F4IZI7, A1L4W5, F4I7B6, Q9C958, Q39026, Q84JR9
intracellular signal transduction				4.24E-03	8/45	B9DFS6, F4J0N1, F4K0Z2, F4I7B6, Q9C958, F4IV25, F4J6F6, Q8W4I7
receptor-mediated endocytosis				6.25E-03	3/3	Q9XI12, F4JRG0, F4JRF7
cellular response to salt stress				1.59E-02	4/12	A8MQG3, Q9SJW3, A1L4W5, Q8L636
mitotic nuclear division	3.89E-03	5/22	Q8LGU6, Q9FMB4, Q8W1Y0, F4IIU4, Q8RWY6	1.71E-02	5/22	Q94BP7, Q9ZVJ3, Q8LEG3, Q8RWY6, F4K3E4
root development				1.85E-02	8/59	Q9C9Q8, Q9LQF2, Q9XIE6, Q946J8, P54887, Q9FVQ1, Q9FHI1, Q39026
deadenylation-dependent decapping of nuclear-transcribed mRNA				1.96E-02	3/5	Q94C98, Q0WPK4, F4J077
protein phosphorylation	1.66E-03	14/169	Q9LVI6, Q9FYC5, Q9S713, Q94AB2, Q8VYG5, F4IPV6, F4I5S1, F4HPS0, O49840, Q9SA26, Q1PDV6, Q8RX85, F4K3Z6, Q9FKL3	2.43E-02	15/169	Q94AB2, O64768, Q9FLW0, Q42438, C0LGN2, F4J0N1, F4K0Z2, Q1PDV6, F4I7B6, Q9C958, F4IV25, F4I5S1, Q9SAJ2, Q9FKL3, Q8W4I7
shoot system development				2.66E-02	5/25	Q9C9Q8, Q9XIE6, Q9M086, Q8RWW0, Q9FVQ1
microtubule cytoskeleton organization				3.54E-02	4/16	Q94BP7, Q9ZVJ3, Q8LEG3, F4K3E4
innate immune response				3.86E-02	5/28	Q9FE20, Q1PDV6, P92948, Q0WPK4, Q9ZUU4
regulation of vesicle fusion				3.86E-02	3/7	O49336, F4KG92, F4JF82
cell differentiation				4.32E-02	5/29	Q946J8, Q8RWW0, P92948, Q94BP0, O22607
cell proliferation				4.82E-02	4/18	Q9C778, Q8LEG3, Q9FHI1, F4K3E4
RNA splicing	8.42E-06	11/59	Q9LU44, P92966, Q8L7W3, Q9LZ82, Q9FMG4, A2RVS6, B6EUA9, O48713, Q9SJA6, Q9SEE9, Q9FYB7			
mRNA splicing, via spliceosome	2.48E-03	8/62	Q9LU44, P92966, Q8LPQ9, O81127, Q9FMG4, B6EUA9, Q9SEE9, Q9FYB7			
lipid transport	4.21E-02	3/11	Q9MA55, F4JFW6, Q8RWD9			
mRNA processing	4.76E-02	7/87	P92966, Q8L7W3, Q9LTT8, A2RVS6, F4I3B3, Q9SJA6, Q9SEE9			

The GO-enrichment in Table 3-1 shows that particularly phospho-peptides from proteins involved in ABA-signalling and osmotic stress regulation were down-regulated. In contrast, especially peptides from proteins associate with posttranscriptional pathways such as RNA splicing, and mRNA processing were upregulated. Furthermore, proteins involved in cytoskeleton movements were found to be differentially phosphorylated and not surprisingly several proteins responsible for general signal transduction and protein phosphorylation could be identified. Within this group some phospho-peptides of proteins, known to be involved in chitin-signalling, were detected in this analysis. For example, PBL27 (AT5G18610, Q1PDV6) and LIK1 (AT3G14840, C0LGN2) were found to be phosphorylated in our experiment and were categorized in GO terms innate immune response and protein phosphorylation, respectively. In PBL27 three residues (Threonine-405, Serine-458 und Serine-462) were up regulated and one residue (Serine-31) was down regulated after chitin treatment compared to water treatment. For LIK1 only one (Serine-967) residue could be found to be down regulated. Based on these results phospho-site mutants were generated by Andrea Salzer in her Bachelor project (Salzer, 2016). In these mutants the differentially regulated phospho-sites were mutated to either mimicking phosphorylation by inserting aspartate or blocking phosphorylation by inserting alanine instead of serine or threonine. Mutation constructs were then transformed into the *pbl27-1* (Shinya et al., 2014) or the *lik1-1* (Le et al., 2014) mutant background, respectively. These stable transformed plant lines need to be further tested to confirm the importance of the de/phosphorylated amino acids in the plant immune response.

Beside these known proteins, only a few candidates specifically connected to plant immunity were identified and are described in more detail in Table 3-2. Within this list especially PBS1 (AVRPPHB SUSCEPTIBLE1) and PAT1 (ARABIDOPSIS HOMOLOG OF YEAST PAT1) are interesting. PBS1 is a receptor-like cytoplasmic kinases like PBL27 or BIK1 as explained in the introduction. As already known, RLCK are crucial for downstream signalling in plant immunity (Liang and Zhou, 2018). PBS1 was found in 2003 to be a target of the effector AVIRULENCE PROTEIN PSEUDOMONAS PHASEOLICOLA B (AvrPphB) coming from *Pseudomonas syringae (Shao et al., 2003)*. They propose the theory that PBS1 as a target for the effector AvrPphB guards other important signalling pathways like BIK1 signalling. The complex of PBS1 – AvrPphB is recognised by the

protein RESISTANCE TO PSEUDOMONAS SYRINGAE 5 (RPS5) and leads to the activation of immunity processes which then leads to ETI (Shao et al., 2003). Therefore, regulation of PBS1 upon chitin treatment is an interesting result and could indicate new regulation of pattern induced immunity pathways. The other candidate PAT1 (phosphorylation downregulated after C8 treatment) was found in complexes with MAP KINASE 4 (MPK4) and was shown to be phosphorylated by MPK4 upon flg22 treatment (Roux et al., 2015). Moreover, it is part of the mRNA decapping machinery. This means that PAT1 might link MPK4 to decapping processes which are essential for mRNA turnover and explains a potential alternative way of MPK4 regulating immune responses (Roux et al., 2015). MPK4 belongs to a signalling cascade which is induced by PRRs for example CERK1 (Bi et al., 2018). Interestingly MPK4 was not found in this data set to be regulated. Also, we wouldn't expect MAPK to be regulated since we tried to harvest the samples before MAPK activation. However, the phosphorylation of amino acids in MPK6 (MAP KINASE 6) were found to be downregulated upon chitin treatment, meaning that we cannot exclude seeing effects after MAPK activation, although we tried to harvest as early as possible. Phosphorylation of MPK3(MAP KINASE 3) was not found to be regulated in our dataset. Nevertheless, these results about MPK4 and PAT1 might be worth to be studied in more detail.

Table 3-2: Proteins with regulated phospho-peptides in the GOBP category of innate immunity

Genecode	AGI	Name	Description	Regulated after C8
Q9FE20	AT5G13160	PBS1	Mutant is defective in perception of *Pseudomonas syringae* avirulence gene *avrPphB (Shao et al., 2003)*.	down
Q1PDV6	AT5G18610	PBL27	Encodes a receptor-like cytoplasmic kinase that is an immediate downstream component of the chitin receptor CERK1 and contributes to the regulation of chitin-induced immunity (Shinya et al., 2014).	down
P92948	AT1G09770	ATCDC5	Member of MYB3R- and R2R3- type MYB- encoding genes. Essential for plant innate immunity. Interacts with MOS4 and PRL1 (The Arabidopsis Information Resource (TAIR) (2018b) https://www.arabidopsis.org/servlets/TairObject?id=28932&type=locus)	down
Q0WPK4	AT1G79090	PAT1	Part of mRNA decapping machinery and is phosphorylated by MPK4 upon flg22 treatment. PBS1 mutants exhibit dwarfism and de-repressed immunity dependent on the immune receptor SUMM2 (Roux et al., 2015).	down
Q9ZUU4	AT2G37220	n/d	Encodes a chloroplast RNA binding protein. A substrate of the type III effector HopU1 (mono-ADP-ribosyltransferase) (The Arabidopsis Information Resource (TAIR) (2018a) https://www.arabidopsis.org/servlets/TairObject?id=32909&type=locus)	down

In general, these findings confirm that the change of experimental design was successful, and that the dataset is reliable. Analysis and verification of regulated proteins needs to be conducted in further experiments and was beyond the scope of this work. In the following chapters the focus will be on the characterization of the phospholipase PLDγ1 which was found to be differentially regulated by chitin and PGN in one of the pre-experiments (data not shown).

3.2 THE ROLE OF PLDr1 IN PLANT INNATE IMMUNITY

3.2.1 PLDγ is a putative interactor of CERK1

As already mentioned in the introduction, PLDs are known to be important in signal transduction and were shown to be also involved in plant innate immunity (Li and Wang, 2019, Zhao, 2015). Whilst accomplishing quantitative phosphoproteomic analyses and facing technical problems as described in the chapter above, the role of PLDδ in controlling powdery mildew fungi defence was shown by Pinosa et al. (2013). At the same time Dr. Xiaokun Liu and Dr. Wei-Lin Wan, in our department, found out that PLDγ3 might be a potential interactor of CERK1 based on the results of researching the 'Membrane-based Interactome Database' (M.I.N.D.) (Jones et al., 2014) shown in Table 3-3. Although in the later adapted phosphoproteomic analysis PLDγ1 could not be found anymore, these observations led to the further characterization of the role of PLDγ-proteins in plant innate immunity.

Table 3-3: Putative interactors of CERK1 based on MIND-database analysis (data set from 04.03.2013)

AGI ID	Name	Subtype
AT1G58520	RXW8, lipases; hydrolases, acting on ester bonds	ERD4 family
AT5G49630	AAP6, amino acid permease 6	AAAP
AT2G46450	ATCNGC12, CNGC12, cyclic nucleotide-gated channel 12	CNGC
AT5G52860	ABC-2 type transporter family protein	ABC
AT2G25600	SPIK, AKT6, Shaker pollen inward K+ channel	K+ channel
AT2G40540	KT2, ATKT2, SHY3, KUP2, ATKUP2, TRK2, potassium transporter 2	KUP
AT5G09400	KUP7, K+ uptake permease 7	KUP
AT3G52080	chx28, cation/hydrogen exchanger 28	Monovalent Cation: Proton Antiporter-2 (CPA2) Family
AT1G79820	SGB1, Major facilitator superfamily protein	STP
AT1G35720	ANNAT1, OXY5, ATOXY5, annexin 1	Annexin (Annexin) Family
AT2G26180	IQD6, IQ-domain 6	IQD
AT2G31280	CPUORF7, conserved peptide upstream open reading frame 7	bHLH
AT4G18780	CESA8, IRX1, ATCESA8, LEW2, cellulose synthase family protein	Cellulose Synthase
AT2G40890	CYP98A3, cytochrome P450, family 98, subfamily A, polypeptide 3	cytochrome P450
AT2G30490	ATC4H, C4H, CYP73A5, REF3, cinnamate-4-hydroxylase	cytochrome P451
AT3G26830	PAD3, CYP71B15, Cytochrome P450 superfamily protein	cytochrome P452
AT3G63420	AGG1, ATAGG1, GG1, Ggamma-subunit 1	G protein beta
AT3G51830	SAC8, SAC domain-containing protein 8	phosphoinositide phosphatase
AT5G63990	Inositol monophosphatase family protein	phosphoinositide phosphatase
AT1G07430	HAI2, highly ABA-induced PP2C gene 2	PP2C
AT4G11840	PLDGAMMA3, phospholipase D gamma 3	Phospholipase D
AT2G01275	RING/FYVE/PHD zinc finger superfamily protein	RING finger
AT5G41990	WNK8, ATWNK8, with no lysine (K) kinase 8	MAPKKK
AT4G08470	MAPKKK10, MEKK3, MAPK/ERK kinase kinase 3	MAPKKK
AT2G43850	Integrin-linked protein kinase family	MAPKKK
AT3G23000	CIPK7, SnRK3.10, PKS7, ATSRPK1, ATSR2, CBL-interacting protein kinase 7	CIPK
AT4G21940	CPK15, calcium-dependent protein kinase 15	CPK
AT1G18890	ATCDPK1, CPK10, CDPK1, AtCPK10, calcium-dependent protein kinase 1	CPK
AT1G69910	Protein kinase superfamily protein	RLK/Pelle
AT3G19300	Protein kinase superfamily protein	RLK/Pelle
AT3G45390	Concanavalin A-like lectin protein kinase family protein	RLK/Pelle
AT3G45430	Concanavalin A-like lectin protein kinase family protein	RLK/Pelle
AT4G11460	CRK30, cysteine-rich RLK (RECEPTOR-like protein kinase) 30	RLK/Pelle
AT1G78860	D-mannose binding lectin protein with Apple-like carbohydrate-binding domain	RLK/Pelle
AT5G38990	Malectin/receptor-like protein kinase family protein	RLK/Pelle
AT4G23220	CRK14, cysteine-rich RLK (RECEPTOR-like protein kinase) 14	RLK/Pelle
AT1G04310	ERS2, ethylene response sensor 2	Histidine Kinase
AT2G26380	Leucine-rich repeat (LRR) family protein	RLP
AT2G33050	AtRLP26, RLP26, receptor like protein 26	RLP
AT3G12180	Cornichon family protein	Cornichon family protein
AT3G10980	PLAC8 family protein	PLAC8 family protein
AT2G01490	phytanoyl-CoA dioxygenase (PhyH) family protein	phytanoyl-CoA dioxygenase (PhyH) family protein
AT1G02380	unknown protein	unknown protein
AT5G23920	unknown protein	unknown protein
AT4G16444	Unknown	Unknown

3.2.2 Characterization of PLDγ T-DNA insertion lines

To verify the function of PLDγ family members in plant immunity T-DNA insertion lines (provided by Mats X. Andersson, University of Gothenburg or ordered at Gabi-Kat, University of Bielefeld) were used for most of the experiments. In Figure 3-3 the gene structures of the three *PLDγ* family members *PLDγ1 (AT4G11850)*, *PLDγ2 (AT4G11830)* and *PLDγ3 (AT4G11840)* are displayed with the corresponding position of the T-DNA insertions.

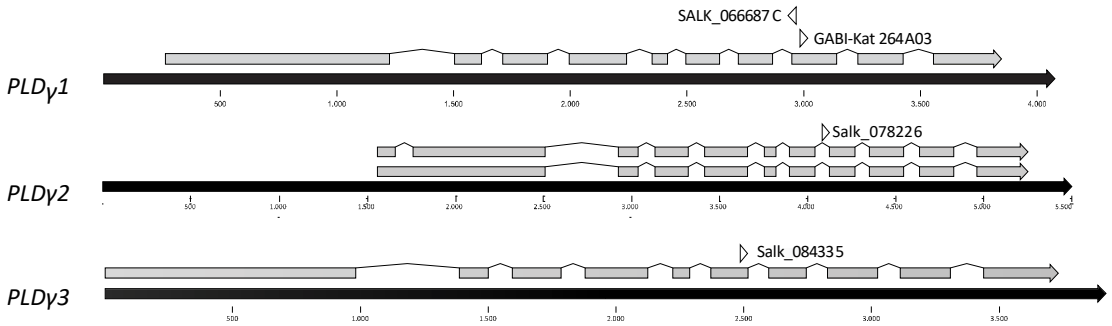

Figure 3-3: T-DNA insertion lines of PLDγ family members

Schematic display of the genes *PLDγ1, PLDγ2 and PLDγ3.* Position of the T-DNA insertions is indicated with arrows above the gene together with the corresponding name of the line. Coding region of the gene are displayed in grey. Thicker bars indicate exons, thin lines correspond to introns. The black bar shows the whole gene including untranslated region as provided by tair database *(The Arabidopsis Information Resource (TAIR), 2019d, The Arabidopsis Information Resource (TAIR), 2019c, The Arabidopsis Information Resource (TAIR), 2019b)*

Quantitative real time PCR was performed to quantify residual transcript levels of the affected gene in the mutants. In *pldγ1-1* (SALK_066687) plants no *PLDγ1*- transcript could be amplified, whereas in the *pldγ1-2* (GABI-Kat 264 A03) mutant residual transcript was detected (Figure 3-4 **A** and **B**). Hence, in all further experiments *pldγ1-1* was addressed to be a true mutant and results from *pldγ1-2* were interpreted with caution. Similar results were obtained for the *pldγ2-1* (Figure 3-4 **C**) and *pldγ3-1* (Figure 3-4 **D**) mutants. Both lines still had residual transcript for the corresponding gene. However, the T-DNA insertion in *pldγ2-1* might not be in an exon but in an intron and could be lost during splicing events. Due to 95 % of similarity (Qin and Wang, 2002) between all three genes, *PLDγ3* specific primers could also bind to the other genes. In pre-experiments *PLDγ1 and PLDγ3* specific primers were tested for cross reactivity with other *PLDγ* genes by using the primers in a PCR with a cDNA clone of the corresponding other gene as template. In these experiments (data not shown) it was observed that *PLDγ1*-specific primers bound to *PLDγ1* and *PLDγ3* cDNA-containing plasmids. But the

efficiency of binding *PLDγ3* was very poor and couldn't be observed in plant cDNA samples. However, primers designed for only binding to *PLDγ3* were able to attach to *PLDγ3* and *PLDγ1* with high efficiency. *PLDγ2* primers and cDNA were not tested because the cloning of *PLDγ2* was not successful, although the study of Qin et al. (2006) showed successful cloning and bacterial expression of all three isoforms. Ordered cDNA clones unfortunately presented empty vector clones or contained only fragments of the gene of interest. But due to the high similarity it might be reasonable to assume that PCR-experiments with *PLDγ2-primers* would be similar to *PLDγ3* results. Therefore, it was not clear whether residual expression of *PLDγ2* and *PLDγ3* was due to incomplete knockouts of the genes or to unspecific binding of the primers to the other genes. Nevertheless, results need to be interpreted carefully. Further T-DNA insertion lines for *PLDγ2* and *PLDγ3* were obtained, but for most of them it was not possible to unambiguously verify the presence of the T-DNA insertion in genotyping PCRs (data not shown). Additionally, residual transcript levels could not be analysed properly. Stable transformed lines with artificial micro RNA constructs silencing all three genes of *PLDγ* were initiated but not analysed further, yet.

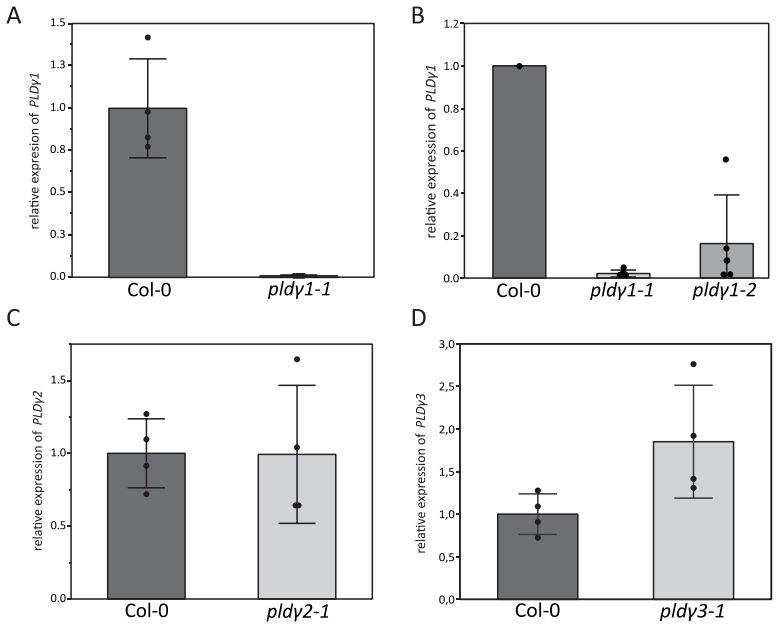

Figure 3-4: Transcript analysis of PLDγ1, PLDγ2 and PLDγ3 in corresponding T-DNA insertion lines by qRT-PCR

RNA was extracted from leaf material of 6-8-week-old wild-type Col-0, *pldγ1-1*, *pldγ1-2*, *pldγ2-1* or *pldγ3-1* plants and subjected to RT-qPCR analysis using gene specific primers. Gene expression was normalized to transcript levels of the elongation factor *EF1*α. Results are presented as the mean of 4 individual plants and plotted as fold induction compared to the respective control, Col-0, which was set to 1. Error bars indicate SD (*n* = 4). **A** Relative *PLDγ1* expression in the *pldγ1-1* mutant. **B** Relative *PLDγ1* expression in *pldγ1-1* and *pldγ1-2* mutants. **C** Relative *PLDγ2* expression in *pldγ2-1* mutant plants. **D** Relative *PLDγ3* expression in the *pldγ3-1* line.

3.2.3 Bacterial and fungal infection in Arabidopsis is negatively regulated by PLDγ1 but not by PLDγ2 and PLDγ3

To characterize the function of PLDγ family members in plant innate immunity T-DNA insertion lines of *PLDγ1*, *PLDγ2* and *PLDγ3* were tested for their resistance towards different pathogens. Infection with the hemibiotrophic bacterium *Pseudomonas syringae* showed that *pldγ1-1* mutants developed a clear resistance towards the pathogen compared to wild-type Col-0 plants after three days of infection (Figure 3-5). In contrast, *pldγ2-1* and *pldγ3-1* lines were not as resistant as *pldγ1-1* plants and the infection rate was similar to wild-type plants.

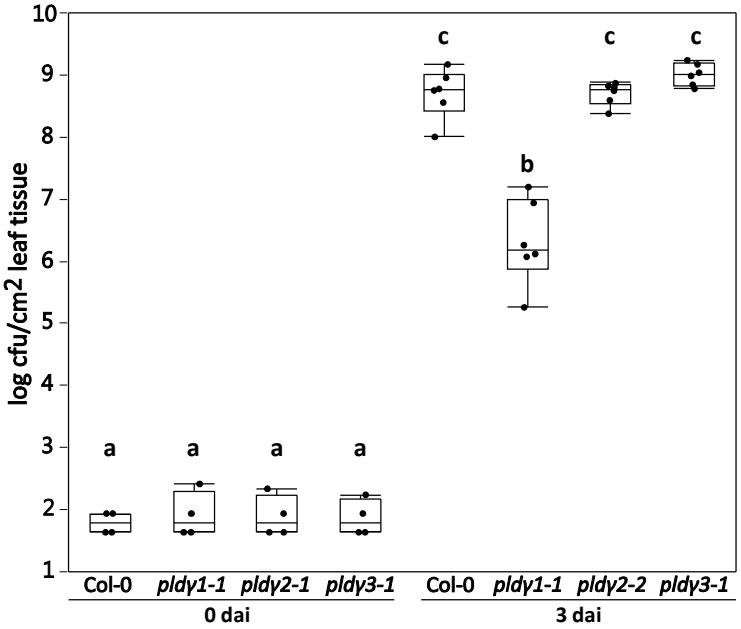

Figure 3-5: Mutants of pldγ1-1 were more resistant to Pseudomonas syringae pv. tomato DC3000 infection than pldγ2-1 and pldγ3-1 or wild-type plants.

Wild-type Col-0, *pldγ1-1*, *pldγ2-1* or *pldγ3-1* plants were infiltrated with 10^4 cfu/mL *Pst* DC3000 and growth of the bacteria was monitored at zero or 3 days after infection (dai). Box plots show the minimum, first quartile, median, third quartile, and a maximum of log cfu/cm^2 leaf tissue (n=4 for 0 dai; n=6 for 3 dai). Labels a-c indicate homogenous groups according to post-hoc comparisons following one-way ANOVA (Tukey-Kramer multiple comparison analysis at a probability level of $p < 0.05$).

Also, the infection with the necrotrophic fungal pathogen *Botrytis cinerea* indicated that only *pldγ1-1* plants were more resistant to the infection, but not *pldγ2-1* and *pldγ3-1* plants. By performing qRT-PCR analysis with specific *Botrytis cinerea* primers, fungal DNA could be quantified in a plant-fungus total DNA mixture. Figure 3-6 **A** points out that the DNA mixture of infected *pldγ1-1* plants contained much less *Botrytis* DNA than mixtures from *pldγ2-1* and *pldγ3-1* mutant or wild-type plants. In additional experiments

could be verified that the fungal DNA content was reduced significantly in *pldγ1-1* plants (Figure 3-6 **B**). However, *pldγ1-2* plants did not show such a clear and more variable phenotype (Figure 3-6 B), which could be explained by residual *PLDγ1* transcript levels in the *pldγ1-2* mutants compared to the *pldγ1-1* line (Figure 3-6 **B**).

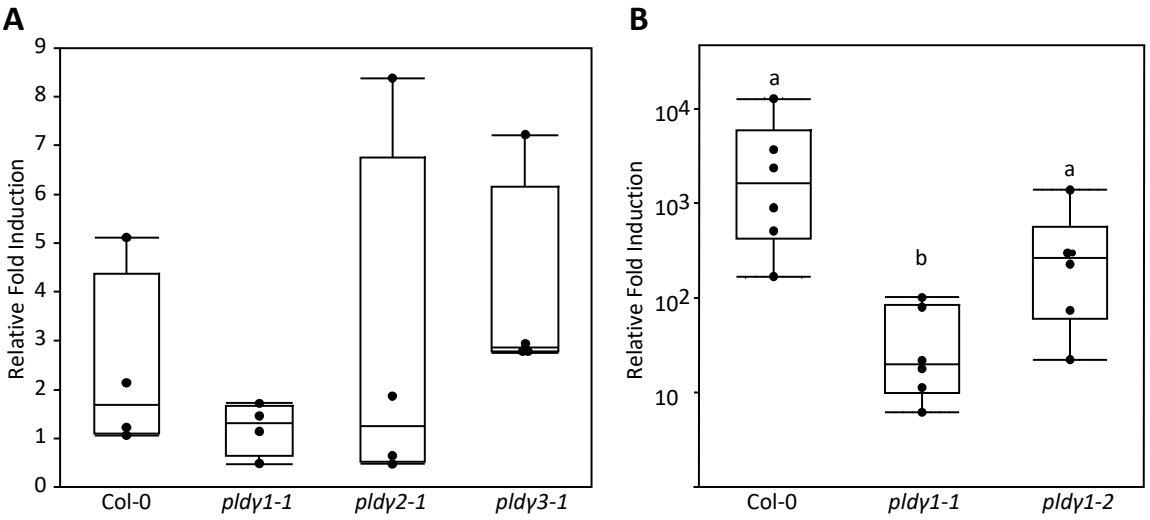

Figure 3-6: Mutants of pldγ1-1 were more resistant to Botrytis cinerea infection compared to wild-type plants

Leaves of 6-week-old plants were inoculated with $5x10^6$/mL *Botrytis cinerea* spores. Three days after inoculation total DNA was extracted from infected leaf material and used for the quantification of fungal biomass via qRT-PCR. The relative amount of *Botrytis cinerea* genomic *Actin*-DNA levels to *Arabidopsis Rubisco* (large subunit) levels was used to quantify fungal biomass. **A** Relative quantification of fungal biomass in wild-type Col-0, *pldγ1-1*, *pldγ2-1* or *pldγ3-1* plants. Box plots show the minimum, first quartile, median, third quartile, and a maximum of fold induction of *Botrytis Actin* (*n=4*) compared to *Botrytis Actin* at 0 dai. **B** Comparison of *Botrytis Actin* levels in wild-type Col-0, *pldγ1-1* or *pldγ1-2* leaf tissue. Box plots show the minimum, first quartile, median, third quartile, and a maximum of fold induction of *Botrytis Actin* (*n=6*) compared to *Botrytis Actin* at 0 dai. Labels a-c indicate homogenous groups according to Kruskal-Wallis one-way ANOVA, followed by an each-pair comparison Wilcoxon rank-sum test with a probability level of $p < 0.05$.

This result is supported by lesion size quantifications of disease symptoms on infected leaves (Figure 3-7 **A**). Again, in *pldγ1-1* plants the lesion sizes of the disease symptoms were significantly smaller than the lesion sizes of the disease symptoms in wild-type or *pldγ1-2* plants.

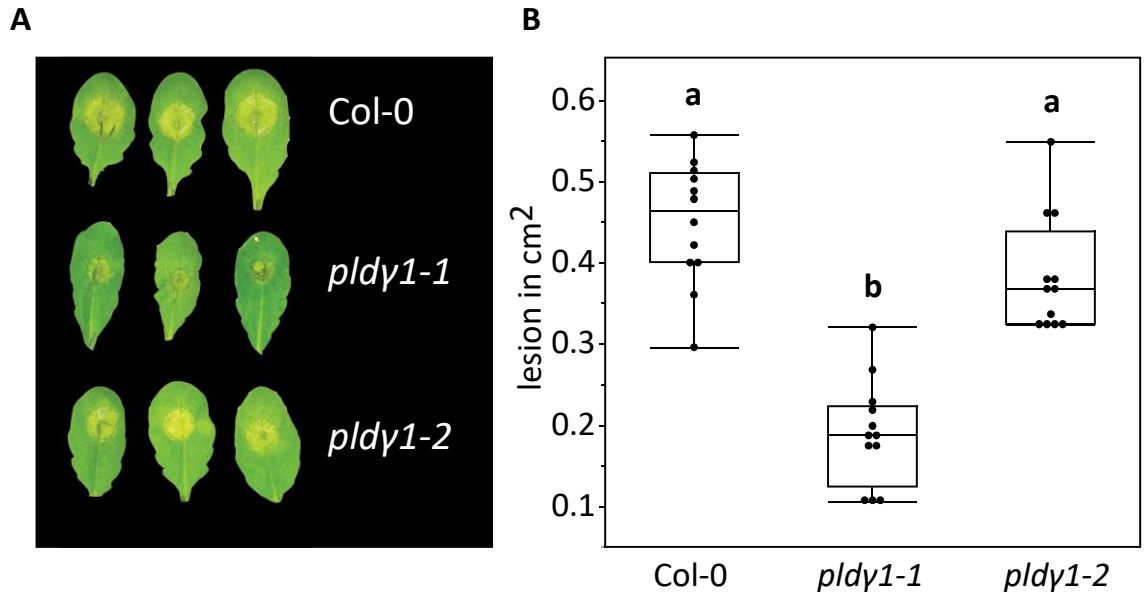

Figure 3-7: pldγ1-1 mutants displayed smaller lesions upon infection with Botrytis cinerea

Wild-type Col-0, *pldγ1-1* or *pldγ1-2* plants were inoculated with 5x10^6 /mL *Botrytis cinerea* spores. Three days after inoculation the plants were monitored. **A** Pictures of representative infected leaves 3 days after infection. **B** Lesion sizes were determined with a pixel-based approach and then calculated using a 1 cm^2 standard. Box plots show the minimum, first quartile, median, third quartile, and a maximum (n=12). Labels a-b indicate homogenous groups according to post-hoc comparisons following one-way ANOVA (Tukey-Kramer multiple comparison analysis at a probability level of $p < 0.05$).

Contrary to *Botrytis* resistance, the infection with *Alternaria brassicicola*, another necrotrophic fungal pathogen, yielded a higher disease index for the *pldγ1-1* mutant, but not for *pldγ2-1* and *pldγ3-1* plants after monitoring day 7, day 10 and day 13 post inoculation. In Figure 3-8 **A** representative leaves after 13 dai are shown. Leaves of *pldγ1-1* showed severe necrotic areas all over the leave. In contrast to that in Col-0 and *pldγ2-1* and *pldγ3-1* necrotic tissues were only visible at the infection sites. Although statistic comparison of the means could only be applied on the data within one monitoring day, the difference of the disease index on day 10 dai and 13 dai between *pldγ1-1* plants and the other lines was significant (Figure 3-8 **B**). However, quantification of the disease index was based on infection symptoms on the leaf (see section 2.6.3). Quantification of *Alternaria* DNA like shown for *Botrytis cinerea* (Figure 3-7 **B**) was not successful, so far. Consequently, it was difficult to prove what was exactly the reason for these enhanced infection symptoms on *pldγ1-1* plants

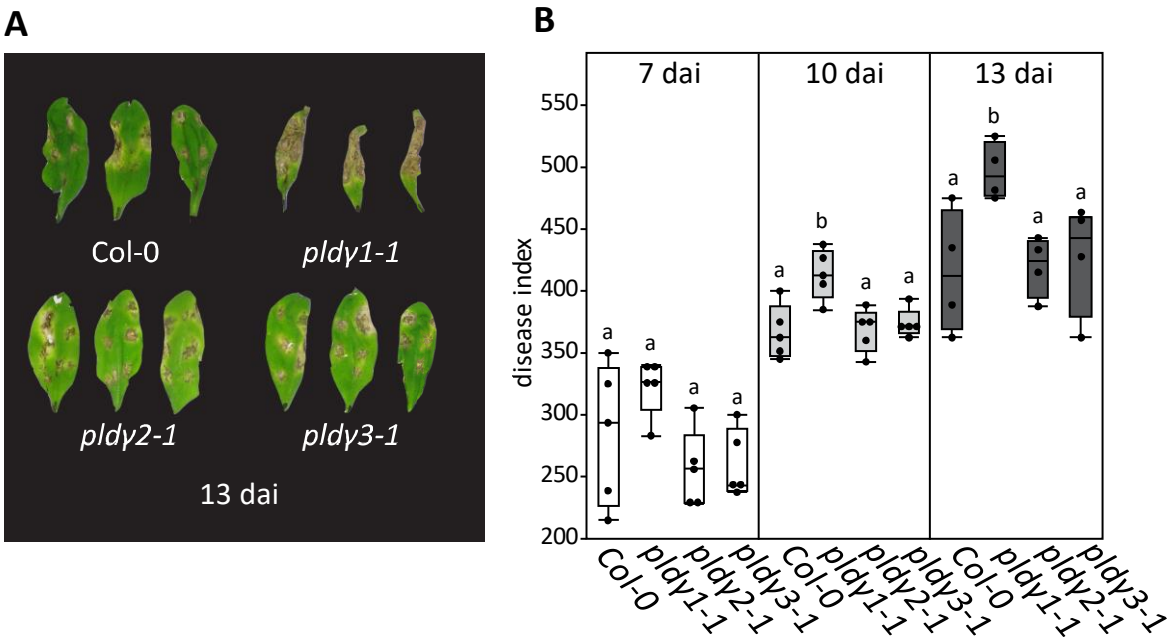

Figure 3-8: Infection with Alternaria brassicicola induced more severe infection symptoms on pldγ1-1 than to pldγ2-1 and pldγ3-1 mutant plants

Leaves of 5-week old wild-type Col-0, *pldγ1-1, pldγ2-1 or pldγ3-1* plants were inoculated with 6x5 µL drops containing $1x10^6$ spores/mL of the necrotrophic fungus *Alternaria brassicicola.* 7, 10 and 13 days after inoculation (dai) disease symptoms were monitored and classified in categories. Out of this the disease index was ascertained. **A** Pictures of representative infected leaves after 13 days of infection. **B** Disease indices of 4 (13 dai) to 5 (7 and 10 dai) independent *Alternaria* infection assays. Box plots showing the minimum, first quartile, median, third quartile, and a maximum (7 and 10 dai n=5; 13 dai n=4). Labels a-b indicate homogenous groups within one monitoring day according to post-hoc comparisons following one-way ANOVA (Dunnet's multiple comparison analysis with wild-type Col-0 as control group at a probability level of $p < 0.05$)

Summarizing, the results of infection assays showed clearly that *pldγ1-1* mutants behaved significantly different than wild-type plants, *pldγ2-1 and pldγ3-1 mutant plants. Pldγ1-1* (and sometimes *pldγ1-2*) mutant plants were more resistant to bacterial *Pseudomonas* and fungal *Botrytis* infection. Surprisingly, *pldγ1-1* plants appeared to react stronger to *Alternaria brassicicola* infection which might lead to the assumption that they were more susceptible. However, for *Alternaria* infections further experiments with more technical replicates and the quantification of fungal biomass would be crucial to distinguish between an enhanced fungal growth in the *pldγ1-1* mutant versus a stronger resistance response.

3.2.4 MAMP induced ROS-production is negatively regulated by PLDγ1

To address the question why *pldγ1-1* plants were more resistant to bacterial and fungal infections, described in the chapter before, early immune responses such as the accumulation of reactive oxygen species (ROS) in a ROS-burst and the activation of MAP-kinases were analysed. Leaf pieces of adult plant leaves were elicited with 1 µM chitin heptamers (C7) or octamers (C8), as a fungal MAMP, and 1 µM flg22, representative of a bacterial MAMP. Oxidative burst results upon flg22 elicitation are displayed exemplarily in Figure 3-9 as a fold induction compared to the ROS-accumulation detected in wild-type plants. As shown in Figure 3-9, *pldγ1-1* plants showed a higher ROS-burst induction after flg22 treatment, while in *pldγ2-1* and *pldγ3-1* plants ROS levels were similar to the wild-type response. Although the results were sometimes variable (in some experiments wild-type like responses or even opposite results were obtained), in general flg22-triggered ROS accumulation was enhanced in *pldγ1-1* leaf pieces compared to *pldγ2-1* and *pldγ3-1*. Similar results were obtained for chitin treatment (Table 3-4). In *pldγ1-1* an enhanced ROS burst towards chitin elicitation could be observed compared to wild-type plants. The summary of all results concerning ROS burst shown in Table 3-4, leads to the assumption that PLDγ1 has a negative regulatory function in the flg22 but also in chitin induced signalling pathway. However, the role of PLDγ2 and PLDγ3 is not clear, which might be caused by the residual transcript levels as shown in chapter 3.2.2. Furthermore, there might be also redundancy effects in the mutants which cause contrary results.

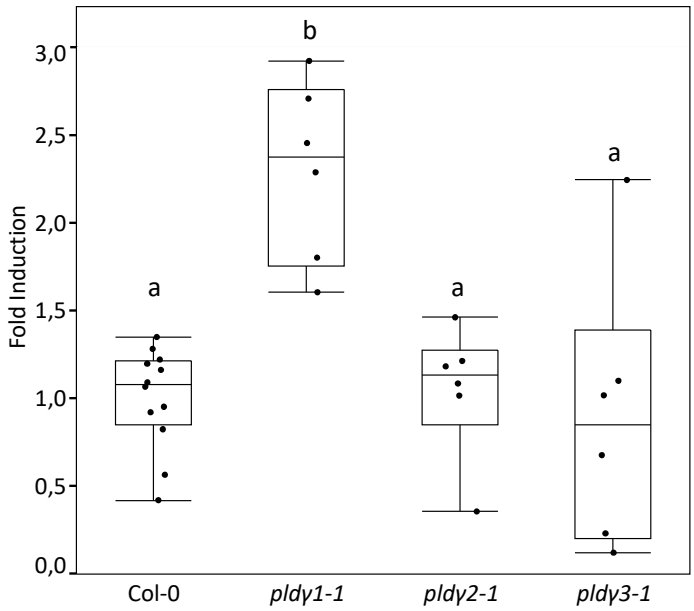

Figure 3-9: The oxidative burst was enhanced in pldγ1-1 but not in pldγ2-1 and pldγ3-1 mutants compared to wild-type plants.

The production of reactive oxygen species was triggered by 1 µM flg22 and water as control in wild-type Col-0, *pldγ1-1, pldγ2-1 or pldγ3-1* plants, measured in relative light units (RLU) and expressed here as fold induction to the mean of Col-0, which was set as 1. Box plots show the minimum, first quartile, median, third quartile, and a maximum of fold induction of peak value minus background value (n≥6). Water treated samples had no peak value, therefore they are not displayed in the figure. Labels a-b indicate homogenous groups according to post-hoc comparisons following one-way ANOVA (Tukey-Kramer multiple comparison analysis at a probability level of $p < 0.05$).

Table 3-4: Summary of all ROS-burst experiments performed in pldγ mutants

line	treatment	response compared to wild-type Col-0			
		higher	equal	lower	total
pldγ1-1	flg22	13	3	2	18
pldγ1-2	flg22	1	2	2	5
pldγ2-1	flg22	2	2	2	6
pldγ3-1	flg22	3	3	4	10
pldγ1-1	C8	12	3	3	18
pldγ1-2	C8	3	1		
pldγ2-1	C8	4	3	2	9
pldγ3-1	C8	3	5	5	13

Another early immune response is the activation of MAP-kinases. It is known that upon infection or elicitation especially MPK3, MPK6 and MPK4/MPK11 play an important role (Thulasi Devendrakumar et al., 2018a, Colcombet and Hirt, 2008). Since PLDγ1 was shown to be involved in ROS burst regulation in Arabidopsis (Figure 3-9 and Table 3-4) it was interesting to know whether MAP-kinase activation is also regulated by PLDγ1. Therefore, seedlings were elicited with 1 µM flg22 and MAP-kinase activation was determined via western blot analysis. The results in Figure 3-10 indicate that PLDγ1-mediated signalling was independent from the activation of MAP-kinases as pldγ1-1 plants had similar activation of MPK3, 6 and 4/11 as wild-type plants upon flg22 stimulation. Here, also PLDγ1 complementation lines, which will be introduced in the next chapter, were used and showed the same level of MAPK activation as wild-type Col-0 plants or the pldγ1-1 mutant.

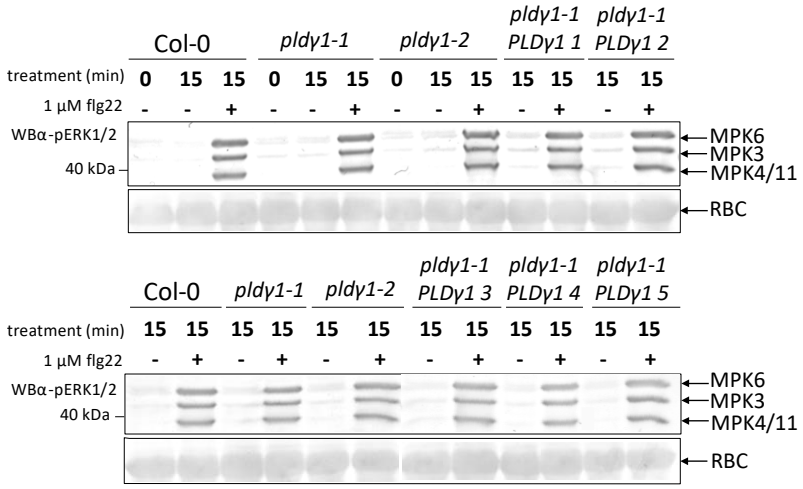

Figure 3-10: MAP kinases are not differently activated in pldγ1-1 and pldγ1-1 PLDγ1 complementation lines

The MAP kinase assay was performed with 10-day-old seedlings which were elicited with 1 µM flg22 for 15 min or water as control. Activation of MAP-kinases was detected using the p44/p42 anti-phospho antibody. Ponceau-S staining of RBC (Ribulose-bis-phosphate-carboxylase large chain) served as loading control.

3.2.5 Generation of complementation lines pldγ1-1 PLDγ1

In order to verify whether *PLDγ1* depletion is responsible for the effects seen in the *pldγ1-1* plants (Section 3.2.3) we transformed *pldγ1-1* plants with a *PLDγ1* cDNA construct linked to a C-terminal GFP tag under the control of the 35S promotor to recover the wild-type phenotype. *PLDγ1* was cloned into a binary vector containing the GFP sequence and then stably transformed via *Agrobacteria* meditated transformation

into *pldγ1-1* plants. In the beginning selection was done with kanamycin-containing ½ MS-plates.

Surviving plants were verified for the presence of *PLDγ1* mRNA and GFP fusion protein as shown in Figure 3-11. In the first generation of transformed plants (T1), displayed in Figure 3-11 **A**-**B**, several plants showed detectable transcript and protein levels of PLDγ1-GFP. However, the PLDγ1-GFP protein was only detectable after immunoprecipitation using a GFP-trap. Also, the fluorescence was not detectable using fluorescence microscopy. Therefore, in the next generation it was envisaged to identify plants with higher or equal expression level of PLDγ1 compared to wild-type plants. Unfortunately, all these selected plants died and/or could not produce seeds due to unknown reasons. Therefore, plants with a lower *PLDγ1-GFP* expression level had to be used. Interestingly, most of those plants also died before flowering. In the end we could only obtain seeds of the lines shown in Figure 3-11 **C** and from two other independent lines coming from plant 1 and 11 in the beginning (data of selection is not shown). In the third generation (T3) general *PLDγ1-GFP* expression levels were low. Nevertheless, there were some plants with similar or higher gene expression levels compared to the wild-type control. However, these plants had problems to flower and to produce seeds, again. Remarkable is the constant tendency that plants with wild-type or higher *PLDγ1-GFP* expression levels were not able to flower or to produce seeds. In contrast, lines expressing *PLDγ1* at a very low level survived hygromycin selection which was used since the T3 selection instead of kanamycin which also might contribute to killing plants. Eventually, we generated stable lines expressing *PLDγ1* in the *pldγ1-1* mutant background (Figure 3-11 **D**-**E** and Table 3-5); though, the expression of *PLDγ1-GFP* was very low.

Table 3-5: Overview of complementation lines

Name	Line	Protein expression
pldγ1-1-PLDγ1 1	12-4-3-2	yes
pldγ1-1-PLDγ1 2	12-8-2-2	yes
pldγ1-1-PLDγ1 3	12-8-4-4	yes
pldγ1-1-PLDγ1 4	12-9-1-3	yes
pldγ1-1-PLDγ1 5	11-13-3-3	not tested
pldγ1-1-PLDγ1 6	1-41-1-1	not tested

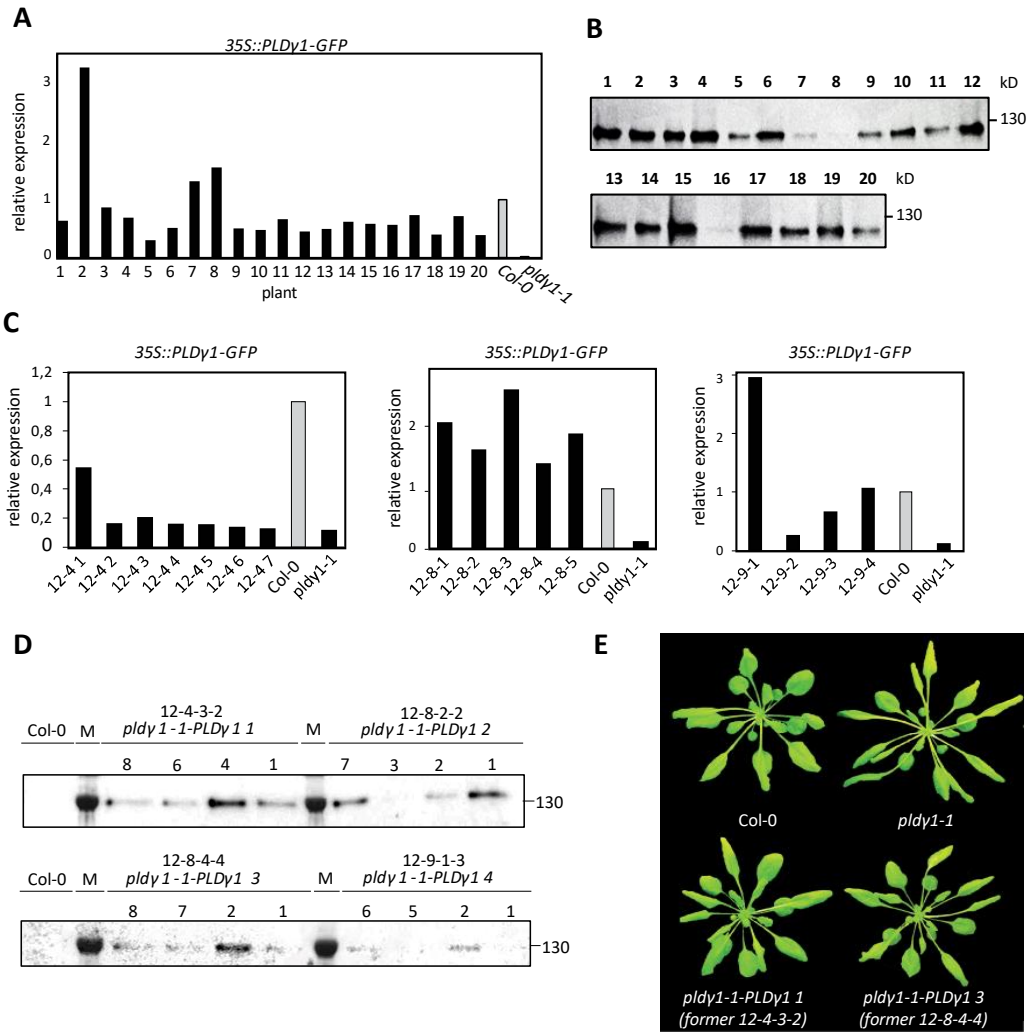

Figure 3-11: Generation of pldγ1-1 PLDγ1 complementation lines

Complementation lines were generated by stable transformation of *pldγ1-1* with PLDγ1-GFP under control of the 35S-Promotor. **A** The T1 generation was verified by qRT-PCR-based transcript analysis of *PLDγ1* and normalized to *EF1α* transcript levels and plotted as fold induction compared to wild-type Col-0 as control, set to 1. **B** WB-analysis of PLDγ1-GFP expression in the T1 generation. PLDγ1-GFP was immunoprecipitated from total protein extracts using Chromotek GFP-agarose beads and detected in western blot analysis using an anti-GFP antibody. **C** qRT-PCR transcript analysis of *PLDγ1* in the T3 generation. Results were normalized to *EF1α* transcript levels and plotted as fold induction compared to wild-type Col-0 as control, set to 1. **D** WB-analysis of PLDγ1-GFP expression in the T3 generation. PLDγ1-GFP was immunoprecipitated using Chromotek GFP-agarose beads followed by western blot analysis as described in **B**. **E** Phenotypical comparison of 8-week old plants of Col-0 and *pldγ1-1-PLDγ1 1 (former 12-4-3-2) and pldγ1-1-PLDγ1 3 (former 12-8-4-4)*.

3.2.6 Resistance of pldγ1 to Pseudomonas infection can be reversed in complementation lines

As described in the last section, complementation lines could be obtained which were next tested for their resistance towards *Pst* DC3000 infection. Although the *PLDγ1-GFP* containing plants had only low levels of protein, Figure 3-12 shows that the complementation lines were as susceptible to *Pst* infection as wild-type plants while the

pldγ1-1 mutant line still was more resistant. The complementation line *pldγ1-1-PLDγ1 1* (former 12-4-3-2, see Table 3-5) was fully complemented regarding the resistance phenotype and had similar infection rates as observed in wild-type plants while the two lines *pldγ1-1-PLDγ1 2 and 3* (former 12-8-2-2 and 12-8-4-4, see Table 3-5) had intermediate phenotypes as they were significantly more susceptible than *pldγ1-1* plants but not as susceptible as wild-type plants. However, the complementation line *pldγ1-1-PLDγ1 4* (former 12-9-3-1, see Table 3-5) showed no complementation in this assay and was still as resistant as *pldγ1-1.* This output correlates with the protein amounts shown in the chapter before. *pldγ1-1-PLDγ1 1* had the highest GFP protein levels while *pldγ1-1-PLDγ1 4* had very little or no expression at all.

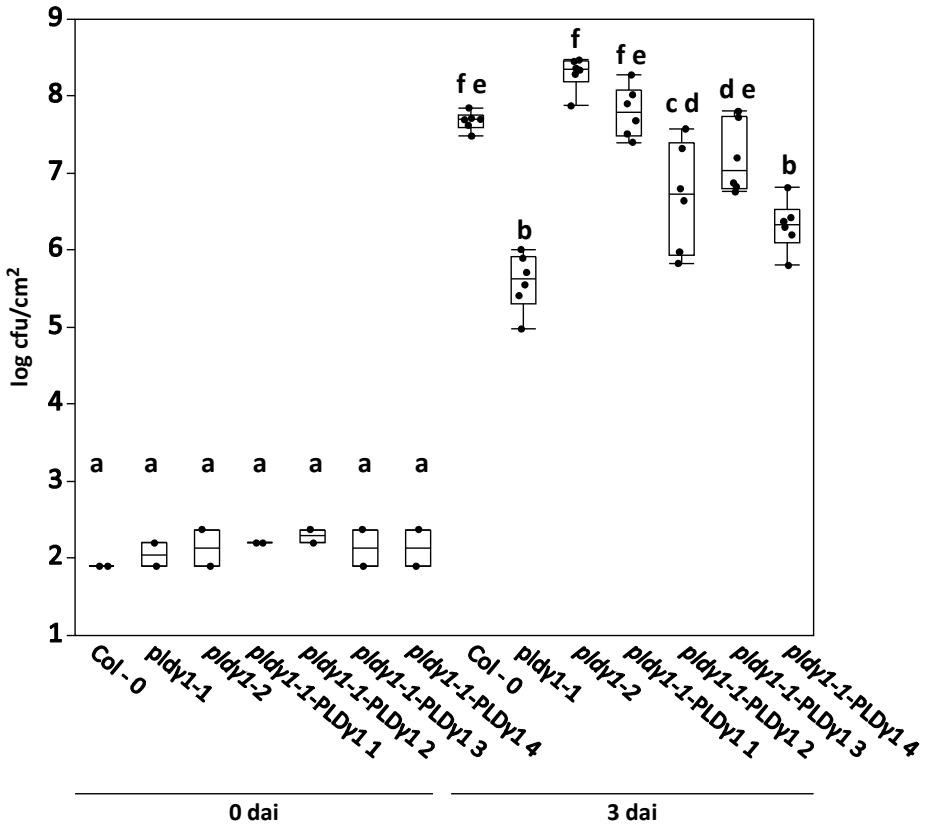

Figure 3-12: Complementation of pldγ1-1 with 35S::PLDγ1-GFP led to wild-type infection levels
Wild-type Col-0, *pldγ1-1, pldγ1-1-PLDγ1 1, pldγ1-1-PLDγ1 2, pldγ1-1-PLDγ1 3* or *pldγ1-1-PLDγ1 4* plants, were infiltrated with 10^4 cfu/mL *Pst* DC3000 and growth of the bacteria was monitored at zero or 3 days after infection (dai). Box plots show the minimum, first quartile, median, third quartile, and a maximum of log cfu/cm^2 (n=4 for 0 dai n=6 for 3 dai). Labels a-c indicate homogenous groups according to post-hoc comparisons following one-way ANOVA (Tukey-Kramer multiple comparison analysis at a probability level of $p < 0.05$).

In a further experiment (Figure 3-13), where two independent complementation lines, *pldγ1-1-PLDγ1 5* and *pldγ1-1-PLDγ1 6* were included (see Table 3-5), the results of the

previous experiment could be repeated for *pldγ1-1-PLDγ1 1* and *pldγ1-1-PLDγ1 2*. Contrary to the previous experiment *pldγ1-1-PLDγ1 4* was complemented this time although it was not as clear as the other two lines mentioned before. The new included independent complementation line *pldγ1-1-PLDγ1 5* showed similar results as *pldγ1-1-PLDγ1 1* and *pldγ1-1-PLDγ1 2* plants, whereas the *pldγ1-1-PLDγ1 6* line behaved as *pldγ1-1-PLDγ1 4* which was not complemented in the experiment before. However, in this experiment all plants could not complement the phenotype of *pldγ1-1* plants completely. They were significantly more susceptible than *pldγ1-1* plants but also significantly more resistant than wild-type plants. Thus, we can as assume that expression of PLDγ1-GFP led to partial complementation. However, summarizing all experiments on the complementation lines, it could be approved that the *pldγ1-1* phenotype could be reversed by the complementation lines showed in this work.

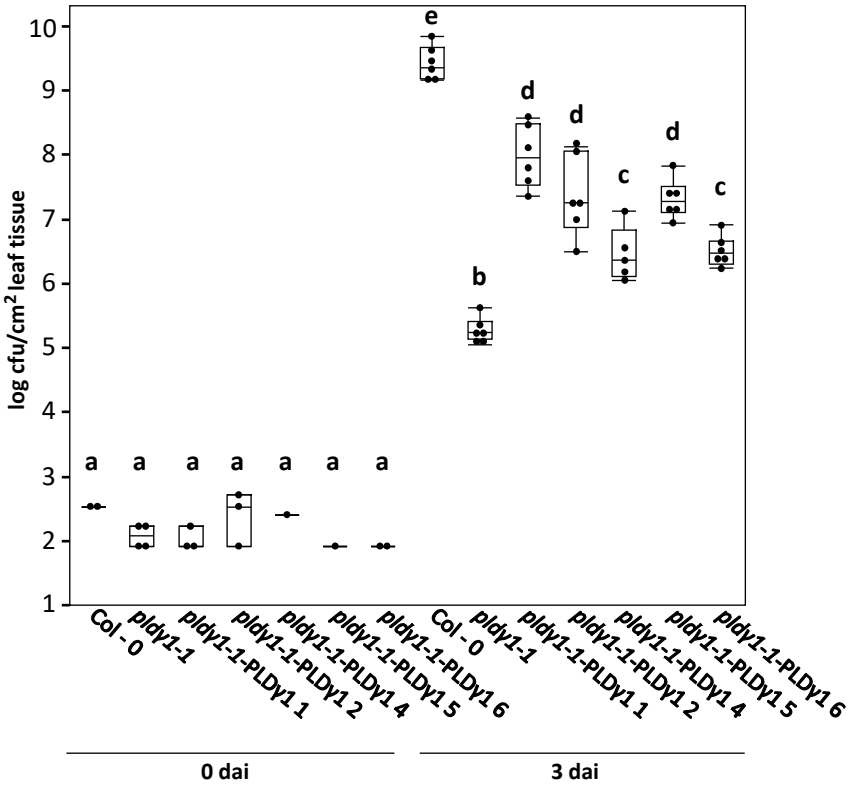

Figure 3-13: Independent complementation of pldγ1-1 with 35S::PLDγ1-GFP showed partial phenotype reversion I Pst infection assays

Wild-type Col-0, *pldγ1-1, pldγ1-1-PLDγ1 1, pldγ1-1-PLDγ1 2, pldγ1-1-PLDγ1 4, pldγ1-1-PLDγ1 5 or pldγ1-1-PLDγ1 6* plants were infiltrated with 10^4 cfu/mL *Pst* DC3000 and growth of the bacteria was monitored at zero or 3 days after infection (dai). Box plots show the minimum, first quartile, median, third quartile, and a maximum of log cfu/cm^2 leaf tissue (n=1-4 for 0 dai n=6 for 3 dai). Labels a-e indicate homogenous groups according to post-hoc comparisons following one-way ANOVA (Tukey-Kramer multiple comparison analysis at a probability level of $p < 0.05$).

To further proof that PLDγ1 was responsible for the observed phenotype ROS burst experiments were done. In these results the complementation of the phenotype described in Figure 3-14, where *pldγ1-1* plants showed a higher ROS burst, could only be reversed by *pldγ1-1-PLDγ1 3* and partly by *pldγ1-1-PLDγ1 4.* Contrary to the *Pst* infection results, *pldγ1-1-PLDγ1 1* and *pldγ1-1-PLDγ1 2* lines did not show a reversed phenotype and the ROS burst was still significantly higher than in wild-type plants, similar to the *pldγ1-1* mutant.

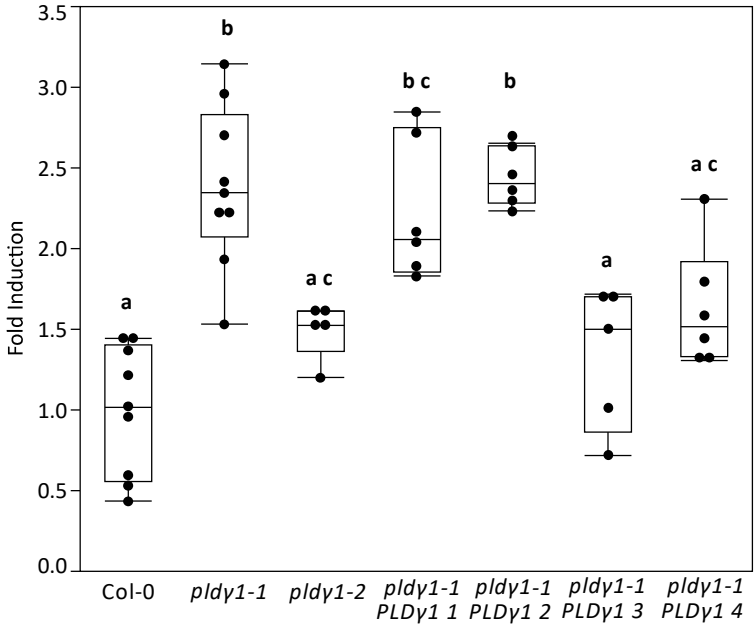

Figure 3-14: Complementation of pldγ1-1 mutant could only reverse elevated ROS levels partially

Production of reactive oxygen species was triggered by 1 µM flg22 and water as control in wild-type Col-0, *pldγ1-1*, *pldγ1-2 and complementation lines* measured in relative light units (RLU) and expressed here as fold induction to the mean of Col-0. Box plots showing the minimum, first quartile, median, third quartile, and a maximum of fold induction of peak value minus background value (n≥6). H_2O-treated samples had no peak value; therefore, they are not shown in the figure. Labels a-c indicate homogenous groups according to post-hoc comparisons following one-way ANOVA (Tukey-Kramer multiple comparison analysis at a probability level of $p < 0.05$).

In summary, the re-insertion of *PLDγ1* into the *pldγ1-1* mutant background could reverse the phenotype for the *Pst* infection for 3 out of 4 complementation lines significantly and for the other lines in a partial way. The complementation of the enhanced ROS-burst phenotype in the *pldγ1-1* mutant was not as clear and partly shows contrary results to the *Pst* results. In these experiments only two lines (*pldγ1-1-PLDγ1 3* and *pldγ1-1-PLDγ1 4)* were able to reverse the higher ROS-burst phenomenon. The

remaining lines still behaved like the *pldγ1-1* plants. However, the ROS-burst phenotype was already variable in earlier tests (see also Table 3-3) and the assay would need to be repeated more often to make a clear statement.

3.2.7 Identification of additional T-DNA insertions in pldγ1-1 (Salk_066687)

Because of the contrary results of *pldγ1-1* and *pldγ1-2* mutant lines, the variability within the ROS measurements and the incomplete complementation observed in some complementation lines we tried to figure out whether *pldγ1-1* might have additional T-DNA insertions in its genome. Therefore, we did a full genome sequencing of the *pldγ1-1* mutant in cooperation with Effthymia Semonidi, Rebecca Schwab and Detlef Weigel from the Max Planck Institute (data not shown). This resulted in the discovery of two additional T-DNA insertions in the promotor region of genes *AT1G77460* and *AT2G31130*, respectively. Meanwhile, these results were also published on the TAIR database and confirmed our results. The importance of these two additional T-DNA insertions was studied in single T-DNA mutants of both genes in a separate Diploma thesis by Raffaele Del Corvo (Del Corvo, 2018). In brief, it was shown that single knockout mutants of the two genes did not lead to the phenotype which could be observed in *pldγ1-1* plants. ROS-burst assays showed similar responses as wild-type plants. For bacterial infection assays the result is unclear because the total growth of the bacteria was quite high and the difference from *pldγ1-1* plants to wild-type plant was very small. Nevertheless, the single knockout plants of *AT1G77460* and *AT2G31130* showed similar responses as wild-type indicating that these genes are not responsible for the phenotype observed in *pldγ1-1* plants.

3.2.8 Generation of a second, independent pldγ1 mutant via TALEN

Due to the problem that *pldγ1-1* had two additional T-DNA insertions, that *pldγ1-2*, *pldγ2-1* and *pldγ3-1* mutants had residual transcript levels and that stably transformed complementation lines delivered partly unexpected results the idea was to generate a second mutant for *PLDγ1*, *PLDγ2* and *PLDγ3* using TAL-effector nucleases (TALENs). These custom-made nucleases can introduce a targeted mutation into a sequence of choice (Zhang et al., 2014). Constructs were cloned in collaboration with Dr. Robert Morbitzer from the department of general genetics of the ZMBP. After stable

transformation of wild-type Col-0 with the constructs, containing a BASTA resistance gene, plants were selected by BASTA application. In the first generation after transformation (T1), expressed TALENs bound to the sequence area of interest and introduced double strand breaks. This could lead to mutation in this area in following generations due to incorrect insertions or deletions by the DNA repair mechanism of the cell. To check whether TALENs were active towards the *PLDγ1*, *PLDγ2* and *PLDγ3* genes the genomic region surrounding the binding area of the TALEN was amplified by PCR with specific primers and obtained fragments were then sequenced. If TALENs are active the alignment of the sequences to the reference sequence will abort/mismatch in the activity region of the nuclease. In Figure 3-15 an example is shown. The sequence accuracy stopped in the midway between the two binding sites of the corresponding TAL-effectors, which indicates that the nucleases have been active in the plant. In theory, for the next generation (T2) PCR analysis combined with restriction enzyme reactions would be used to verify positive candidates. TALENs were designed to remove a specific restriction site by introducing a sequence mutation in the area of interest. The PCR fragments from the PCR reaction used already in the T1 generation would be treated with the restriction enzyme Tat1 (W'GTAC) which binds inside the sequence of interest. If a mutation was introduced the restriction site would not be present any longer and no digestion fragments would be detected in an agarose-gel analysis. In contrast, fragments without a mutation would still be cut by the enzyme to generate two fragments of different sizes which could be separated in an agarose gel electrophoresis. Unfortunately, this method was not successful in this study, restriction analysis always showed the digestion of the PCR fragment. Therefore, this fragment was sent for sequencing to see whether a mutation was inserted on a different position before or behind the restriction site. The obtained sequencing results showed that the sequence alignment stops direct behind the restriction site indicating that potential mutation must be introduced behind the restriction site which therefore cannot be used for analyses as envisaged. So, PCR fragments were sequenced instead of doing restriction site analysis.

In the T1 generation three plants were found to have a putative insertion in the *PLDγ1* gene. Thus, in the T2 generation for each of these three lines 40 different plants were sequenced to determine whether a mutation or frameshift was inserted. Eventually, no

plant could be found showing a mutation in *PLDγ1*. Since this method didn't work out for *PLDγ1* the other lines were transformed but not analysed in further generations.

A

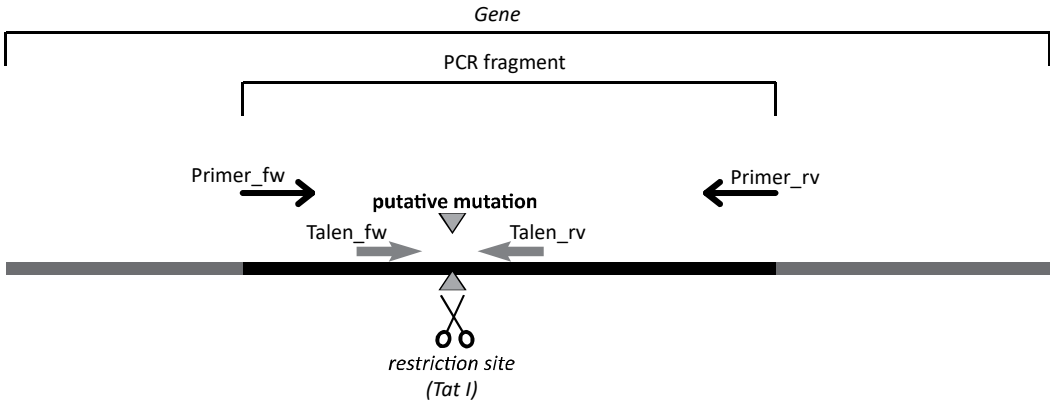

B

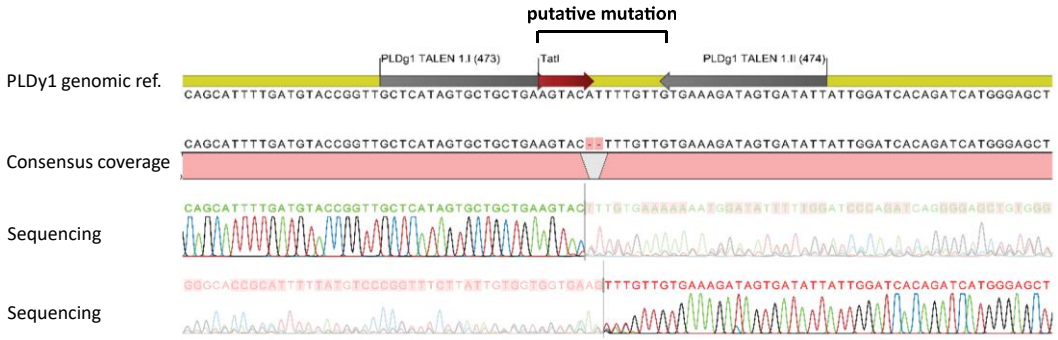

Figure 3-15: Schematic display of working steps using TALENs to generate new mutants

Schematic display of identifying plants with mutated *PLDγ1* Sequences introduced by the TALEN technique. **A** TALEN sequences were designed to bind inside the gene of *PLDγ1* and induce a double strand DNA break and a putative mutation within the restriction site of *Tat*I. Primers flanking the putative mutation area were designed to produce PCR fragments which can be treated with *Tat*I to identify positive candidates which would lack the *Tat*I restriction site due to TALEN activity. These PCR fragments can be sequenced to validate the mutation. **B** sequence analysis of a PCR fragment from **A** with a putative introduced mutation (here deletion of two base pairs). In this case, the TALEN-induced mutation was outside the *Tat*I restriction site making mutant identification via restriction site analysis impossible.

3.3 FINDING THE REASON FOR THE PLDΓ1-1 PHENOTYPE IN DIFFERENT DOWNSTREAM PATHWAYS

To address the question what causes the phenotype of *pldγ1-1,* downstream pathways were analysed. Beside the induction of MAP-kinase activation and ROS-burst analysis (see results in section 3.2.4) the production of PA and the effect on phytohormone levels were tested.

3.3.1 PA levels are not affected in the pldγ1-1 mutant

One of the main functions of PLDs is the synthesis of PA (Berg et al., 2018). To examine the role of PLDγ1 PA levels were checked in seedlings of the corresponding *pld*-mutant lines, wild-type Col-0 plants and the *bir2-1* mutant as controls. BIR2 was shown to be a negative regulator of FLS2-BAK1 mediated defence pathways (Halter et al., 2014). PLDγ1- and BIR2-deficient plants show a similar phenotype in infection studies and early immune responses like ROS-production. Therefore, the *bir2-1* mutant line was included in this analysis. Radioactive $^{32}P_i$ labelling was used to visualise newly generated phospholipid structures. After elicitation a classical lipid extraction was performed which were then separated using thin layer chromatography. In the end PA was quantified using phosphoimaging. The results showed that the basal levels of PA in untreated plants was not affected by genetic inactivation of *PLDγ1* (Figure 3-16 **A**). All lines were still able to produce PA and not only in an untreated state but also after applying 300 mM of NaCl for 30 min as a strong abiotic stimulus (Figure 3-16 B, **C**). To check whether specific MAMP elicitation influences PA release, seedlings were treated with 1 µM flg22 for 30 min. In Figure 3-16 **D** and **E** it is shown that PA levels did not differ between *pldγ1* mutant plants and the control wild-type Col-0 or the *bir2-1* mutant. However, there was a difference between treated and untreated plants of the same mutant line, indicating that flg22 treatment led to higher PA accumulation. But since there was no difference between *pldγ1* mutant plants and the wild-type plants it could be assumed that either PLDγ1 had no measurable impact on PA release or this technique was not sensitive enough to detect very small differences.

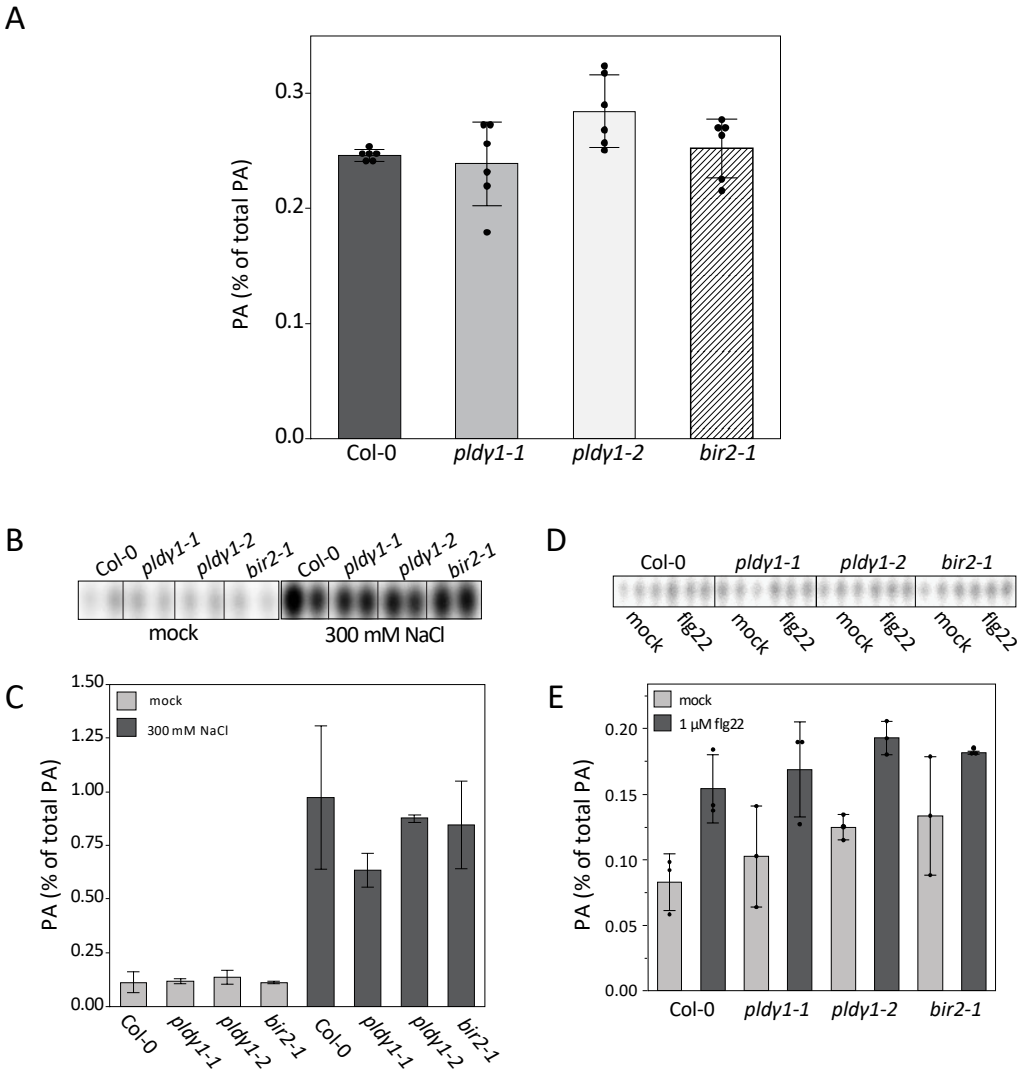

Figure 3-16: Phosphatidic acid levels were not changed significantly in pldγ1 mutant lines compared to wild-type plants

5-day old seedlings of Col-0, *pldγ1-1*, *pldγ1-2* or the *bir2-1* mutant were labelled with $^{32}P_i$ for 16 h and then treated for 15 min with elicitor or cell-free medium (mock) as indicated. Lipids were extracted, separated by EtAc-TLC and the radioactivity incorporated into the PA was quantified by phosphoimaging. Data represent the average of 2-6 biological replicates and are expressed in relation to the radioactivity of the total phospholipids. **A** Basal PA levels in Col-0, *pldγ1-1*, *pldγ1-2* or *bir2-1* plants (n=6) **B-C** PA spots on EtAc-TLC mock and NaCl (300 mM) treatment of Col-0, *pldγ1-1*, *pldγ1-2* or *bir2-1* seedlings (n=2) and corresponding quantification. **D-E** PA spots on EtAc-TLC of mock and flg22 (1 µM) treatment of Col-0, *pldγ1-1*, *pldγ1-2* or *bir2-1* lines(n=3) and corresponding quantification.

3.3.2 JA levels are elevated

Plant hormones play an important role in plant immunity and are responsible for lots of reactions. They are especially needed to induce cell death to avoid spreading of the pathogen and then gaining systemic resistance (Shine et al., 2019, Saijo et al., 2018, Andersen et al., 2018, Zhang et al., 2017) . SA and JA are prominent candidates and were shown to be induced after pathogen attack to activate downstream pathways. SA is often correlated with biotrophic infection while JA was associated with necrotrophic

infection (Zhang et al., 2018b). However, this differentiation is difficult since there is considerable crosstalk between these two hormone pathways and is not fully understood how the hormones regulate each other (Zhang et al., 2018b). Nevertheless, the measuring of SA and JA can give us a deeper insight into which signalling pathways involve PLDγ1.

Therefore, we determined hormone levels in different, untreated mutant lines via gas chromatography followed by mass spectrometry in co-operation with Dr. Joachim Kilian from the ZMBP analytics department. Preliminary results indicated that SA levels were not affected in *pldγ1-1* or *pldγ1-1* complementation lines although the technical replicates varied a lot within one line (Figure 3-17 **A**). Interestingly, in this experiment JA levels were significantly elevated in the *pldγ1-1* mutant but not in the complementation lines (Figure 3-17 **B**). This leads to the assumption that PLDγ1 might have an influence on the JA pathway itself or on its regulation, but results must be repeated in independent experiments with more replicates.

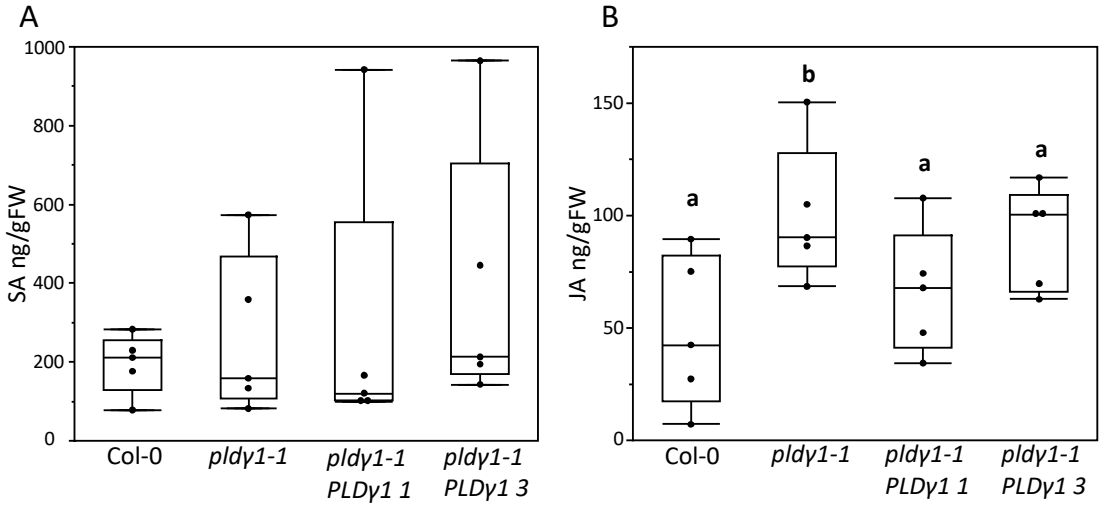

Figure 3-17: SA-levels are not affected in pldγ1-1 mutants but JA levels are elevated

Quantification of salicylic acid **A** and jasmonic acid **B** in 8-week old untreated leaves of Col-0 wild-type plants or *pldγ1-1*, *pldγ1-1 PLDγ1 1* and *pldγ1-1 PLDγ1 3* lines by gas chromatography/mass spectrometry analysis. Box plots show the minimum, first quartile, median, third quartile, and a maximum of the values represented in ng/g fresh weight (FW) (n=5). Labels a-b indicate homogenous groups according to post-hoc comparisons following one-way ANOVA (Dunnet's multiple comparison analysis with Col-0 as control group at a probability level of $p < 0.05$).

3.4 PLDγ1 CAN BE FOUND IN COMPLEX WITH BIR2 AND BIR3

3.4.1 Transiently expressed PLDγ1 binds to BIR2 and BIR3 in N. benthamiana

As PLDγ1 is involved in flg22-induced ROS-production, we next addressed the question whether PLDγ1 interacts with some known proteins of plant immunity at the plasma membrane such as FLS2 and BAK1 as the two first components starting flg22-induced signalling (Chinchilla et al., 2007, Heese et al., 2007). To analyse complex formation, PLDγ1 containing a C-terminal MYC-tag was transiently co-expressed in *Nicotiana benthamiana* together with either FLS2 or BAK1 which had a C-terminal GFP tag. After three days of expression the leaves were infiltrated with flg22 to see whether potential interaction is flg22-dependent or not. After protein extraction the samples were immuno-purified using agarose beads coated with GFP or MYC binding proteins. Eventually, the samples were analysed via a western blot assay using GFP- or and MYC-tag antibodies. Figure 3-18 shows that PLDγ1 does not interact with FLS2 (Figure 3-18 **A**) or BAK1 (Figure 3-18 **B**). All proteins were expressed and could be precipitated with the corresponding affinity beads. Since within on experiment the same source material was used for GFP and MYC-immuno-precipitation, the detected proteins in the precipitate function as an evidence for successful protein expression of the proteins in the whole experiment.

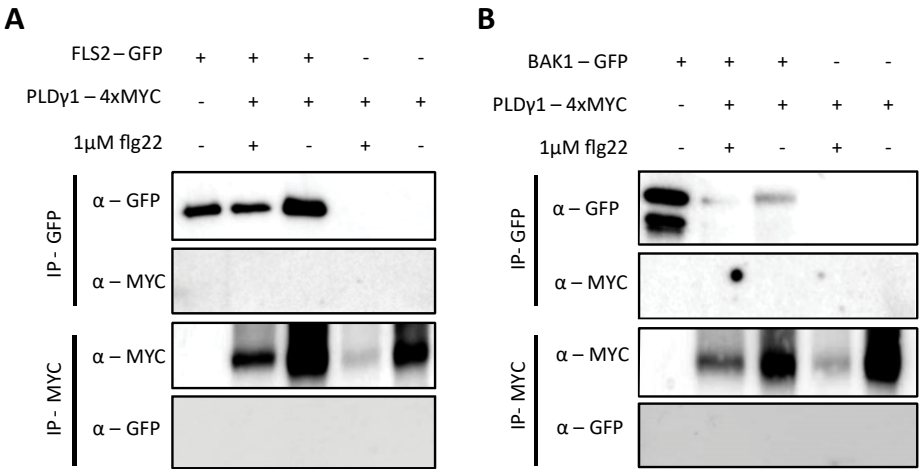

Figure 3-18: PLDγ1 does not interact with FLS2 or BAK1

Western blot analysis of transiently expressed proteins in *N. benthamiana* three days after infiltration. PLDγ1-4xMYC was either co-expressed with FLS2-GFP **A** or BAK1-GFP **B**. Three days post *Agrobacterium* infiltration, leaf material was harvested 5 min after 1 µM flg22 (+) or water (-) treatment. After protein extraction the proteins were immuno-purified with GFP-trap or MYC-trap beads, respectively, as indicated. For different immuno-precipitations within one experiment the same source material was used. Immunoprecipitated and co-immunoprecipitated proteins were detected with tag-specific antibodies.

Even though FLS2 and BAK1 could not be found in complex with PLDγ1 we thought about other proteins and realized that the phenotype of the *pldγ1-1* mutant is similar to the phenotype of *bir2-1*, which was shown to be a negative regulator of flg22 mediated immunity (Halter et al., 2014). Like *pldγ1-1*, *bir2-1* mutant plants react with higher ROS-burst after flg22-stimulation, show higher resistance to Pst infection and also have higher disease indices in Alternaria infection (Halter et al., 2014). Additionally, Sarina Schulze, a colleague working on downstream interaction partners of BIR3, found PLDγ1 among BIR3-interacting proteins (data not shown). Thus, we tested whether PLDγ1 interacts with BIR2 and BIR3. The results shown in Figure 3-19. A-C indicate that transiently expressed PLDγ1 and BIR2 with different tagged versions interact with each other and can be co-purified. The protein band of the co-immunoprecipitated protein in (A) is stronger after flg22 treatment which indicates that this interaction might be flg22 dependent. Also, for BIR3 an interaction could be found in this assay shown in Figure 3-19 **D**-**F**. In this case there is no obvious difference in interaction strength with or without flg22 pre-treatment. These interaction assays indicate that PLDγ1 interacts with BIR2 and BIR3 or that they are found together in a same protein complex which could be pulled down. Whether there is a direct interaction between PLDγ1 and BIR2 and BIR3 needs to be verified in other interaction assays. Also, the influence of flg22 to the interaction needs to be studied in more detail.

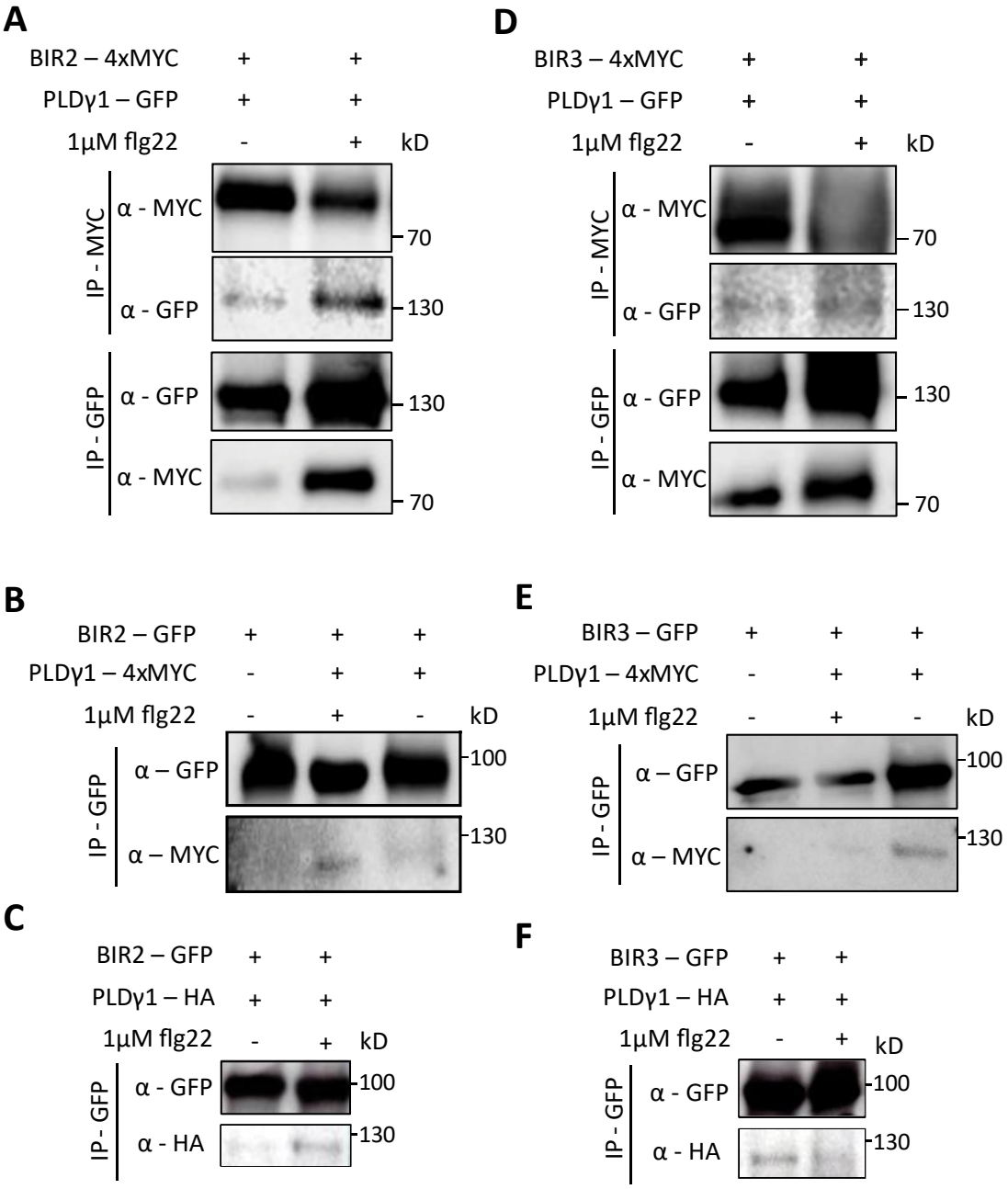

Figure 3-19: PLDγ1 can be found in complex with BIR2 and BIR3

Western Blot analysis of transiently expressed proteins in *N. benthamiana* three days after infiltration. Leaf material was harvested 5 min after 1 µM flg22 (+) or water (-) treatment. After protein extraction the proteins were pulled down with GFP-trap or MYC-trap beads, as indicated. For different pull-downs within one experiment the same source material was used. Immunoprecipitated and co-immunoprecipitated proteins were detected with tag-specific antibodies. **A** Co-immunoprecipitation of BIR2-4xMYC and PLDγ1-GFP pulled down with MYC-trap beads and GFP-trap beads, respectively. **B** Co-immunoprecipitation of BIR2-GFP and PLDγ1-4xMYC pulled down with GFP-trap beads. **C** Co-immunoprecipitation of BIR2-GFP and PLDγ1-HA pulled down with GFP-trap beads. **D** Co-immunoprecipitation of BIR3-4xMYC and PLDγ1-GFP pulled down with MYC-trap beads and GFP-trap beads. **E** Co-immunoprecipitation of BIR3-GFP and PLDγ1-4xMYC pulled down with GFP-trap beads. **F** Co-immunoprecipitation of BIR3-GFP and PLDγ1-HA pulled down with GFP-trap beads.

3.4.2 Alternative methods to test interaction of PLDγ1 with BIR2 need to be optimized

In the chapter before complex formation of PLDγ1 with BIR2 and BIR3 could be shown in immuno-precipitation assays. To analyze whether this complex formation is based on a direct protein-protein-interaction the yeast to hybrid system was chosen. In preliminary experiments the interaction of PLDγ1 with BIR2-kinase domain could not be determined (data not shown). However, the expression of all proteins could not be detected in a western blot analysis. There were technical problems to detect especially MYC-tagged proteins as the MYC-antibody bound unspecific to a lot of proteins on the membrane. Especially, strong unspecific bands with the expected sizes of BIR2-4x-MYC or PLDγ1-4x-MYC were detected in samples without expressing BIR2 or PLDγ1, making interpretation of the results impossible. To conclude whether PLDγ1 and BIR2 interact directly this experiment needs to be repeated and protein expression must be confirmed.

Moreover, other methods like bimolecular fluorescence complementation (BiFC) or FLIM-FRET- analyses (Fluorescence Lifetime Imaging Microscopy - Förster Resonance Energy Transfer) should be considered since these would be *in vivo* studies in a plant system. The Student Raffaele Del Corvo did some BiFC-interaction analysis in his diploma thesis, showing that there is a weak interaction of PLDγ1 with BIR2, although the detection of expressed proteins was also questionable (Del Corvo, 2018).

4 DISCUSSION

4.1 GENERAL ASPECTS

The plant innate immune system is a very complex network of different responses which are tightly regulated. Several levels and different signals ensure the survival of the plant in danger situations. The plant needs to balance defence responses, growth and yield. Enhanced defence responses lead to less growth and consequently often less yields which concerns especially crop production and food supply (Ning et al., 2017). Nevertheless, the plant evolved a sophisticated system to protect itself against abiotic but also biotic stresses. In the introduction an overview of different aspects is given. However, the exact mechanisms and regulation of these defence mechanisms remain mostly unknown. Especially, the understanding of the downstream signalling of danger signal receptor pathways and its regulation is just beginning (Wan et al., 2019). Initially, the focus of this work was to study CERK1-downstream signalling using phosphoproteomic analyses (section 3.1). This eventually changed to the characterization of the protein PLDγ1 and its involvement in plant innate immune system. One major reason for this is that initially phosphoproteomic analysis in cooperation with the proteome centre was facing a lot of technical issues. Sample collection and protein extraction needed to be optimized. During this time more and more results on PLDγ1, which was identified as candidate protein in the first phosphoproteomics analysis, as being involved in plant immunity were obtained. Therefore, the focus of this final thesis is the characterization of PLDγ1. However, the latest phosphoproteomic results, shown as compressed data sets in section 3.1, have high potential for new information and findings. Preliminary analysis indicated that in general the latest data set is reliable and some interesting candidates, already explained and discussed in section 3.1, should be investigated in the future. This dataset might contain new information especially for CERK1-function but also general immune downstream signalling. However, as mentioned above the following chapters are focusing on the function of the protein PLDγ1.

4.2 PLDγ1 IS PART OF THE IMMUNE PATHWAY IN ARABIDOPSIS AS NEGATIVE REGULATOR

Phospholipases are well-known proteins in a lot of signal transduction and regulation aspects in plants. Especially phospholipases of the subgroup D are connected to stress responses and plant immunity (Li and Wang, 2019, Hong et al., 2016, Zhao, 2015). PLDβ1 was found to be a negative regulator in different plants. In Arabidopsis PLDβ1 depletion leads to enhanced resistance against *Pseudomonas syringae* pv*. tomato DC3000* (*Pst*) infection, higher ROS-levels and SA accumulation upon infection. (Zhao et al., 2013b). In *Rice* it was also shown to function in a similar way. Mutants of *OsPLDβ1* were more resistant against bacterial infection and had elevated defence responses up o infection (Yamaguchi et al., 2009). Bargmann et al. (2006) demonstrated a negative regulatory function of PLDβ1 in tomato suspension culture up on xylanase treatment. In this study it was shown that PLDγ1 also works as a negative regulator of plant immunity. The results in 3.2.3 showed that genetic loss of *PLDγ1* leads to enhanced resistance against *Pst* infection, as demonstrated for PLDβ1. This effect could be reversed in *pldγ1-1*-lines complemented with the *PLDγ1* gene under a 35S-promotor. Infection and growth of the necrotrophic fungus *Botrytis cinerea* was also restricted in *pldγ1-1* plants. Contrary to this, the infection with another necrotrophic fungus, *Alternaria brassicicola*, led to higher infection symptoms. However, it is not yet fully understood how pathogens, especially fungi, infect plants. Studies in the last years, reviewed in Zhang et al. (2018b), demonstrated that for fungal defence especially JA-pathways are activated while SA dependent signalling is important for hemibiotrophic defence responses like *Pst*. Our preliminary results shown in 3.3.2 indicate that JA levels might be increased in *pldγ1-1* plants in a non-infected state but not in the complemented lines, while SA levels are not affected. However, repetition of those experiments performed by colleagues gave varying results and preliminary transcript analysis of JA- and SA-depended genes did not show any deregulation compared to wild-type plants (personal communication Dr. Andrea Gust). It would be necessary to test hormone levels before and after infection in *pldγ1-1* plants to make a final statement. However, AbuQamar et al. (2017) is giving an overview of a lot of contrary studies regarding JA and SA influences in fungal infection, making it clear that the crosstalk between the involved hormones in pathogen infection is highly complex and not understood completely yet. Hence, it is not impossible to have

different results with *Botrytis* and *Alternaria* infections in the *pldγ1-1* mutant. There might be differences in either infection strategies of these two fungi which could explain different results in our infection assays or differences in recognition of the pathogens. El Oirdi et al. (2011) showed that *Botrytis* infection in tomato for example activates a SA-dependent pathway which is different from other necrotrophic fungi. Hence, although both *Alternaria* and *Botrytis* belong to the family of necrotrophic fungi, plant resistance to the two fungi might involve different immune signalling pathways, also differentially involving PLDγ1. Also, not clear, if strong necrosis upon *Alternaria* infection is a disease symptom or an increased resistance phenotype, e.g. cell death. *Alternaria* growth/biomass need to be determined! However, both would lead in the end to more susceptible plants due to necrotroph's lifestyle.

Furthermore, it was demonstrated recently that the same protein can work as positive and negative regulator in different pathways. Wan et al. (2018) showed that the RLCK BIK1 is working as positive regulator in RLK-mediated pathways and has a negative regulator function in RLP-mediated signalling. This might be also an explanation for different outcomes in different assays as explained before.

Mutants in negative regulators in innate plant immunity usually show a stronger ROS-burst upon infection or elicitation. As mentioned before mutants of *PLDβ*, a known negative regulator in plant immunity, show higher ROS levels upon *Pst* and *Botrytis* infection (Zhao et al., 2013a). Mutants of *BIR2* and *BIR3*, which are also negative regulators preventing BAK1 from binding to FLS2 and activating downstream processes, displayed also enhanced ROS production (Halter et al., 2014, Imkampe et al., 2017). Although the results of ROS-burst measurements in *pldγ1-1* were varying sometimes in most of the experiments *pldγ1* mutants demonstrated enhanced ROS production indicating that PLDγ1 also has a negative regulatory function. The other isoforms PLDγ2 and PLDγ3 did not show this phenotype. However, it cannot be ruled out that for PLDγ2 and PLDγ3 inappropriate mutant lines were used as explained in 3.2.2. Nevertheless, in a recent study from Premkumar et al. (2018) the same seedstocks as in our study were used and apparently confirmed as proper mutant lines. In their experiments, protoplasts of *pldγ3* mutants showed increased ROS levels after hypoxia treatment. Interestingly, *PLDγ1*- and *PLDγ2*- deficient plants did not have the same effect. But comparing the non-treated samples, *pldγ1* and *pldγ2* mutants showed slightly higher ROS levels than non-

treated wild-type samples in their study (Premkumar et al., 2018)Fig 6 A). Because of the homology of the genes their results come along with the results of the *pldγ1-1* phenotype observed in this thesis, showing a higher ROS burst after flg22 treatment. Due to missing regulation of immunity pathways by PLDγ1, ROS levels could be already increased in non - infected or non- stimulated states as also indicated in Premkumar et al. (2018).

Some of the complementation lines could reverse the phenotype of *pldγ1-1* in the ROS assay but some could not. Interestingly, these results do not fit well with the results obtained for those complementation lines in *Pst*-infection assays. While the strongest rescue effect in *Pst*-infection was found in *pldγ1-1-PLDγ1 1* and *pldγ1-1-PLDγ1 2* lines, exact those lines were not complemented in the ROS-burst measurements. In contrast, *pldγ1-1-PLDγ1 3 and pldγ1-1-PLDγ1 4* showed only partial complementation in *Pst*-infection or even no complementation (Figure 3-12 and Figure 3-13). But these lines (*pldγ1-1-PLDγ1 3 and pldγ1-1-PLDγ1 4)* showed similar results as wild-type plants in ROS-burst assays. However, ROS-burst measurements might not be the most reliable assay to proof complementation, since the results were varying before (chapter 3.2.4) and only a high number of samples and repetitions could generate a reliable conclusion. Furthermore, the activation of ROS is a tightly regulated system (Liu and He, 2016b). Variation in protein amount can influence the outcome. Overexpression lines of known negative regulators usually decrease ROS accumulation dramatically, as shown for example in *bir3*-mutants (Imkampe et al., 2017). Although the mRNA levels of the complementation lines used in these assays were tested and proved to be similar to wild-type levels or even lower, the gene *PLDγ1* itself is under the control of a 35S-promotor. For future studies it would be necessary to work with complementation line containing the native promotor to make a clear statement. Nevertheless, these contrary results might be an indication that later resistance effects are regulated independently from early immune responses (ROS-burst and MAPK activation). In this study no differences in MAPK activation could be detected in *PLDγ1*-deficient plants after 15 min (Figure 3-10).But, it was shown that early immune responses like MAPK, ROS or CDPKs (Ca^{2+}-burst was not tested in this work but is also a very important indicator for early immune responses and connected to ROS-burst (Boudsocq et al., 2010)) can be activated independently (Liu and He, 2016a, Boudsocq et al., 2010). Therefore, it might

be that PLDγ1 is more involved in ROS-burst signalling than in MAPK signalling or is working downstream of MAPK activation. However, it would be interesting to test with more replicates whether in non-stimulated plants MAPKs are already activated. Another interesting aspect would be if in *pldγ1-1* plants MAPKs are activated more rapidly after flg22 treatment and/or if the activation might be prolonged.

Overall, although there might be some discrepancies in results obtained for ROS accumulation, PLDγ1 seems to be involved in plant immunity and works most likely as a negative regulator of plant resistance towards both fungal and bacterial pathogens.

4.3 ADDITIONAL T-DNA INSERTIONS IN PLDΓ1-1 AND MISSING INDEPENDENT MUTANT LINE COMPLICATE THE SITUATION

Most of the phenotypes described for *PLDγ1*-deficient plants were demonstrated in the mutant line *pldγ1-1*. The results of the independent *pldγ1-2* line were variable and hence not reliable. Some of the phenotypes observed in the *pldγ1-1* mutant could be reversed in complementation lines which indicates that PLDγ1 is indeed responsible for these effects. However, it is necessary to exclude that other proteins or a combination of various mutations are responsible for the mutant phenotypes shown in this work. The issue that the gene sequence of *PLDγ1* and the other two isoforms *PLDγ2* and *PLDγ3* are very alike complicates this problem. Besides redundancy in functional characterization the genetic characterization of other T-DNA insertion lines of all three genes was very difficult since most of the primes could bind in all three gene sequences. Additionally, the T-DNA insertion lines which were available for PLDγ2 and PLDγ3 were unsuitable because they had residual transcript levels of the respective gene. The effort to generate a second mutant for PLDγ1 using TAL-effector nucleases was not successful. Although other groups and studies were able to generate homozygous mutants using TALEN - systems in our case we could not obtain any mutant lines in T2 generations. Consultation with other scientists working with the same system gave us the information that in general this technique is difficult to apply in *Arabidopsis* and that they have similar problems as we had. However, a possibility to identify a successful *pldγ1* mutant line could be to increase sample sizes during screening of plants with potential TALEN-induced mutations. Alternatively, the generation of artificial micro RNA lines silencing all 3 *PLD*γ genes was started but the transgenic lines were not analysed further, so far.

These lines are, however, very interesting because all 3 genes would be silenced, and no redundancy effect could occur. Apart from that the method of CRISPR/Cas (Cong et al., 2013, Feng et al., 2013, Wolter et al., 2019) should be considered to generate an independent mutant lines.

Another strategy to confirm that the lack of *PLDγ1* was the course of the observed mutant phenotypes was to sequence the whole genome to find putative additional T-DNA in other regions than PLDγ1. The identified additional insertion sites affected the promotor region of the genes *AT1G77460* and *AT2G31130*, respectively. *AT1G77460* encodes for a protein named CELLULOSE SYNTHASE INTERACTIVE 3 (CSI3) which is involved in cellulose synthesis (Lei et al., 2013). The main barrier for pathogens is the cell wall. Cell wall components can be target of virulence factors of pathogens or can be a source for DAMPs after infection to start immune responses (Bacete et al., 2018, Malinovsky et al., 2014, Liu et al., 2014, Hückelhoven, 2007). Therefore, changes in the cell wall composition, for example due to non-functional CSI3, could have enormous effects on immunity. Because of that, single knock-out mutants of CIS3 were tested by the student Raffaele Del Corvo. The other affected gene *AT2G31130* encodes for an hypothetical protein (The Arabidopsis Information Resource (TAIR), 2019a) . Single knock- out mutants for this gene were also tested within the work of R. Del Corvo. The results of his work is summarized briefly in section 3.2.7, however, it was revealed that genetic inactivation of these two genes are most likely not responsible for the phenotypes observed in *pldγ1-1* plants (Del Corvo, 2018). But it cannot be ruled out that a mis regulation, due to the mutation in the promotor region, and/or the combination together with the *PLDγ1* mutation do have accumulative effects. Considering that the leaf structures in *pldγ1-1* plants were different to the wild-type sometimes (mentioned in section 4.5), these findings should be taken into account and phenotype responsibility of *PLDγ1*-inactivation must be proven by independent mutant lines.

4.4 THE ROLE OF PHOSPHATIDIC ACID IN PLDΓ1 DEPENDENT STRESS SIGNALLING

Phospholipases D (PLDs) in general, as PA producing enzymes, have an important function in danger signal recognition and plant immunity (Li and Wang, 2019). The role of PA itself within these pathways, however, is not fully understood yet. PA was found

to interact with several known proteins in plant immunity. For example, PA was shown to bind to RESPIRATORY BURST OXIDASE HOMOLOG D (RbohD) and RbohF, which contribute to ROS accumulation as an early defence response (Zhang et al., 2009). Intriguingly, *pldγ1* mutants (assumingly producing less PA) show an increased production of ROS upon MAMP-treatment (see section 3.2.4 and Figure 3-9). So far it has, however, not been shown whether PA also exerts a negative regulatory function on the plant immune response. Furthermore, PA was found to bind to 3'-PHOSPHOINOSITIDE-DEPENDENT PROTEIN KINASE 1 (PDK1) (Anthony et al., 2006), a key player in the ROS-induced OXI1 pathway. This pathway was found to be important for establishing fungal resistance (Anthony et al., 2006) and is responsible for implementing growth promotion effects to *Piriformospora idica* (*P. indica*) (Camehl et al., 2011). Moreover, MPK6 was found as a PA target upon salt stress conditions (Yu et al., 2010). Interestingly, within the PDK1/OXI1 – pathway MPK6 is also involved and somehow regulated by PA-activated PDK1 (Camehl et al., 2011). Another study by Howden et al. (2011) discovered that in the phosphoproteome of OXI1-deficient plants phosphorylation of PLDγ - proteins were elevated indicating that not only PLDα1 (Camehl et al., 2011) but also PLDγ might be affected in this pathway, possibly not as a direct target but as an protein involved indirectly in the whole signalling cascade (Howden et al., 2011). In order to clarify the function of PLDγ1, PA was measured in *pldγ1-1* mutant plants and compared to wild-type and *bir2-1* plants. Our experiments, in quantifying PA, didn't show any differences suggesting that PA levels are not changed after genetic inactivation of *PLDγ1* (see section 3.3.1.) and after flg22 treatment. But, measuring flg22-depended PA accumulation changes in *Arabidopsis* plants is difficult and failed in another study as well (D'Ambrosio et al., 2017), although in tomato cell culture a dramatic increase of PA after xylanase elicitation could be observed (van der Luit et al., 2000). In the experiment shown in Figure 3-16 at least a general PA increase was noticed after flg22 treatment in radioactively labelled seedlings. Though, there is no difference between *pldγ1-1* and wild-type plants. As already discussed in D'Ambrosio et al. (2017) also redundancy among the PLDs might be one reason for that. *Arabidopsis* plants contain 12 PLD isoforms. The probability of redundant function of different isoforms is quite high, since it is known that also other PLDs might be involved in the same signalling pathways. These proteins including the intact forms of the PLDγ2 and

PLDγ3 are still functional in *pldγ1-1* mutants and could compensate for the loss of PLDγ1 function. However, the clear phenotypes of *pldγ1-1* mutants with respect to elevated MAMP-induced ROS-levels and increased bacterial and fungal resistance indicate that other PLDs cannot compensate all these functions. Another reason for unaltered PA levels in the *pldγ1-1* mutant compared to wild-type plants could be technical limitations of measuring small differences in PA amounts (D'Ambrosio et al., 2017). Notably, in the common PA-determination method used in this thesis (Munnik and Zarza, 2013) apart from PLD-generated PA also PLC-generated PA is measured. Hence, subtle changes of PA in the big PA pool might not be detectable with this technique but might still have an enormous effect on immune signalling. Although no PA changes were detected in *pldγ1-1* plants compared to the wild-type control, it could still have an impact on plant innate immunity. Triple mutation of all PLDγ isoforms would thus be a good starting point to analyse PA levels again. Application of synthetic PA and a possible phenotype reversion was another strategy to analyses PA importance in this pathway. First experiments on PA application were performed but failed on the application itself. We used syringe-infiltration for PA application, however, we could not prove the uptake of PA into the cells and did not see an effect on plant immune responses after PA-treatment. However, this should be optimized and studied further. Eventually, no statement about the impact of PLDγ1 derived PA in plant innate immunity could be made and remains to be studied.

In any case, so far PA would be a positive regulator, but in this thesis a PA-producing enzyme is apparently a negative regulator. This raise the question whether PA produced by PLDγ1 could regulate immune responses negatively. So far, no examples for negative regulatory function of PA are known. As long as we cannot demonstrate that the phenotype of *pldγ1-1* plants is caused by PLDγ1 produced PA, however, this remains elusive.

4.5 DEFENCE PATHWAYS MUST BE TIGHT REGULATED – PLDΓ1 INTERPLAY WITH BIR2 AND BIR3

As already explained before immune pathways need tight control and regulation. In the flg22 recognition and signalling pathway several regulation steps are known but also a lot of questions are still open. The observation that *PLDγ1* deficient plants produced

more flg22-induced ROS led to the question where and how this protein works in this signalling pathway. Therefore, protein interaction studies with prominent proteins of the flg22 recognition pathway were performed. Within these assays an interaction of PLDγ1 with FLS2 and BAK1 could be excluded, indicating that PLDγ1 must act downstream of these two proteins. After we noticed that *pldγ1-1* plants had similar phenotypes as *BIR2*- and *BIR3*- deficient plants, PLDγ1 interaction with BIR2 and BIR3 was tested. Importantly, my colleague Sarina Schulze found PLDγ1 to bind to BIR3 in her pulldown assays in *Arabidopsis bir3-yfp-overexpressor* lines. Indeed, in transient interaction assays with PLDγ1 and BIR2 and BIR3, fused to different epitope-tags, these proteins could be found in a complex. Whether these proteins interact directly was analyzed using BIFC assays by the diploma student Raffaele Del Corvo (Del Corvo, 2018). However, these results remain unclear and need further repetition and optimization. Nevertheless, finding PLDγ1 in a complex with BIR2 and BIR3 in a co-immunoprecipitation approach raises the question what the role of PLDγ1 is and whether it might regulate BIR2. In Halter et al. (2014) and Imkampe et al. (2017) the model of a guarding protein of BIR2 and BAK1 was proposed. The idea was that the guarding protein senses when BAK1 is not controlled by BIR2. Subsequently, cell-death responses would be activated. If PLDγ1 would be this guard protein, its genetic inactivation would result in disturbance of BAK1/BIR2-complex. Subsequent the loss of negative regulation of BAK1 through the loss of PLDγ would have similar effects as observed in *bir*2- knock out plants, as reported earlier (Halter et al., 2014). Although, one would expect uncontrolled BAK1 leads to the same phenotype as BAK1 -overexpression, this is only partly true. Similar to *bir2-1* BAK1-overexpressor lines are more resistant to *Pst* infections and have enhanced early immune response upon flg22 treatment (Domínguez-Ferreras et al., 2015), but, the growth phenotype differs to BIR2 or BIR3-deficient plants. Although *bir2-1* plants show slightly smaller leaves and beginning of autoimmune responses (Imkampe, 2015) it is not nearly as strong as in BAK1 overexpressing plants which suffer from strong dwarf phenotype and constantly activated autoimmunity which leads to strong necrosis (Domínguez-Ferreras et al., 2015). For *BIR3*-deficient plants this growth-phenotype is not known so far (Imkampe, 2015).

Nevertheless, all this is pure speculation and needs to be tested in future experiments since the guard of BAK1/BIR2 is expected to be a R-protein. Most of the R-genes in planta are members of proteins containing a nucleotide-binding-site (NBS) domain and leucine-rich-repeats (LRR), and are therefore named NBS-LRR-proteins (McHale et al., 2006). PLDγ1, however, does not have any of these characteristics.

Another, more probable scenario could be that PLDγ1, as a phospholipase, modifies cell membrane structures and would be responsible for the right localization and insertion of BIR2 and BIR3, as they belong to transmembrane proteins. In the case of *pldγ1-1* mutants BIR2 and BIR3 and possibly other proteins might not be inserted or localized right into the membrane and would have similar effects as genetic inactivation or a misfolded protein. However, for this a direct interaction of BIR2 or BIR3 with PLDγ1 is not necessary. But, until now we can only show that PLDγ1 is in a complex together with BIR2 and BIR3 proteins. A direct interaction could not be shown, yet. As mentioned in the introduction recent studies showed that components which are necessary for a fast signalling activation upon infection are clustered together in so called nanoclusters (Gu et al., 2017, Bücherl et al., 2017). If PLDγ1 is together with BIR2 or BIR3 in one nanocluster, it could alter the membrane for a right incorporation and localization of the BIR2 or BIR3 protein. It could also play a role in facilitating the separation of BIR2 and BAK1 by changing the membrane structure and ensures right recycling of BIR2. In our pull-down experiments PLDγ1 and BIR2 association is elevated after flg22 treatment. Interestingly in Mammals the function of PLD in vesicle trafficking, exocytosis and recycling of receptor proteins through endocytosis is already known for a while (Donaldson, 2009, Egea-Jimenez and Zimmermann, 2018). ADP-ribosylation factors can activate PLDs and therefore facilitate membrane trafficking (Donaldson, 2009).PLD2 was shown to alter membrane structure to build exosomes and involved in exocytosis (Egea-Jimenez and Zimmermann, 2018). Intriguingly, in some experiments the observation of a different leaf structure and texture was made in *pldγ1* mutants. This might be caused by structural membrane changes and/or cytoskeleton rearrangements. PLDs were associated with actin and microtubule remodeling and sequentially immune defenses (Pleskot et al., 2013). Though, this observation of different leave structures needs to be quantified.

Taken together the results of our interaction studies suggest that PLDγ1 is found together with BIR2 and BIR3 in a protein complex. At least for the PLDγ1/BIR2 interaction, this complex formation seems to be flg22 dependent. The importance of this complex formation, however, remains elusive and needs further investigation.

4.6 OUTLOOK

Results in this thesis could show that the protein PLDγ1 has an impact in plant immunity and is most likely working as a negative regulator. The interaction of PLDγ1 with BIR2 and BIR3 might indicate an interplay of those proteins with PLDγ1 in regulation of danger signal receptors at the plasma membrane. However, the exact role of PLDγ1 and where it is acting remains to be studied in further experiments.

I would like to mention some interesting aspects which weren't studied in detail, yet, but might contribute to answer the question of the function of PLDγ1. As already mentioned, PLDs and PA are correlated to cytoskeleton remodelling (Pleskot et al., 2013) which is worth to be studied further. A few years ago, a cooperation with Prof. Dr. Christopher J. Staiger of the Purdue University in the United States was started to characterize the function of PLDγ1 in actin remodelling mechanisms. Unfortunately, the complicated genetic background and homology of the PLDγ family hampered the generation of reporter lines needed for these analyses which were also performed in the study from Li et al. (2015). Nevertheless, this should not be forgotten und maybe tried again.

Another interesting aspect of this project is the implication of PLDγ1 in the PDK1/ OXI1 pathway together with MPK6 as explained in section 4.4. PLDγ1 might be involved in this signalling pathway. Interestingly, personal communication of Prof. Dr. Heribert Hirt of the King Abdullah University of Science and Technology in Saudi Arabia indicated that PLDγ1 might be phosphorylated by MPK6. These preliminary results need to be confirmed and studied further before making any proposition. However, all these facts indicate that PLDγ1 has a regulatory function in plant immunity and reveal once again that plant immunity pathways are tightly regulated and that there are a lot of aspects to be studied in the future (Wan et al., 2019).

5 SUMMARY

Plant innate immunity is mediated by pattern-recognition-receptors which can recognize danger signals from different pathogens. Upon recognition a machinery of different signalling pathways is activated to trigger downstream defence responses. One well characterized signalling pathway is mediated by the receptor kinase (RK) FLS2 which binds the bacterial flagellin epitope flg22 and recruits the co-receptor kinase BAK1 to induce downstream signalling. To prevent activation of immunity pathways without infection BAK1 is negatively regulated by the two RKs BIR2 and BIR3. This work demonstrates that the phospholipase PLDγ1 is also involved as negative regulator in FLS2-mediated immune signalling. PLDγ1-deficient plants showed a higher resistance towards bacterial and fungal infection. Early immune responses, like the accumulation of reactive oxygen species but not the activation of mitogen-activated protein kinases, were elevated. These findings could be validated in corresponding complementation plants overexpressing PLDγ1 in the *pldγ1-1* mutant background. Furthermore, *pldγ1-1* mutant plants were tested for PA accumulation after flg22 treatment, since the biochemical function of PLDs is the hydrolysis of phospholipids, which results in the generation of the second messenger PA. However, mutants of *PLDγ1* showed no difference in PA accumulation after flg22 treatment implying that PA itself is most likely not responsible for this phenotype. Importantly, PLDγ1 is located at the plasma membrane and the *pld1-1* mutant phenotype resembles that of *bir2* mutants. Indeed, PLDγ1 was found together with BIR2 and BIR3 in a complex as observed in co-immunoprecipitation assays; however, so far, no direct protein-protein interaction could be confirmed. Future work will now be needed to address the question whether PLDγ1 is necessary for BIR2 or BIR3 regulation or whether PLDγ1 affects BIR2/ BIR3 protein stability or integration into the plasma membrane.

6 ZUSAMMENFASSUNG

Die basale Pflanzenimmunität wird unter anderem durch Rezeptoren (Pattern recognition receptors (PRR)) vermittelt, welche die molekularen Muster bestimmter Gefahrensignale von Pathogenen erkennen. Nach der Perzeption dieser Komponenten wird eine Maschinerie verschiedener Signalwege aktiviert, um gezielte Abwehrmechanismen zu initiieren. Die Rezeptorkinase (RK) FLS2, ein bekanntes PRR-Beispiel, erkennt als Gefahrensignal flg22, ein Epitop des bakteriellen Proteins Flagellin. Durch die Bindung von flg22 an FLS2 wird die Ko-Rezeptorkinase BAK1 rekrutiert und weitere Signalkaskaden werden induziert. Um zu verhindern, dass Abwehrmechanismen dauerhaft aktiviert sind, wird die Interaktion zwischen FLS2 und BAK1 durch die Negativregulatoren BIR2 und BIR3 kontrolliert. Diese Arbeit zeigt, dass die Phospholipase PLDγ1 ebenso als Negativregulator an dem FLS2-vermittelten Immunsignalweg beteiligt ist. Mutationen im *PLDγ1* Gen führen in den entsprechenden Pflanzen zu einer verstärkten Resistenz gegen Infektionen mit Bakterien sowie Pilzen. Des Weiteren konnte gezeigt werden, dass frühe Immunantworten, wie z.B. der oxidative Burst, aber nicht die Aktivierung von mitogen-aktivierten Proteinkinasen, in der *pldγ1-1* Mutante erhöht waren. Diese Ergebnisse konnten in entsprechenden Komplementationspflanzen mit überexprimierter *PLDγ1* im *pldγ1-1*-Mutantenhintergrund bestätigt werden. Phospholipasen sind für die Hydrolyse von Phospholipiden zuständig. Dabei entsteht Phosphatiditsäure (PA), welches als Signalmolekül bekannt ist. Jedoch konnte in *pldγ1-1* Pflanzen keine veränderte PA-Akkumulation vor oder nach flg22-Behandlung im Vergleich zum Wildtyp festgestellt werden. Daraus lässt sich schließen, dass PA höchstwahrscheinlich nicht für den beschriebene Phänotyp der *pldγ1-1* Mutante verantwortlich ist. Allerdings ist PLDγ1 an der Plasmamembran zu finden und der Phänotyp der *pld1-1*-Mutanten ähnelt dem der *bir2*-Mutation. In Co-Immunpräzipitations-Assays konnte PLDγ1 in dieser Arbeit in einem Proteinkomplex mit BIR2 bzw. BIR3 nachgewiesen werden, eine direkte Interaktion konnte allerdings bisher nicht gezeigt werden. Für zukünftige Arbeiten stellt sich nun die Frage, ob PLDγ1 für die Regulation von BIR2 oder BIR3 notwendig ist oder für deren Stabilisierung oder richtige Plasmamembran-Integration verantwortlich ist.

7 REFERENCES

NEB Tm Calculator [Online]. Available: http://tmcalculator.neb.com/#!/ [Accessed 2017].

ABUQAMAR, S., MOUSTAFA, K. & TRAN, L. S. 2017. Mechanisms and strategies of plant defense against Botrytis cinerea. *Crit Rev Biotechnol,* 37**,** 262-274.

ADAM, A. L., NAGY, Z. A., KATAY, G., MERGENTHALER, E. & VICZIAN, O. 2018. Signals of Systemic Immunity in Plants: Progress and Open Questions. *Int J Mol Sci,* 19.

ALOULOU, A., ALI, Y. B., BEZZINE, S., GARGOURI, Y. & GELB, M. H. 2012. Phospholipases: an overview. *Methods Mol Biol,* 861**,** 63-85.

ANDERSEN, E. J., ALI, S., BYAMUKAMA, E., YEN, Y. & NEPAL, M. P. 2018. Disease Resistance Mechanisms in Plants. *Genes (Basel),* 9.

ANTHONY, R. G., KHAN, S., COSTA, J., PAIS, M. S. & BOGRE, L. 2006. The Arabidopsis protein kinase PTI1-2 is activated by convergent phosphatidic acid and oxidative stress signaling pathways downstream of PDK1 and OXI1. *J Biol Chem,* 281**,** 37536-46.

AO, Y., LI, Z., FENG, D., XIONG, F., LIU, J., LI, J. F., WANG, M., WANG, J., LIU, B. & WANG, H. B. 2014. OsCERK1 and OsRLCK176 play important roles in peptidoglycan and chitin signaling in rice innate immunity. *Plant J,* 80**,** 1072-84.

BACETE, L., MELIDA, H., MIEDES, E. & MOLINA, A. 2018. Plant cell wall-mediated immunity: cell wall changes trigger disease resistance responses. *Plant J,* 93**,** 614-636.

BARGMANN, B. O., LAXALT, A. M., RIET, B. T., SCHOUTEN, E., VAN LEEUWEN, W., DEKKER, H. L., DE KOSTER, C. G., HARING, M. A. & MUNNIK, T. 2006. LePLDbeta1 activation and relocalization in suspension-cultured tomato cells treated with xylanase. *Plant J,* 45**,** 358-68.

BERG, J. M., TYMOCZKO, J. L., GATTO, G. J. & STRYER, L. 2018. *Stryer Biochemie*, Springer Spektrum.

BI, G., ZHOU, Z., WANG, W., LI, L., RAO, S., WU, Y., ZHANG, X., MENKE, F. L. H., CHEN, S. & ZHOU, J.-M. 2018. Receptor-Like Cytoplasmic Kinases Directly Link Diverse Pattern Recognition Receptors to the Activation of Mitogen-Activated Protein Kinase Cascades in Arabidopsis. *The Plant Cell,* 30**,** 1543-1561.

BOERSEMA, P. J., RAIJMAKERS, R., LEMEER, S., MOHAMMED, S. & HECK, A. J. 2009. Multiplex peptide stable isotope dimethyl labeling for quantitative proteomics. *Nat Protoc,* 4**,** 484-94.

BÖHM, H., ALBERT, I., FAN, L., REINHARD, A. & NÜRNBERGER, T. 2014. Immune receptor complexes at the plant cell surface. *Current Opinion in Plant Biology,* 20**,** 47-54.

BOLLER, T. & FELIX, G. 2009. A renaissance of elicitors: perception of microbe-associated molecular patterns and danger signals by pattern-recognition receptors. *Annu Rev Plant Biol,* 60**,** 379-406.

BOUDSOCQ, M., WILLMANN, M. R., MCCORMACK, M., LEE, H., SHAN, L., HE, P., BUSH, J., CHENG, S. H. & SHEEN, J. 2010. Differential innate immune signalling via Ca(2+) sensor protein kinases. *Nature,* 464**,** 418-22.

BOUTROT, F. & ZIPFEL, C. 2017. Function, Discovery, and Exploitation of Plant Pattern Recognition Receptors for Broad-Spectrum Disease Resistance. *Annual Review of Phytopathology,* 55**,** 257-286.

BRADFORD, M. M. 1976. A rapid and sensitive method for the quantitation of microgram quantities of protein utilizing the principle of protein-dye binding. *Anal Biochem,* 72**,** 248-54.

BÜCHERL, C. A., JARSCH, I. K., SCHUDOMA, C., SEGONZAC, C., MBENGUE, M., ROBATZEK, S., MACLEAN, D., OTT, T. & ZIPFEL, C. 2017. Plant immune and growth receptors share common signalling components but localise to distinct plasma membrane nanodomains. *Elife,* 6.

CAMEHL, I., DRZEWIECKI, C., VADASSERY, J., SHAHOLLARI, B., SHERAMETI, I., FORZANI, C., MUNNIK, T., HIRT, H. & OELMÜLLER, R. 2011. The OXI1 Kinase Pathway Mediates Piriformospora indica-Induced Growth Promotion in Arabidopsis. *PLOS Pathogens,* 7**,** e1002051.

CAO, Y., LIANG, Y., TANAKA, K., NGUYEN, C. T., JEDRZEJCZAK, R. P., JOACHIMIAK, A. & STACEY, G. 2014. *The kinase LYK5 is a major chitin receptor in Arabidopsis and forms a chitin-induced complex with related kinase CERK1*.

CHINCHILLA, D., SHAN, L., HE, P., DE VRIES, S. & KEMMERLING, B. 2009. One for all: the receptor-associated kinase BAK1. *Trends in Plant Science,* 14**,** 535-541.

CHINCHILLA, D., ZIPFEL, C., ROBATZEK, S., KEMMERLING, B., NÜRNBERGER, T., JONES, J. D. G., FELIX, G. & BOLLER, T. 2007. A flagellin-induced complex of the receptor FLS2 and BAK1 initiates plant defence. *Nature,* 448**,** 497.

CHOMCZYNSKI, P. & SACCHI, N. 1987. Single-step method of RNA isolation by acid guanidinium thiocyanate-phenol-chloroform extraction. *Analytical Biochemistry,* 162**,** 156-159.

CLOUGH, S. J. & BENT, A. F. 1998. Floral dip: a simplified method forAgrobacterium-mediated transformation ofArabidopsis thaliana. *The Plant Journal,* 16**,** 735-743.

COLCOMBET, J. & HIRT, H. 2008. Arabidopsis MAPKs: a complex signalling network involved in multiple biological processes. *Biochem J,* 413**,** 217-26.

CONG, L., RAN, F. A., COX, D., LIN, S., BARRETTO, R., HABIB, N., HSU, P. D., WU, X., JIANG, W., MARRAFFINI, L. A. & ZHANG, F. 2013. Multiplex genome engineering using CRISPR/Cas systems. *Science,* 339**,** 819-23.

COUTO, D. & ZIPFEL, C. 2016. Regulation of pattern recognition receptor signalling in plants. *Nature Reviews Immunology,* 16**,** 537.

COX, J., MATIC, I., HILGER, M., NAGARAJ, N., SELBACH, M., OLSEN, J. V. & MANN, M. 2009. A practical guide to the MaxQuant computational platform for SILAC-based quantitative proteomics. *Nat Protoc,* 4**,** 698-705.

CRUZ-RAMIREZ, A., OROPEZA-ABURTO, A., RAZO-HERNANDEZ, F., RAMIREZ-CHAVEZ, E. & HERRERA-ESTRELLA, L. 2006. Phospholipase DZ2 plays an important role in extraplastidic galactolipid biosynthesis and phosphate recycling in Arabidopsis roots. *Proc Natl Acad Sci U S A,* 103**,** 6765-70.

CVETESIC, N., SEMANJSKI, M., SOUFI, B., KRUG, K., GRUIC-SOVULJ, I. & MACEK, B. 2016. Proteome-wide measurement of non-canonical bacterial mistranslation by quantitative mass spectrometry of protein modifications. *Scientific Reports,* 6**,** 28631.

D'AMBROSIO, J. M., COUTO, D., FABRO, G., SCUFFI, D., LAMATTINA, L., MUNNIK, T., ANDERSSON, M. X., ÁLVAREZ, M. E., ZIPFEL, C. & LAXALT, A. M. 2017.

Phospholipase C2 Affects MAMP-Triggered Immunity by Modulating ROS Production. *Plant Physiology,* 175**,** 970-981.

DE TORRES ZABELA, M., FERNANDEZ-DELMOND, I., NIITTYLA, T., SANCHEZ, P. & GRANT, M. 2002. Differential Expression of Genes Encoding Arabidopsis Phospholipases After Challenge with Virulent or Avirulent Pseudomonas Isolates. *Molecular Plant-Microbe Interactions,* 15**,** 808-816.

DEL CORVO, R. 2018. *Charakterisierung einer T-DNA-Insertionslinie und möglicher Interaktionspartner der Phospholipase Dγ1 in Arabidopsis thaliana.* Diplomarbeit, Eberhard Karls Universität Tübingen.

DOMÍNGUEZ-FERRERAS, A., KISS-PAPP, M., JEHLE, A. K., FELIX, G. & CHINCHILLA, D. 2015. An Overdose of the Arabidopsis Coreceptor BRASSINOSTEROID INSENSITIVE1-ASSOCIATED RECEPTOR KINASE1 or Its Ectodomain Causes Autoimmunity in a SUPPRESSOR OF BIR1-1-Dependent Manner. *Plant physiology,* 168**,** 1106-1121.

DONALDSON, J. G. 2009. Phospholipase D in endocytosis and endosomal recycling pathways. *Biochim Biophys Acta,* 1791**,** 845-9.

EDWARDS, K., JOHNSTONE, C. & THOMPSON, C. 1991. A simple and rapid method for the preparation of plant genomic DNA for PCR analysis. *Nucleic Acids Research,* 19**,** 1349.

EGEA-JIMENEZ, A. L. & ZIMMERMANN, P. 2018. Phospholipase D and phosphatidic acid in the biogenesis and cargo loading of extracellular vesicles. *J Lipid Res,* 59**,** 1554-1560.

EL OIRDI, M., EL RAHMAN, T. A., RIGANO, L., EL HADRAMI, A., RODRIGUEZ, M. C., DAAYF, F., VOJNOV, A. & BOUARAB, K. 2011. Botrytis cinerea manipulates the antagonistic effects between immune pathways to promote disease development in tomato. *Plant Cell,* 23**,** 2405-21.

ELMORE, J. M., LIU, J., SMITH, B., PHINNEY, B. & COAKER, G. 2012. Quantitative proteomics reveals dynamic changes in the plasma membrane proteome during Arabidopsis immune signaling. *Molecular & Cellular Proteomics*.

ENGLER, C. & MARILLONNET, S. 2014. Golden Gate cloning. *Methods Mol Biol,* 1116**,** 119-31.

FENG, Z., ZHANG, B., DING, W., LIU, X., YANG, D. L., WEI, P., CAO, F., ZHU, S., ZHANG, F., MAO, Y. & ZHU, J. K. 2013. Efficient genome editing in plants using a CRISPR/Cas system. *Cell Res,* 23**,** 1229-32.

FU, Z. Q. & DONG, X. 2013. Systemic acquired resistance: turning local infection into global defense. *Annu Rev Plant Biol,* 64**,** 839-63.

GAO, H. B., CHU, Y. J. & XUE, H. W. 2013. Phosphatidic acid (PA) binds PP2AA1 to regulate PP2A activity and PIN1 polar localization. *Mol Plant,* 6**,** 1692-702.

GARDINER, J. C., HARPER, J. D., WEERAKOON, N. D., COLLINGS, D. A., RITCHIE, S., GILROY, S., CYR, R. J. & MARC, J. 2001. A 90-kD phospholipase D from tobacco binds to microtubules and the plasma membrane. *Plant Cell,* 13**,** 2143-58.

GÓMEZ-GÓMEZ, L. & BOLLER, T. 2000. FLS2: An LRR Receptor–like Kinase Involved in the Perception of the Bacterial Elicitor Flagellin in Arabidopsis. *Molecular Cell,* 5**,** 1003-1011.

GU, Y., ZAVALIEV, R. & DONG, X. 2017. Membrane Trafficking in Plant Immunity. *Molecular plant,* 10**,** 1026-1034.

GUST, A. A. & FELIX, G. 2014. Receptor like proteins associate with SOBIR1-type of adaptors to form bimolecular receptor kinases. *Curr Opin Plant Biol,* 21**,** 104-111.

GUST, A. A., PRUITT, R. & NÜRNBERGER, T. 2017. Sensing Danger: Key to Activating Plant Immunity. *Trends Plant Sci,* 22**,** 779-791.

GUST, A. A., WILLMANN, R., DESAKI, Y., GRABHERR, H. M. & NÜRNBERGER, T. 2012. Plant LysM proteins: modules mediating symbiosis and immunity. *Trends Plant Sci,* 17**,** 495-502.

HALTER, T., IMKAMPE, J., MAZZOTTA, S., WIERZBA, M., POSTEL, S., BÜCHERL, C., KIEFER, C., STAHL, M., CHINCHILLA, D., WANG, X., NÜRNBERGER, T., ZIPFEL, C., CLOUSE, S., BORST, JAN W., BOEREN, S., DE VRIES, SACCO C., TAX, F. & KEMMERLING, B. 2014. The Leucine-Rich Repeat Receptor Kinase BIR2 Is a Negative Regulator of BAK1 in Plant Immunity. *Current Biology,* 24**,** 134-143.

HARRISON, S. J., MOTT, E. K., PARSLEY, K., ASPINALL, S., GRAY, J. C. & COTTAGE, A. 2006. A rapid and robust method of identifying transformed Arabidopsis thaliana seedlings following floral dip transformation. *Plant Methods,* 2**,** 19.

HAYAFUNE, M., BERISIO, R., MARCHETTI, R., SILIPO, A., KAYAMA, M., DESAKI, Y., ARIMA, S., SQUEGLIA, F., RUGGIERO, A., TOKUYASU, K., MOLINARO, A., KAKU, H. & SHIBUYA, N. 2014. Chitin-induced activation of immune signaling by the rice receptor CEBiP relies on a unique sandwich-type dimerization. *Proc Natl Acad Sci U S A,* 111**,** E404-13.

HEESE, A., HANN, D. R., GIMENEZ-IBANEZ, S., JONES, A. M. E., HE, K., LI, J., SCHROEDER, J. I., PECK, S. C. & RATHJEN, J. P. 2007. The receptor-like kinase SERK3/BAK1 is a central regulator of innate immunity in plants. *Proceedings of the National Academy of Sciences,* 104**,** 12217-12222.

HEGENAUER, V., FÜRST, U., KAISER, B., SMOKER, M., ZIPFEL, C., FELIX, G., STAHL, M. & ALBERT, M. 2016. Detection of the plant parasite Cuscuta reflexa by a tomato cell surface receptor. *Science,* 353**,** 478-81.

HONG, Y., DEVAIAH, S. P., BAHN, S. C., THAMASANDRA, B. N., LI, M., WELTI, R. & WANG, X. 2009. Phospholipase D epsilon and phosphatidic acid enhance Arabidopsis nitrogen signaling and growth. *Plant J,* 58**,** 376-87.

HONG, Y., PAN, X., WELTI, R. & WANG, X. 2008. The effect of phospholipase Dalpha3 on Arabidopsis response to hyperosmotic stress and glucose. *Plant Signal Behav,* 3**,** 1099-100.

HONG, Y., ZHAO, J., GUO, L., KIM, S.-C., DENG, X., WANG, G., ZHANG, G., LI, M. & WANG, X. 2016. Plant phospholipases D and C and their diverse functions in stress responses. *Progress in Lipid Research,* 62**,** 55-74.

HOWDEN, A. J., SALEK, M., MIGUET, L., PULLEN, M., THOMAS, B., KNIGHT, M. R. & SWEETLOVE, L. J. 2011. The phosphoproteome of Arabidopsis plants lacking the oxidative signal-inducible1 (OXI1) protein kinase. *New Phytol,* 190**,** 49-56.

HUANG, D. W., SHERMAN, B. T. & LEMPICKI, R. A. 2008. Systematic and integrative analysis of large gene lists using DAVID bioinformatics resources. *Nature Protocols,* 4**,** 44.

HUANG, S., GAO, L., BLANCHOIN, L. & STAIGER, C. J. 2006. Heterodimeric capping protein from Arabidopsis is regulated by phosphatidic acid. *Mol Biol Cell,* 17**,** 1946-58.

HÜCKELHOVEN, R. 2007. Cell wall-associated mechanisms of disease resistance and susceptibility. *Annu Rev Phytopathol,* 45**,** 101-27.

IMKAMPE, J. 2015. *Analysis on the BAK1-interacting RLKs BIR2 and BIR3, two proteins that differentially regulate BAK1-dependent pathways.* Dissertation, Eberhard

Karls Universität. Available: http://dx.doi.org/10.15496/publikation-8019 [Accessed 15.08.2019].

IMKAMPE, J., HALTER, T., HUANG, S., SCHULZE, S., MAZZOTTA, S., SCHMIDT, N., MANSTRETTA, R., POSTEL, S., WIERZBA, M., YANG, Y., VAN DONGEN, W., STAHL, M., ZIPFEL, C., GOSHE, M. B., CLOUSE, S., DE VRIES, S. C., TAX, F., WANG, X. & KEMMERLING, B. 2017. The Arabidopsis Leucine-Rich Repeat Receptor Kinase BIR3 Negatively Regulates BAK1 Receptor Complex Formation and Stabilizes BAK1. *Plant Cell,* 29**,** 2285-2303.

INOUE, H., NOJIMA, H. & OKAYAMA, H. 1990. High efficiency transformation of Escherichia coli with plasmids. *Gene,* 96**,** 23-28.

JONES, A. M., XUAN, Y., XU, M., WANG, R. S., HO, C. H., LALONDE, S., YOU, C. H., SARDI, M. I., PARSA, S. A., SMITH-VALLE, E., SU, T., FRAZER, K. A., PILOT, G., PRATELLI, R., GROSSMANN, G., ACHARYA, B. R., HU, H. C., ENGINEER, C., VILLIERS, F., JU, C., TAKEDA, K., SU, Z., DONG, Q., ASSMANN, S. M., CHEN, J., KWAK, J. M., SCHROEDER, J. I., ALBERT, R., RHEE, S. Y. & FROMMER, W. B. 2014. Border control--a membrane-linked interactome of Arabidopsis. *Science,* 344**,** 711-6.

JONES, J. D. & DANGL, J. L. 2006. The plant immune system. *Nature,* 444**,** 323-9.

KADOTA, Y., SKLENAR, J., DERBYSHIRE, P., STRANSFELD, L., ASAI, S., NTOUKAKIS, V., JONES, J. D., SHIRASU, K., MENKE, F., JONES, A. & ZIPFEL, C. 2014. Direct regulation of the NADPH oxidase RBOHD by the PRR-associated kinase BIK1 during plant immunity. *Mol Cell,* 54**,** 43-55.

KAISER, B., VOGG, G., FÜRST, U. B. & ALBERT, M. 2015. Parasitic plants of the genus Cuscuta and their interaction with susceptible and resistant host plants. *Front Plant Sci,* 6**,** 45.

KAKU, H., NISHIZAWA, Y., ISHII-MINAMI, N., AKIMOTO-TOMIYAMA, C., DOHMAE, N., TAKIO, K., MINAMI, E. & SHIBUYA, N. 2006. Plant cells recognize chitin fragments for defense signaling through a plasma membrane receptor. *Proc Natl Acad Sci U S A,* 103**,** 11086-91.

KATAGIRI, T., TAKAHASHI, S. & SHINOZAKI, K. 2001. Involvement of a novel Arabidopsis phospholipase D, AtPLDdelta, in dehydration-inducible accumulation of phosphatidic acid in stress signalling. *Plant J,* 26**,** 595-605.

KUSNER, D. J., BARTON, J. A., QIN, C., WANG, X. & IYER, S. S. 2003. Evolutionary conservation of physical and functional interactions between phospholipase D and actin. *Arch Biochem Biophys,* 412**,** 231-41.

LAEMMLI, U. K. 1970. Cleavage of Structural Proteins during the Assembly of the Head of Bacteriophage T4. *Nature,* 227**,** 680.

LE, M. H., CAO, Y., ZHANG, X. C. & STACEY, G. 2014. LIK1, a CERK1-interacting kinase, regulates plant immune responses in Arabidopsis. *PLoS One,* 9**,** e102245.

LEI, L., LI, S., DU, J., BASHLINE, L. & GU, Y. 2013. CELLULOSE SYNTHASE INTERACTIVE3 Regulates Cellulose Biosynthesis in Both a Microtubule-Dependent and Microtubule-Independent Manner in Arabidopsis. *The Plant Cell,* 25**,** 4912-4923.

LI, G. & XUE, H. W. 2007. Arabidopsis PLDzeta2 regulates vesicle trafficking and is required for auxin response. *Plant Cell,* 19**,** 281-95.

LI, J., HENTY-RIDILLA, J. L., HUANG, S., WANG, X., BLANCHOIN, L. & STAIGER, C. J. 2012. Capping protein modulates the dynamic behavior of actin filaments in response to phosphatidic acid in Arabidopsis. *Plant Cell,* 24**,** 3742-54.

LI, J., HENTY-RIDILLA, J. L., STAIGER, B. H., DAY, B. & STAIGER, C. J. 2015. Capping protein integrates multiple MAMP signalling pathways to modulate actin dynamics during plant innate immunity. *Nat Commun,* 6.

LI, J. & WANG, X. 2019. Phospholipase D and phosphatidic acid in plant immunity. *Plant Sci,* 279**,** 45-50.

LI, M., WELTI, R. & WANG, X. 2006. Quantitative profiling of Arabidopsis polar glycerolipids in response to phosphorus starvation. Roles of phospholipases D zeta1 and D zeta2 in phosphatidylcholine hydrolysis and digalactosyldiacylglycerol accumulation in phosphorus-starved plants. *Plant Physiol,* 142**,** 750-61.

LI, W., LI, M., ZHANG, W., WELTI, R. & WANG, X. 2004. The plasma membrane-bound phospholipase Ddelta enhances freezing tolerance in Arabidopsis thaliana. *Nat Biotechnol,* 22**,** 427-33.

LI, W., WANG, R., LI, M., LI, L., WANG, C., WELTI, R. & WANG, X. 2008. Differential degradation of extraplastidic and plastidic lipids during freezing and post-freezing recovery in Arabidopsis thaliana. *J Biol Chem,* 283**,** 461-8.

LIANG, X. & ZHOU, J. M. 2018. Receptor-Like Cytoplasmic Kinases: Central Players in Plant Receptor Kinase-Mediated Signaling. *Annu Rev Plant Biol,* 69**,** 267-299.

LIEBRAND, T. W., VAN DEN BURG, H. A. & JOOSTEN, M. H. 2014. Two for all: receptor-associated kinases SOBIR1 and BAK1. *Trends Plant Sci,* 19**,** 123-32.

LIN, W., LI, B., LU, D., CHEN, S., ZHU, N., HE, P. & SHAN, L. 2014. Tyrosine phosphorylation of protein kinase complex BAK1/BIK1 mediates Arabidopsis innate immunity. *Proceedings of the National Academy of Sciences,* 111**,** 3632-3637.

LISCOVITCH, M. 1989. Phosphatidylethanol biosynthesis in ethanol-exposed NG108-15 neuroblastoma X glioma hybrid cells. Evidence for activation of a phospholipase D phosphatidyl transferase activity by protein kinase C. *J Biol Chem,* 264**,** 1450-6.

LIU, B., LI, J. F., AO, Y., QU, J., LI, Z., SU, J., ZHANG, Y., LIU, J., FENG, D., QI, K., HE, Y., WANG, J. & WANG, H. B. 2012a. Lysin motif-containing proteins LYP4 and LYP6 play dual roles in peptidoglycan and chitin perception in rice innate immunity. *Plant Cell,* 24**,** 3406-19.

LIU, T., LIU, Z., SONG, C., HU, Y., HAN, Z., SHE, J., FAN, F., WANG, J., JIN, C., CHANG, J., ZHOU, J. M. & CHAI, J. 2012b. Chitin-induced dimerization activates a plant immune receptor. *Science,* 336**,** 1160-4.

LIU, X., GRABHERR, H. M., WILLMANN, R., KOLB, D., BRUNNER, F., BERTSCHE, U., KÜHNER, D., FRANZ-WACHTEL, M., AMIN, B., FELIX, G., ONGENA, M., NÜRNBERGER, T. & GUST, A. A. 2014. Host-induced bacterial cell wall decomposition mediates pattern-triggered immunity in Arabidopsis. *eLife,* 3**,** e01990.

LIU, Y. & HE, C. 2016a. Regulation of plant reactive oxygen species (ROS) in stress responses: learning from AtRBOHD. *Plant Cell Reports,* 35**,** 995-1007.

LIU, Y. & HE, C. 2016b. A review of redox signaling and the control of MAP kinase pathway in plants. *Redox biology,* 11**,** 192-204.

LIU, Y., HUANG, X., LI, M., HE, P. & ZHANG, Y. 2016. Loss-of-function of Arabidopsis receptor-like kinase BIR1 activates cell death and defense responses mediated by BAK1 and SOBIR1. *New Phytol,* 212**,** 637-645.

LIVAK, K. J. & SCHMITTGEN, T. D. 2001. Analysis of Relative Gene Expression Data Using Real-Time Quantitative PCR and the 2−ΔΔCT Method. *Methods,* 25**,** 402-408.

LU, D., LIN, W., GAO, X., WU, S., CHENG, C., AVILA, J., HEESE, A., DEVARENNE, T. P., HE, P. & SHAN, L. 2011. Direct ubiquitination of pattern recognition receptor FLS2 attenuates plant innate immunity. *Science,* 332**,** 1439-42.

LU, D., WU, S., GAO, X., ZHANG, Y., SHAN, L. & HE, P. 2010. A receptor-like cytoplasmic kinase, BIK1, associates with a flagellin receptor complex to initiate plant innate immunity. *Proc Natl Acad Sci U S A,* 107**,** 496-501.

MA, C., LIU, Y., BAI, B., HAN, Z., TANG, J., ZHANG, H., YAGHMAIEAN, H., ZHANG, Y. & CHAI, J. 2017. Structural basis for BIR1-mediated negative regulation of plant immunity. *Cell Res,* 27**,** 1521-1524.

MALINOVSKY, F. G., FANGEL, J. U. & WILLATS, W. G. 2014. The role of the cell wall in plant immunity. *Front Plant Sci,* 5**,** 178.

MANOSALVA, P., MANOHAR, M., VON REUSS, S. H., CHEN, S., KOCH, A., KAPLAN, F., CHOE, A., MICIKAS, R. J., WANG, X. & KOGEL, K. H. 2015. Conserved nematode signalling molecules elicit plant defenses and pathogen resistance. 6**,** 7795.

MCHALE, L., TAN, X., KOEHL, P. & MICHELMORE, R. W. 2006. Plant NBS-LRR proteins: adaptable guards. *Genome biology,* 7**,** 212-212.

MIEDES, E., VANHOLME, R., BOERJAN, W. & MOLINA, A. 2014. The role of the secondary cell wall in plant resistance to pathogens. *Frontiers in Plant Science,* 5.

MITHÖFER, A. & BOLAND, W. 2008. Recognition of herbivory-associated molecular patterns. *Plant Physiol,* 146**,** 825-31.

MIYA, A., ALBERT, P., SHINYA, T., DESAKI, Y., ICHIMURA, K., SHIRASU, K., NARUSAKA, Y., KAWAKAMI, N., KAKU, H. & SHIBUYA, N. 2007. CERK1, a LysM receptor kinase, is essential for chitin elicitor signaling in Arabidopsis. *Proc Natl Acad Sci U S A,* 104**,** 19613-8.

MUNNIK, T. & LAXALT, A. M. 2013. Measuring PLD activity in vivo. *Methods Mol Biol,* 1009**,** 219-31.

MUNNIK, T. & ZARZA, X. 2013. Analyzing plant signaling phospholipids through 32Pi-labeling and TLC. *Methods Mol Biol,* 1009**,** 3-15.

NAKAGAWA, T., KUROSE, T., HINO, T., TANAKA, K., KAWAMUKAI, M., NIWA, Y., TOYOOKA, K., MATSUOKA, K., JINBO, T. & KIMURA, T. 2007. Development of series of gateway binary vectors, pGWBs, for realizing efficient construction of fusion genes for plant transformation. *J Biosci Bioeng,* 104**,** 34-41.

NAKAZAWA, Y., SAGANE, Y., SAKURAI, S.-I., UCHINO, M., SATO, H., TOEDA, K. & TAKANO, K. 2011. Large-Scale Production of Phospholipase D from Streptomyces racemochromogenes and Its Application to Soybean Lecithin Modification. *Applied Biochemistry and Biotechnology,* 165**,** 1494-1506.

NING, Y., LIU, W. & WANG, G. L. 2017. Balancing Immunity and Yield in Crop Plants. *Trends Plant Sci,* 22**,** 1069-1079.

OSBOURN, A. 1996. Preformed Antimicrobial Compounds and Plant Defense against Fungal Attack. *Plant Cell,* 8**,** 1821-31.

PETUTSCHNIG, E. K., JONES, A. M., SERAZETDINOVA, L., LIPKA, U. & LIPKA, V. 2010. The lysin motif receptor-like kinase (LysM-RLK) CERK1 is a major chitin-binding protein in Arabidopsis thaliana and subject to chitin-induced phosphorylation. *J Biol Chem,* 285**,** 28902-11.

PINOSA, F., BUHOT, N., KWAAITAAL, M., FAHLBERG, P., THORDAL-CHRISTENSEN, H., ELLERSTROM, M. & ANDERSSON, M. X. 2013. Arabidopsis phospholipase ddelta is involved in basal defense and nonhost resistance to powdery mildew fungi. *Plant Physiol,* 163**,** 896-906.

PLESKOT, R., LI, J., ZARSKY, V., POTOCKY, M. & STAIGER, C. J. 2013. Regulation of cytoskeletal dynamics by phospholipase D and phosphatidic acid. *Trends Plant Sci,* 18**,** 496-504.

POSTEL, S., KÜFNER, I., BEUTER, C., MAZZOTTA, S., SCHWEDT, A., BORLOTTI, A., HALTER, T., KEMMERLING, B. & NÜRNBERGER, T. 2010. The multifunctional leucine-rich repeat receptor kinase BAK1 is implicated in Arabidopsis development and immunity. *Eur J Cell Biol,* 89**,** 169-74.

PREMKUMAR, A., LINDBERG, S., LAGER, I., RASMUSSEN, U. & SCHULZ, A. 2018. Arabidopsis PLDs with C2-domain function distinctively in hypoxia. *Physiol Plant*.

QIN, C., LI, M., QIN, W., BAHN, S. C., WANG, C. & WANG, X. 2006. Expression and characterization of Arabidopsis phospholipase Dγ2. *Biochimica et Biophysica Acta (BBA) - Molecular and Cell Biology of Lipids,* 1761**,** 1450-1458.

QIN, C. & WANG, X. 2002. The Arabidopsis phospholipase D family. Characterization of a calcium-independent and phosphatidylcholine-selective PLD zeta 1 with distinct regulatory domains. *Plant Physiol,* 128**,** 1057-68.

ROUX, M. E., RASMUSSEN, M. W., PALMA, K., LOLLE, S., REGUE, A. M., BETHKE, G., GLAZEBROOK, J., ZHANG, W., SIEBURTH, L., LARSEN, M. R., MUNDY, J. & PETERSEN, M. 2015. The mRNA decay factor PAT1 functions in a pathway including MAP kinase 4 and immune receptor SUMM2. *Embo j,* 34**,** 593-608.

RUBARTELLI, A. & LOTZE, M. T. 2007. Inside, outside, upside down: damage-associated molecular-pattern molecules (DAMPs) and redox. *Trends Immunol,* 28**,** 429-36.

SAIJO, Y., LOO, E. P. & YASUDA, S. 2018. Pattern recognition receptors and signaling in plant-microbe interactions. *Plant J,* 93**,** 592-613.

SALZER, A. 2016. *Charakterisierung von möglichen Interaktoren der Lysin-Motiv Rezeptorkinase CERK1.* Bachelor Thesis, Eberhard Karls Universität.

SANG, Y., ZHENG, S., LI, W., HUANG, B. & WANG, X. 2001. Regulation of plant water loss by manipulating the expression of phospholipase Dalpha. *Plant J,* 28**,** 135-44.

SCHLÖFFEL, M. A., KÄSBAUER, C. & GUST, A. A. 2019. Interplay of plant glycan hydrolases and LysM proteins in plant-Bacteria interactions. *Int J Med Microbiol,* 309**,** 252-257.

SHAO, F., GOLSTEIN, C., ADE, J., STOUTEMYER, M., DIXON, J. E. & INNES, R. W. 2003. Cleavage of Arabidopsis PBS1 by a bacterial type III effector. *Science,* 301**,** 1230-3.

SHIMIZU, T., NAKANO, T., TAKAMIZAWA, D., DESAKI, Y., ISHII-MINAMI, N., NISHIZAWA, Y., MINAMI, E., OKADA, K., YAMANE, H., KAKU, H. & SHIBUYA, N. 2010. Two LysM receptor molecules, CEBiP and OsCERK1, cooperatively regulate chitin elicitor signaling in rice. *Plant J,* 64**,** 204-14.

SHINE, M. B., XIAO, X., KACHROO, P. & KACHROO, A. 2019. Signaling mechanisms underlying systemic acquired resistance to microbial pathogens. *Plant Sci,* 279**,** 81-86.

SHINYA, T., YAMAGUCHI, K., DESAKI, Y., YAMADA, K., NARISAWA, T., KOBAYASHI, Y., MAEDA, K., SUZUKI, M., TANIMOTO, T., TAKEDA, J., NAKASHIMA, M., FUNAMA, R., NARUSAKA, M., NARUSAKA, Y., KAKU, H., KAWASAKI, T. & SHIBUYA, N. 2014. Selective regulation of the chitin-induced defense response by the Arabidopsis receptor-like cytoplasmic kinase PBL27. *Plant J,* 79**,** 56-66.

SPAT, P., MACEK, B. & FORCHHAMMER, K. 2015. Phosphoproteome of the cyanobacterium Synechocystis sp. PCC 6803 and its dynamics during nitrogen starvation. *Front Microbiol,* 6**,** 248.

SPOEL, S. H. & DONG, X. 2012. How do plants achieve immunity? Defence without specialized immune cells. *Nature Reviews Immunology,* 12**,** 89.

THE ARABIDOPSIS INFORMATION RESOURCE (TAIR). 2018a. *AT2G37220* [Online]. on www.arabidopsis.org. Available: https://www.arabidopsis.org/servlets/TairObject?id=32909&type=locus [Accessed 20.11.2018 2018].

THE ARABIDOPSIS INFORMATION RESOURCE (TAIR). 2018b. *ATCDC5* [Online]. on www.arabidopsis.org. Available: https://www.arabidopsis.org/servlets/TairObject?id=28932&type=locus [Accessed 20.11.2018 2018].

THE ARABIDOPSIS INFORMATION RESOURCE (TAIR). 2019a. *AT2G31130* [Online]. www.arabidopsis.org. Available: https://www.arabidopsis.org/servlets/TairObject?id=33918&type=locus [Accessed 05.03.2019 2019].

THE ARABIDOPSIS INFORMATION RESOURCE (TAIR). 2019b. *AT4G11830* [Online]. www.arabidopsis.org. Available: https://www.arabidopsis.org/servlets/TairObject?id=129739&type=locus [Accessed 08.08.2019 2019].

THE ARABIDOPSIS INFORMATION RESOURCE (TAIR). 2019c. *AT4G11840* [Online]. www.arabidopsis.org. Available: https://www.arabidopsis.org/servlets/TairObject?id=129741&type=locus [Accessed 08.08.2019 2019].

THE ARABIDOPSIS INFORMATION RESOURCE (TAIR). 2019d. *AT4G11850* [Online]. www.arabidopsis.org. Available: https://www.arabidopsis.org/servlets/TairObject?id=129743&type=locus [Accessed 08.08.2019 2019].

THOMMA, B. P., NELISSEN, I., EGGERMONT, K. & BROEKAERT, W. F. 1999. Deficiency in phytoalexin production causes enhanced susceptibility of Arabidopsis thaliana to the fungus Alternaria brassicicola. *Plant J,* 19**,** 163-71.

THOMMA, B. P. H. J., NÜRNBERGER, T. & JOOSTEN, M. H. A. J. 2011. Of PAMPs and Effectors: The Blurred PTI-ETI Dichotomy. *The Plant Cell,* 23**,** 4-15.

THULASI DEVENDRAKUMAR, K., LI, X. & ZHANG, Y. 2018a. MAP kinase signalling: interplays between plant PAMP- and effector-triggered immunity. *Cell Mol Life Sci,* 75**,** 2981-2989.

THULASI DEVENDRAKUMAR, K., LI, X. & ZHANG, Y. 2018b. MAP kinase signalling: interplays between plant PAMP- and effector-triggered immunity. *Cellular and Molecular Life Sciences,* 75**,** 2981-2989.

VAN DER LUIT, A. H., PIATTI, T., VAN DOORN, A., MUSGRAVE, A., FELIX, G., BOLLER, T. & MUNNIK, T. 2000. Elicitation of suspension-cultured tomato cells triggers the formation of phosphatidic acid and diacylglycerol pyrophosphate. *Plant Physiol,* 123**,** 1507-16.

VOINNET, O., RIVAS, S., MESTRE, P. & BAULCOMBE, D. 2003. Retracted: An enhanced transient expression system in plants based on suppression of gene silencing by the p19 protein of tomato bushy stunt virus. *The Plant Journal,* 33**,** 949-956.

WAN, J., ZHANG, X. C. & STACEY, G. 2008. Chitin signaling and plant disease resistance. *Plant Signal Behav,* 3**,** 831-3.

WAN, W. L., FRÖHLICH, K., PRUITT, R. N., NÜRNBERGER, T. & ZHANG, L. 2019. Plant cell surface immune receptor complex signaling. *Curr Opin Plant Biol,* 50**,** 18-28.

WAN, W. L., ZHANG, L., PRUITT, R., ZAIDEM, M., BRUGMAN, R., MA, X., KROL, E., PERRAKI, A., KILIAN, J., GROSSMANN, G., STAHL, M., SHAN, L., ZIPFEL, C., VAN KAN, J. A. L., HEDRICH, R., WEIGEL, D., GUST, A. A. & NÜRNBERGER, T. 2018. Comparing Arabidopsis receptor kinase and receptor protein-mediated immune signaling reveals BIK1-dependent differences. *New Phytol*.

WANG, G., RYU, S. & WANG, X. 2012. Plant Phospholipases: An Overview. *In:* SANDOVAL, G. (ed.) *Lipases and Phospholipases.* Humana Press.

WANG, Z.-Y. 2012. Brassinosteroids modulate plant immunity at multiple levels. *Proceedings of the National Academy of Sciences,* 109**,** 7-8.

WILLMANN, R., LAJUNEN, H. M., ERBS, G., NEWMAN, M. A., KOLB, D., TSUDA, K., KATAGIRI, F., FLIEGMANN, J., BONO, J. J., CULLIMORE, J. V., JEHLE, A. K., GÖTZ, F., KULIK, A., MOLINARO, A., LIPKA, V., GUST, A. A. & NÜRNBERGER, T. 2011. Arabidopsis lysin-motif proteins LYM1 LYM3 CERK1 mediate bacterial peptidoglycan sensing and immunity to bacterial infection. *Proc Natl Acad Sci U S A,* 108**,** 19824-9.

WOLTER, F., SCHINDELE, P. & PUCHTA, H. 2019. Plant breeding at the speed of light: the power of CRISPR/Cas to generate directed genetic diversity at multiple sites. *BMC Plant Biol,* 19**,** 176.

WU, P., GAO, H. B., ZHANG, L. L., XUE, H. W. & LIN, W. H. 2014. Phosphatidic acid regulates BZR1 activity and brassinosteroid signal of Arabidopsis. *Mol Plant,* 7**,** 445-7.

YAMADA, K., YAMAGUCHI, K., SHIRAKAWA, T., NAKAGAMI, H., MINE, A., ISHIKAWA, K., FUJIWARA, M., NARUSAKA, M., NARUSAKA, Y., ICHIMURA, K., KOBAYASHI, Y., MATSUI, H., NOMURA, Y., NOMOTO, M., TADA, Y., FUKAO, Y., FUKAMIZO, T., TSUDA, K., SHIRASU, K., SHIBUYA, N. & KAWASAKI, T. 2016. The Arabidopsis CERK1-associated kinase PBL27 connects chitin perception to MAPK activation. *Embo j,* 35**,** 2468-2483.

YAMAGUCHI, T., KURODA, M., YAMAKAWA, H., ASHIZAWA, T., HIRAYAE, K., KURIMOTO, L., SHINYA, T. & SHIBUYA, N. 2009. Suppression of a phospholipase D gene, OsPLDbeta1, activates defense responses and increases disease resistance in rice. *Plant Physiol,* 150**,** 308-19.

YANG, S. F., FREER, S. & BENSON, A. A. 1967. Transphosphatidylation by Phospholipase D. *Journal of Biological Chemistry,* 242**,** 477-484.

YU, L., NIE, J., CAO, C., JIN, Y., YAN, M., WANG, F., LIU, J., XIAO, Y., LIANG, Y. & ZHANG, W. 2010. Phosphatidic acid mediates salt stress response by regulation of MPK6 in Arabidopsis thaliana. *New Phytol,* 188**,** 762-73.

YU, X., FENG, B., HE, P. & SHAN, L. 2017. From Chaos to Harmony: Responses and Signaling upon Microbial Pattern Recognition. *Annu Rev Phytopathol,* 55**,** 109-137.

ZHANG, J., LI, W., XIANG, T., LIU, Z., LALUK, K., DING, X., ZOU, Y., GAO, M., ZHANG, X., CHEN, S., MENGISTE, T., ZHANG, Y. & ZHOU, J.-M. 2010. Receptor-like Cytoplasmic Kinases Integrate Signaling from Multiple Plant Immune Receptors and Are Targeted by a Pseudomonas syringae Effector. *Cell Host & Microbe,* 7**,** 290-301.

ZHANG, L., ZHANG, F., MELOTTO, M., YAO, J. & HE, S. Y. 2017. Jasmonate signaling and manipulation by pathogens and insects. *J Exp Bot,* 68**,** 1371-1385.

ZHANG, M., WANG, F., LI, S., WANG, Y., BAI, Y. & XU, X. 2014. TALE: A tale of genome editing. *Progress in Biophysics and Molecular Biology,* 114**,** 25-32.

ZHANG, Q., BERKEY, R., BLAKESLEE, J. J., LIN, J., MA, X., KING, H., LIDDLE, A., GUO, L., MUNNIK, T., WANG, X. & XIAO, S. 2018a. Arabidopsis phospholipase Dalpha1 and Ddelta oppositely modulate EDS1- and SA-independent basal resistance against adapted powdery mildew. *J Exp Bot,* 69**,** 3675-3688.

ZHANG, W., ZHAO, F., JIANG, L., CHEN, C., WU, L. & LIU, Z. 2018b. Different Pathogen Defense Strategies in Arabidopsis: More than Pathogen Recognition. *Cells,* 7.

ZHANG, Y., ZHU, H., ZHANG, Q., LI, M., YAN, M., WANG, R., WANG, L., WELTI, R., ZHANG, W. & WANG, X. 2009. Phospholipase dalpha1 and phosphatidic acid regulate NADPH oxidase activity and production of reactive oxygen species in ABA-mediated stomatal closure in Arabidopsis. *Plant Cell,* 21**,** 2357-77.

ZHAO, J. 2015. Phospholipase D and phosphatidic acid in plant defence response: from protein-protein and lipid-protein interactions to hormone signalling. *J Exp Bot,* 66**,** 1721-36.

ZHAO, J., DEVAIAH, S. P., WANG, C., LI, M., WELTI, R. & WANG, X. 2013a. Arabidopsis phospholipase Dbeta1 modulates defense responses to bacterial and fungal pathogens. *New Phytol,* 199**,** 228-40.

ZHAO, J., DEVAIAH, S. P., WANG, C., LI, M., WELTI, R. & WANG, X. 2013b. Arabidopsis phospholipase Dβ1 modulates defense responses to bacterial and fungal pathogens. *New Phytologist,* 199**,** 228-240.

ZHAO, J., WANG, C., BEDAIR, M., WELTI, R., SUMNER, L. W., BAXTER, I. & WANG, X. 2011. Suppression of phospholipase Dgammas confers increased aluminum resistance in Arabidopsis thaliana. *PLoS One,* 6**,** e28086.

ZHAO, J. & WANG, X. 2013. Biochemical Analysis of the Interaction Between Phospholipase Dα1 and GTP-Binding Protein α-Subunit from Arabidopsis thaliana. *In:* RUNNING, M. P. (ed.) *G Protein-Coupled Receptor Signaling in Plants: Methods and Protocols.* Totowa, NJ: Humana Press.

ZHONG, C.-L., ZHANG, C. & LIU, J.-Z. 2018. Hetero-trimeric G protein signaling in plant immunity. *Journal of Experimental Botany***,** ery426-ery426.

8 APPENDIX

DANKSAGUNG

Ich bedanke mich bei

Andrea, für die Verfügungstellung dieses Themas, deine Betreuung und Unterstützung in den letzten Jahren, die wissenschaftlichen Ratschläge und Diskussionen und die Freiheit eigene Erfahrungen sammeln zu dürfen und dieses Projekt möglichst selbständig durchzuführen zu können. Auch bedanke ich mich für die Übernahme der ersten Berichterstatterin.

Thorsten für die Möglichkeit an deinem Lehrstuhl meine Doktorarbeit zu absolvieren, deine wissenschaftlichen Einschätzungen und Ideen. Danke, für die Übernahme des zweiten Berichterstatters.

meinen Kollegen aus N1 Christina Steidele, Wei-Lin Wan, Xiaokun Liu, Dagmar Kolb, Zana Kikic, Birgit Löffelhardt und allen anderen aus der Pflanzenbiochemie, Gärtnerei und Central facilities für die gute Zusammenarbeit, gegenseitige Unterstützung, Unterhaltungen, Diskussionen und schönen lustigen Momente.

Andrea Salzer für die beste Bachelor Studentin und Hiwi, die man haben kann.

Christoph für den besten Baykollegen und Freund, den man sich vorstellen kann, für viele lustige und philosophische Momente und Diskussionen und dass man sich auf dich verlassen kann.

Sarina für deine Freundschaft, dein offenes Ohr in jeder Lebenssituation, Ratschläge, Aufmerksamkeiten, Spaß haben, wissenschaftlichen Austausch und Spekulationen, Korrekturlesen, Babysitting. Danke, du hast mir oft Mut gemacht.

Katja für deine Freundschaft, Unterstützung, Motivation, Essen, Urlaube, wissenschaftliche Diskussionen, Pst-Assay, Korrekturlesen und Statistik-Nachhilfe. Danke, ohne dich wäre ich manchmal verloren gewesen.

meinen Eltern für die Ermöglichung meiner Ausbildung, dass ihr immer an mich glaubt und mich unterstützt und ihr mir gezeigt habt, wie ich in dieser Welt bestehen kann und was wirklich wichtig ist.

Robert und Henry Emil, meine Familie, mein Halt und meine Zukunft. Danke, ohne euch hätte ich es nicht geschafft.

CURRICULUM VITAE

Maria Alejandra Schlöffel

Geburtsdatum und -Ort	23.12.1988 Ciudad Bolivar, Colombia

Akademische Ausbildung

Seit 02/2014	**Eberhard Karls Universität Tübingen** Promotion Pflanzenbiochemie "Functional characterization of PLDγ1 in *Arabidopsis thaliana* innate immunity"
10/2011 – 12/2013	**Justus-Liebig-Universität Gießen** Master of Science Agrobiotechnology „A reverse genetic approach to identify homoserine lactones receptor(s) in plants"
10/2008 – 09/2011	**Justus-Liebig-Universität Gießen** Bachelor of Science Biology „Impact of singlet oxygen to the thylakoid ATP-Synthase"
2008	**Adolf-Reichwein-Schule Limburg** Abitur

Praktika und Forschungsaufenthalte im Ausland

08/2018 – 09/2018	**Botanische Exkursion Kolumbien** „Neotropic diversity of adaptations, a glance through plant physiology and plant-animal interactions."
11/2017 – 12/2017	**Universität von Amsterdam, Niederlande Pflanzenphysiologie** Gastforschungsaufenthalt zur Erlernung neuer Techniken
09/2013 – 12/2013	**ABiTEP GmbH Berlin** Praktikum in Forschung und Entwicklung
08/2010 – 10/2010	**INVEMAR, Santa Marta, Kolumbien** Meeresbiologische Praktikum

Publikationen

Schlöffel et al. (2019): Interplay of plant glycan hydrolases and LysM proteins in plant-bacteria interactions. — *Int J Med Microbiol*.

Fuchs et al. (2018): The fungal ligand chitin directly binds TLR2 and triggers inflammation dependent on oligomer size. — *EMBO Reports*